

ABSTRACTS PRESENTED  
AT THE 4<sup>TH</sup> BRAINN CONGRESS  
BRAZILIAN INSTITUTE OF NEUROSCIENCE  
AND NEUROTECHNOLOGY (CEDIP-FAPESP)

MARCH 27<sup>th</sup> TO 29<sup>th</sup> 2017 - CAMPINAS, SP, BRAZIL

PART II

Um **NOVO PASSO**  
para uma vida com  
**NOVAS POSSIBILIDADES**



**Keppra®**  
levetiracetam



- ▶ **Keppra® é o único FAE considerado nível A de evidência para o tratamento de crises focais, em terapia adjuvante, pelos guidelines da ILAE\*, em pediatria<sup>1</sup>**
- ▶ **Keppra® solução oral, em terapia adjuvante, se mostrou bem tolerado no tratamento de crises focais em crianças a partir de 1 mês de idade, crises mioclônicas (incluindo epilepsia mioclônica juvenil) a partir de 12 anos e em crises tônico-clônicas primariamente generalizadas a partir dos 6 anos de idade<sup>2,3,4,5</sup>**

\*International League Against Epilepsy

**CONTRAINDICAÇÃO:** Hipersensibilidade ao princípio ativo ou a outros derivados da pirrolidona ou a qualquer um dos excipientes. **INTERAÇÃO MEDICAMENTOSA:** Foram observados relatos isolados de diminuição de eficácia quando o laxante osmótico macrogol foi administrado concomitantemente a levetiracetam oral. Assim, a administração oral de macrogol não deve ser realizada dentro de 1 hora (antes ou após) da administração de levetiracetam.

**Referência Bibliográfica:** 1. Wilmschurst JM, Summary of recommendations for the management of infantile seizures: Task Force Report for the ILAE Commission of Pediatrics. - Epilepsia. 2015 Aug; 56(8): 1185-97. 2. Berkovic; Placebo-controlled study of levetiracetam in idiopathic generalized epilepsy - Neurology 2007; 69: 1751-1760. 3. Piña Garza; Adjunctive levetiracetam in infants and young children with refractory partial-onset seizures - Epilepsia. 50(5): 1141-1149, 2009. 4. Noachtar et al.; Levetiracetam for the treatment of idiopathic generalized epilepsy with myoclonic seizures - Neurology. 2008 Feb 19; 70(8): 607-16. 5. Glauser; Double-blind placebo-controlled trial of adjunctive levetiracetam in pediatric partial seizures - Neurology. 2006 Jun 13; 66(11): 1654-60.

**Keppra® (levetiracetam).** **Apresentação:** Frasco de vidro âmbar contendo 150 mL de solução oral (100 mg/mL), acompanhado de uma seringa de 3 mL para administração. **Indicações:** é indicado como monoterapia para o tratamento de crises parciais, com ou sem generalização secundária em pacientes a partir dos 16 anos com diagnóstico recente de epilepsia. Keppra® também é indicado como terapia adjuvante no tratamento de: - crises convulsivas parciais em adultos, crianças e bebês a partir de 1 mês de idade, com epilepsia; - crises convulsivas mioclônicas em adultos e adolescentes a partir dos 12 anos, com epilepsia mioclônica juvenil; - crises convulsivas tônico-clônicas primárias generalizadas em adultos e crianças com mais de 6 anos de idade, com epilepsia idiopática generalizada. **Contraindicações:** Hipersensibilidade ao princípio ativo ou a outros derivados da pirrolidona ou a qualquer um dos excipientes. **Cuidados e Advertências:** para informações completas de advertências, vide bula do produto. A administração oral de Keppra® em pacientes com comprometimento renal poderá necessitar de um ajuste da dose. Foram notificados suicídio, tentativa de suicídio e ideias e comportamento suicida em pacientes tratados com levetiracetam. **Gravidez** categoria C de risco de gravidez. Este medicamento não deve ser utilizado por mulheres grávidas sem orientação médica ou do cirurgião-dentista. Levetiracetam é excretado no leite humano materno. **Keppra®** é um medicamento. Durante seu uso, não dirija veículos ou opere máquinas, pois sua agilidade e atenção podem estar prejudicadas. **Interações medicamentosas (vide bula completa do produto):** Dados indicam que levetiracetam não influencia as concentrações séricas de medicamentos antiepilépticos existentes (fenitoína, carbamazepina, ácido valproico, fenobarbital, lamotrigina, gabapentina e primidona) e que estes medicamentos antiepilépticos não influenciam a farmacocinética de levetiracetam. A probenecida (500 mg quatro vezes ao dia), um agente bloqueador da secreção tubular renal, mostrou inibir a depuração renal do metabólito primário, mas não a do levetiracetam. Contudo, a concentração deste metabólito permanece baixa. Levetiracetam 1000 mg por dia não influenciou a farmacocinética dos contraceptivos orais (etinilestradiol e levonorgestrel). Foram observados relatos isolados de diminuição de eficácia quando o laxante osmótico macrogol foi administrado concomitantemente a levetiracetam oral. Assim, a administração oral de macrogol não deve ser realizada dentro de 1 hora (antes ou após) da administração de levetiracetam. A extensão de absorção do levetiracetam não sofreu qualquer alteração com a ingestão de alimentos, mas a taxa de absorção diminuiu ligeiramente. Não estão disponíveis dados sobre a interação do levetiracetam com o álcool. **Reações Adversas:** para informações completas de reações adversas, vide bula do produto. Os eventos adversos mais comumente reportados nos estudos clínicos foram astenia, fadiga, dor de cabeça e sonolência. Adicionalmente às reações adversas relatadas durante os estudos clínicos, as seguintes reações adversas foram reportadas na experiência pós-comercialização, além de outras mencionadas na bula completa do produto: comportamento anormal, raiva, ataque de pânico, ansiedade, estado de confusão, alucinação, distúrbios psicóticos, suicídio, tentativa de suicídio e ideação suicida, parestesia, coreoatetose, discinesia, letargia. **Posologia:** A dose inicial recomendada para monoterapia no tratamento de crises parciais, com ou sem generalização secundária em pacientes a partir dos 16 anos com diagnóstico recente de epilepsia, é de 250 mg (2,5 mL) duas vezes ao dia, a qual poderá ser aumentada para uma dose terapêutica inicial de 500 mg (5 mL) duas vezes ao dia, após duas semanas. A dose máxima é de 1500 mg (15 mL) duas vezes ao dia. Nos casos de terapia adjuvante, para adultos e crianças acima de 12 anos e com peso igual ou superior a 50 kg, a dose terapêutica inicial é de 500 mg/duas vezes ao dia (5 mL/duas vezes ao dia). Esta dose poderá ser iniciada no primeiro dia de tratamento, a dose diária poderá ser aumentada até o máximo de 1500 mg/duas vezes ao dia (15 mL/duas vezes ao dia). Ainda nos casos de terapia adjuvante, para adolescentes, crianças e bebês a partir dos 6 meses com peso inferior a 50 kg a dose terapêutica inicial é de 10 mg/kg (0,1 mL/kg) duas vezes ao dia, a dose pode ser aumentada até 30 mg/kg (0,3 mL/kg) duas vezes ao dia. A alteração das doses não deve exceder aumentos ou reduções de 10 mg/kg (0,1 mL/kg) duas vezes ao dia, a cada duas semanas. Deve ser utilizada a dose eficaz mais baixa. A posologia em crianças com peso igual ou superior a 50 kg é igual à dos adultos. Nos casos de terapia adjuvante para bebês com mais de 1 mês e menos de 6 meses de idade a dose terapêutica inicial é de 7 mg/kg (0,07 mL/kg) duas vezes ao dia, a dose pode ser aumentada para um máximo de 21 mg/kg (0,21 mL/kg) duas vezes ao dia. A alteração das doses não deve exceder aumentos ou reduções de 7 mg/kg (0,07 mL/kg) duas vezes ao dia a cada duas semanas. Deve ser utilizada a dose eficaz mais baixa. A solução oral é a forma farmacêutica ideal para uso em bebês. **USO ADULTO E PEDIÁTRICO ACIMA DE 01 MÊS DE IDADE. USO ORAL VENDA SOB PRESCRIÇÃO MÉDICA – SO PODE SER VENDIDO COM RETENÇÃO DA RECEITA. SE PERSISTIREM OS SINTOMAS, O MÉDICO DEVERÁ SER CONSULTADO.** Para maiores informações, consulte a bula completa do produto. (0302040021R8 Rev. Agosto 2015). [www.ucb-biopharma.com.br](http://www.ucb-biopharma.com.br) Reg. MS – 1.2361.0083

## CORPO EDITORIAL

### Editores Científicos

Fernando Cendes – Departamento de Neurologia, Faculdade de Ciências Médicas, Unicamp, Campinas/SP/Brasil.

João Pereira Leite – Departamento de Neurociências e Ciências do Comportamento, Faculdade de Medicina, USP, Ribeirão Preto/SP/Brasil.

### Editores Associados

Li Li Min – Departamento de Neurologia, Faculdade de Ciências Médicas, Unicamp, Campinas/SP/Brasil.

Carlos Eduardo Silvado – Setor de Epilepsia e EEG, Hospital de Clínicas, UFPR, Curitiba, PR/Brasil.

## Conselho Editorial

- André Palmieri – Divisão de Neurologia, PUC Porto Alegre, RS/Brasil.
- Áurea Nogueira de Melo – Departamento de Medicina Clínica, Centro de Ciências da Saúde, UFRN, Natal, RN/Brasil.
- Bernardo Dalla Bernardina – Università de Verona, Verona/Itália.
- Elza Marcia Yacubian – Unidade de Pesquisa e Tratamento das Epilepsias, Unifesp, São Paulo, SP/Brasil.
- Esper A. Cavalheiro – Departamento de Neurologia e Neurocirurgia, Unifesp, São Paulo, SP/Brasil.
- Fernando Tenório Gameleira – Programa de Cirurgia de Epilepsia do Hospital Universitário, UFAL, Maceió, AL/Brasil.
- Francisco José Martins Arruda – Departamento de Neurofisiologia Clínica, Instituto de Neurologia de Goiânia, Goiânia, GO/Brasil.
- Frederick Anderman – Montreal Neurological Institute, McGill University, Montreal/Canadá.
- Fulvio Alexandre Scorza – Neurologia Experimental, Unifesp, São Paulo, SP/Brasil.

- Gilson Edmar Gonçalves e Silva – Departamento de Neurologia, Faculdade de Medicina, UFPE, Recife, PE/Brasil.
- Íscia Lopes-Cendes – Departamento de Genética Médica, Faculdade de Ciências Médicas, Unicamp, Campinas, SP/Brasil.
- J. W. A. S. Sander – National Hospital for Neurology and Neurosurgery, London/UK
- Júlio Velluti – Instituto de Investigaciones Biológicas Clemente Estable, Montevideo/Uruguai
- Magda Lahorgue Nunes, PUC, Porto Alegre, RS/Brasil.
- Maria Carolina Doretto – Departamento de Fisiologia e Biofísica, ICB-UFMG, Belo Horizonte, MG/Brasil.
- Marielza Fernandez Veiga – Hospital Universitário “Edgard dos Santos”, UFBA, Salvador, BA/Brasil.
- Marilisa Mantovani Guerreiro – Departamento de Neurologia, Faculdade de Ciências Médicas, Unicamp, Campinas, SP/Brasil.
- Mirna Wetters Portuguez – Divisão de Neurologia, Departamento de Medicina Interna e

Pediatria, Faculdade de Medicina, PUC, Porto Alegre, RS/Brasil.

- Natalio Fejerman – Hospital de Pediatria “Juan P. Garrahan”, Buenos Aires/Argentina.
- Norberto Garcia Cairasco – Departamento de Fisiologia, Faculdade de Medicina, USP, Ribeirão Preto, SP/Brasil.
- Paula T. Fernandes – Faculdade de Educação Física, Unicamp, Campinas, SP/Brasil.
- Raul Ruggia – Hospital das Clínicas, Faculdade de Medicina, Montevideo/Uruguai.
- Roger Walz – Departamento de Clínica Médica, Hospital Universitário da UFSC, Centro de Cirurgia de Epilepsia de Santa Catarina (Cepesc), SC/Brasil.
- Shlomo Shinnar – Albert Einstein College of Medicine, New York/USA.
- Solomon L. Moshé – Albert Einstein College of Medicine, New York/USA.
- Wagner Afonso Teixeira – Serviço de Epilepsia e Eletroencefalografia, Hospital de Base de Brasília, Brasília, DF/Brasil.

## EXPEDIENTE

Editor Consultivo – Arthur Tadeu de Assis  
Editora Executiva – Ana Carolina de Assis

Editora Administrativa – Atha Comunicação Editora  
Contato – revistajecn@outlook.com

## Ficha Catalográfica

Journal of Epilepsy and Clinical Neurophysiology (Revista de Epilepsia e Neurofisiologia Clínica) / Liga Brasileira de Epilepsia. – Vol. 23, n.1, mar 2017.

v.1, 1995 – JLBE: Jornal da Liga Brasileira de Epilepsia

v.2 a 7 (n. 2, jun. 2001) Brazilian Journal of Epilepsy and Clinical Neurophysiology (Jornal Brasileiro de Epilepsia e Neurofisiologia Clínica)

Publicação trimestral.

ISSN 1676-2649

CDD: 616.8

CDU: 616.853(05)

616.8-092(05)

616.8-073(05)

### Índice para Catálogo Sistemático:

Epilepsia – Periódicos – 616.853(05);

Neurofisiologia – Periódicos – 616.8-092(5);

Eletroencefalografia – Periódicos – 616.8-073(05);

Eletroencefalografia – Periódicos – 616.8-073(05);

Neurologia – Fisiologia – Periódicos – 616.8-092(05).

O BRAINN Congress é um encontro que visa reunir pesquisadores e estudantes (graduação e pós-graduação) que trabalham em neurociência, neurotecnologia e áreas afins. O principal objetivo é promover comunicação e colaborações mais fortes, a fim de alcançar padrões de pesquisa de alta qualidade.

O Congresso é uma iniciativa do projeto BRAINN (*Brazilian Institute of Neuroscience and Neurotechnology*), que é um Centro de Pesquisa, Inovação e Disseminação (RIDC) da Fundação de Pesquisa de São Paulo (FAPESP). O BRAINN congrega pesquisadores de muitas áreas (neurologia, física, engenharia elétrica, psicologia, entre outros), provenientes principalmente da Universidade de Campinas - UNICAMP e do Centro de Tecnologia da Informação Renato Archer, que é um centro federal de pesquisa e desenvolvimento; mas também de outras instituições brasileiras, como Universidade Federal do ABC, Universidade Federal de São Paulo, Pontifícia Universidade Católica do Rio Grande do Sul, entre outras; bem como algumas instituições estrangeiras, como a Universidade de Montreal e University College London, entre outras.

Como o próprio nome indica o projeto BRAINN concentra-se na pesquisa científica básica em neurociência, juntamente com o desenvolvimento de tecnologias que podem auxiliar no diagnóstico, prognóstico e tratamento de doenças neurológicas, principalmente, mas não restrito a, epilepsia e acidente vascular cerebral.

Nesta edição do *Journal of Epilepsy and Clinical Neurophysiology* estamos publicando a segunda parte dos resumos do 4th BRAINN Congress de 2017.

---

# ABSTRACTS PRESENTED AT THE 4<sup>TH</sup> BRAINN CONGRESS BRAZILIAN INSTITUTE OF NEUROSCIENCE AND NEUROTECHNOLOGY (CEDIP-FAPESP) MARCH 27<sup>th</sup> TO 29<sup>th</sup> 2017 - CAMPINAS, SP, BRAZIL PART II

EVIDENCE OF AGE-RELATED MODULATION OF PARTIAL DIRECTED COHERENCE IN AREAS EXHIBITING CORTICAL THINNING.....	80
B. H. Vieira, C. E. G. Salmon	
IMPROVED SISCOM FOR MORE ACCURATE LOCATION OF SEIZURE-ONSET ZONE.....	80
L. S. Watanabe, S.T. Wu, B. J. Amorim	
GRAPH THEORY APPLIED TO A LONGITUDINAL STUDY OF PATIENTS WITH MILD COGNITIVE IMPAIRMENT AND ALZHEIMER'S DISEASE.....	81
S. C. Guzmán, M. Weiler, M. L. Balthazar, G. Castellano	
CAN DIFFERENT DISTRIBUTION OF NORMAL VARIATION IMPACT MOLECULAR TESTING IN THE CLINICAL CONTEXT? A STUDY IN THE BRAZILIAN POPULATION.....	81
C. S. Rocha, B. S. Carvalho, I. Lopes-Cendes *for the BIPMed Collaborative Group	
THE BRAZILIAN INITIATIVE ON PRECISION MEDICINE (BIPMED): IMPACT AFTER ONE YEAR.....	81
I. Lopes-Cendes, C. S. Rocha, W. Souza, B. S. Carvalho*for t he BIPMed Collaborative Group	
COMPARISON BETWEEN THREE DIFFERENT METHODS OF CO-REGISTRATION FOR AN OPEN SOURCE NEURONAVIGATION SYSTEM .....	82
F. S. Otsuka, R. H. Matsuda, V. H. Souza, O. Baffa	
A VOXEL BASED MORPHOMETRY STUDY OF TREATMENT-RESISTANT PATIENTS WITH GENERALIZED EPILEPSIES.....	82
M. S. Polydoro, D. S. Garcia, M. K. Alvim, A. Ishikawa, L. Montanher, M. E. Morita, F. Cendes, C. L. Yasuda	
DISTINCT FUNCTIONAL AND STRUCTURAL NETWORK ABNORMALITIES IN PATIENTS WITH FOCAL EPILEPSIES .....	83
Gonçalves, R.M., Campos, B.M., Cendes F , Coan, A.C.	
HOW A DRUG CAN MAKE YOUR BRAIN FORGET THE WORDS? A LANGUAGE FUNCTIONAL MRI STUDY WITH TOPIRAMATE IN EPILEPSY AND HEADACHE.....	83
A. Ishikawa, R. J. Mariano, B. M. Campos, T. M. Lopes, T. A. Zanão, B. Braga, D.S. Garcia, A. L. C. Costa, F. Cendes, C.L. Yasuda	
TRACT INTEGRITY ALTERATIONS THROUGHOUT LIFE SPAN .....	84
M. S. Pinto, B. H. Vieira, A. C. Santos, C. E. G. Salmon	
ASSOCIATIONS BETWEEN ENVIRONMENTAL FACTORS AND DEFAULT MODE NETWORK DEVELOPMENT DURING CHILDHOOD.....	84
K. Rebello, J. R. Sato	
THE IMPACT OF HIPPOCAMPAL ATROPHY ON BRAIN ATROPHY: SIDE MATTERS .....	85
J.C.V. Moreira, M.K. Alvim, G. Artoni, A. Ishikawa, D. S. Garcia, B.M. Campos, M. E. Morita, F. Cendes, C. L. Yasuda	
A METHOD FOR EXTRACTION OF CORPUS CALLOSUM'S SHAPE SIGNATURE.....	85
W. G. Herrera, A. Costa, L. Rittner	
TOPOGRAPHY OF BRAIN ATROPHY IN HUNTINGTON'S DISEASE: A VOXEL-BASED MORPHOMETRY STUDY .....	85
J. Guitti, P.C. Azevedo, I.Cendes, C.Yasuda <sup>1</sup> , F.Cendes,	
OPERATIONAL AND STRATEGIC MENTAL MODELS REVEAL DIFFERENT BRAIN ACTIVATION.....	86
G. S. Spagnol, L. M. Li	
IMU HEAD TRACKING WITH FIXED PAN-TILT LASER FOR WHEELCHAIR NAVIGATION.....	86
G. M. Pereira <sup>1</sup> , E. Rohmer <sup>1</sup>	
ABNORMAL INTER-INTRANETWORK CONNECTIVITY IN PATIENTS WITH GENERALIZED EPILEPSIES .....	87
D. S. Garcia, M. Polydoro, M. K. Alvim, A. Ishikawa, B. M. Campos, L. L. Montanher, M. E. Morita, F. Cendes, C. L. Yasuda	
CORTICAL SURFACE ANALYSIS IN PATIENTS WITH GENERALIZED EPILEPSIES .....	87
D. S. Garcia, M. K. Alvim, M. Polydoro, A. Ishikawa, L. L. Montanher, M. E. Morita, F. Cendes, C. L. Yasuda	
CONTRALATERAL HIPPOCAMPAL ATROPHY AFTER TEMPORAL LOBE SURGERY: VOLUMETRIC ANALYSIS OF PREOPERATIVE AND LONG-TERM POSTOPERATIVE MRI .....	88
B. F. Silva, A. Ishikawa, I. Amaral, D. S. Garcia, Morita, M. E. Alvim, M.K. Ghizoni, E. Tedeschi, H. F. Cendes, C. L. Yasuda	

POSTOPERATIVE DYNAMIC CHANGES ON CONTRALATERAL HIPPOCAMPUS: MANUAL VOLUMETRY AND RELAXOMETRY ANALYSES .....	88
I. Amaral, B. F. Silva, A. Ishikawa, D. S. Garcia, M. E. Morita, M.K. Alvim, E. Ghizoni, H. Tedeschi, F. Cendes, F. C. L. Yasuda	
VIDEO AND KNOWLEDGE STRUCTURE FOR AN AUDIOVISUAL SYSTEM BASED ON ANIMATIONS TO SUPPORT LEARNING ABOUT EPILEPSY .....	89
F. N. Akhras, C.S.M. Castro, L. S. M. Pereira, G. S. A. Nascimento, T. E. Hatta	
COMPUTER AIDED DESIGN FOR TRANSPOSING A 2D BRAIN MODEL INTO A 3D EDUCATIONAL OBJECT .....	89
C. Rondinoni, J. H. Barbosa, A. C. dos Santos, C. E. G. Salmon, E. Amaro	
TRANSCRIPTOME PROFILE OF HIPPOCAMPUS CA3 IN THE PILOCARPINE MODEL OF TEMPORAL LOBE EPILEPSY.....	90
H. B. Matos, A. S. Vieira, A. M. Canto, S. C. R. B. Carvalho, V. D. B. Pascoal, R. Glioli, I. Lopes-Cendes	
SEGMENTATION OF CORTICAL CYTOARCHITECTONICS FROM IN WHOLE BRAIN THICK NISSL SECTIONS.....	90
C. Rondinoni, E. Alho, H. Heinsen, L. Grinberg, E. Amaro Jr	
MCP-1 IS RELATED WITH FUNCTIONAL CONNECTIVITY AND PHOSPHO-TAU PROTEIN IN AMNESTIC MILD COGNITIVE IMPAIRMENT .....	90
T. N. C. Magalhães, C.V. L. Teixeira, M. Weiler, B. M. de Campos, A. Moraes, V. O. Boldrini, L. M. B. Santos, L. Talib, O. Forlenza, F. Cendes, M. L. F. Balthazar	
OPEN SOURCE WEB-BASED TOOL FOR SELECTION OF THE SPECTRA OF INTEREST ON MAGNETIC RESONANCE SPECTROSCOPY IMAGING (MRSI) .....	91
D. P. Rodrigues, S. Appenzeller, L. Rittner	
MULTIMODAL VISUALIZATION OF DTI GLYPHS FOR DIFFUSIVITY TENSOR ASSESSMENT .....	91
R. Voltoline, C.L. Yasuda, S-T. Wu	
SEIZURE CONTROL AND HIPPOCAMPAL SCLEROSIS ARE RELATED TO METABOLIC ALTERATIONS IN MESIAL TEMPORAL LOBE EPILEPSY .....	92
L.R. Pimentel-Silva, R.F. Casseb, M.K.M. Alvim, R. Barbosa, N. Volpato, M.H. Nogueira, C.L. Yasuda, F. Cendes	
IDENTIFICATION OF THE DISTRIBUTION OF HLA ALLELES IN THE BRAZILIAN POPULATION AND IN NEUROLOGICAL PHENOTYPES POSSIBLY ASSOCIATED WITH AUTOIMMUNITY.....	92
T. K. de Araujo, N. Watanabe, R. Barbosa, F. Cendes, I. Lopes-Cendes	
DETERMINING THE BURDEN OF COPY NUMBER VARIATION IN PATIENTS WITH EPILEPSY .....	93
T. K. de Araujo, F. R. Torres, R. Secolin, M. K. M. Alvim, C. S. Rocha, M. E. Morita, C.L. Yasuda, B. S. Carvalho, F. Cendes, I. Lopes-Cendes	
<sup>1</sup> H-MAGNETIC RESONANCE SPECTROSCOPY IN THE RAT MODEL OF TEMPORAL LOBE EPILEPSY INDUCED BY PERFORANT PATHWAY STIMULATION .....	93
R. Barbosa, A. H. B. Matos, B. M. Campos, R. F. Casseb, L. R. Pimentel-Silva, J. Francischinelli, M. M. Cordeiro, R. Glioli, I. Lopes-Cendes, A. S. Vieira, F. Cendes	
AEROBIC PHYSICAL EXERCISE PROGRAM CAN IMPROVE QUALITY OF LIFE IN PATIENTS WITH TEMPORAL LOBE EPILEPSY .....	94
N. Volpato, J. Kobashigawa, C.L. Yasuda, F. Cendes	
EFFECTS OF AEROBIC EXERCISE ON PROGRESSION OF HIPPOCAMPAL VOLUME AND COGNITION IN AMNESTIC MILD COGNITIVE IMPAIRMENT DUE TO AD .....	94
B. V. L. Teixeira, T. J. Rezende, T. N. Magalhães, M. Weiler, A. F. M. K. C. Cassani, D. Q. de Almeida, T. Q. A. C. Silva, H. P. G. Joaquim, L. L. Talib, O. V. Forlenza, M. P. Franco, P. E. Nechio, P. T. Fernandes, F. Cendes, M. L. F. Balthazar	
EFFECT OF ORTHOGRAPHIC NEIGHBORHOOD DENSITY IN READING .....	94
K. Lukasova, T. Vasconcelos, D. Gomes, E. Amaro	
PREDICTION OF TEMPORAL DECISION BASED ON ELECTROPHYSIOLOGICAL ACTIVITY OF RATS PRE-FRONTAL CORTEX .....	95
G. C. Tunes, M. B. Reyes, D. C. Soriano	
COMPUTATION OF BRAIN MIDSAGITTAL PLANE THROUGH DTI-BASED DIVERGENCE MAP .....	95
G. R. Pinheiro, G. S. Cover, L. Rittner	
APPLICATION AND CHARACTERIZATION OF NEURAL PROBES.....	96
E. V. Dias, A. S. Vieira, R. Panepucci, R. Covolan, I. T. L. Cendes, F. Cendes	
MOTOR ADAPTATION THROUGH THE PREDICTIVE SACCADDES: FMRI STUDY OF THE EYE MOVEMENTS.....	96
T. Vasconcelos, D. Gomes, E. Amaro, K. Lukasova	
E-STREET VIRTUAL REALITY FOR SPATIAL ORIENTATION IN URBAN ENVIRONMENT .....	97
A. F. Brandão, D. R. C. Dias, G. G. Paiva, M. P. Guimarães, L. C. Trevelin, G. Castellano	
FUNCTIONAL CONNECTIVITY OF DEFAULT MODE NETWORK IN ISCHEMIC STROKE: A PROSPECTIVE STUDY .....	97
J. E. Vicentini, S.R.M. de Almeida, B.M. de Campos, L. Valler, L. M. Li	



COMMON CAROTID LUMEN SEGMENTATION USING CINE FAST SPIN ECHO MAGNETIC RESONANCE IMAGING.....	97
L. Rodrigues, R. Souza, L. Rittner, Richard Frayne, R. Lotufo	
A FEASIBILITY EVALUATION OF EEG DATA ACQUIRED USING A NEUROFEEDBACK TRAINING INTERFACE: PRELIMINARY RESULTS .....	98
L. T. Menezes, C. A. Stefano Filho, G. Castellano	
DEFAULT MODE NETWORK IN TLE PATIENTS WITH AND WITHOUT HIPPOCAMPAL ATROPHY .....	98
T. A. Zano, T. M. Lopes, B. M. Campos, M. H. Nogueira, C. L. Yasuda, F. Cendes	
CORTICAL SURFACE ANALYSIS IN PARKINSON DISEASE PATIENTS.....	99
R. Guimarães, L. Campos, L. Piovesana, P. Azevedo, C. Yasuda, J. C. Moreira, D. Garcia, A. D'Abreu, F. Cendes	
BICLUSTERING IN THE ANALYSIS AND IDENTIFICATION OF BIOMARKERS .....	99
R. Veroneze, F. J. Von Zuben	
MOTION ARTIFACTS AND SLICE TIMING CORRECTION CAN INFLUENCE BOLD RESTING STATE RESULTS .....	99
W. A. A. Rocha, A. C. Carvalho, S. L. Novi, R. M. Forti, A. Quiroga, M. M. Cordeiro, C. L. Yasuda, R. C. Mesquita, A. Saa	
ORTHOSTATIC TREMOR: A CASE REPORT .....	100
A.R. Coimbra Neto, P. C. Azevedo, L. G. Piovesana	
MULTIELECTRODE ARRAYS FOR CELL POTENTIAL MEASUREMENTS: TESTING NOVEL INSULATING LAYER BETWEEN ELECTRODES AND CULTURE.....	101
V. P. Gomes, A. D. Barros, J. B. Destro-Filho, J. W. Swart	
HIERARCHICAL OBSERVATION MODELING IN FMRI: SLIDING WINDOW 2.0.....	101
R. F. Casseb, A. Sojoudi, G. Castellano, M. C. França Jr, B. Goodyear	
PYTHON-BASED VIRTUAL KEYBOARD DESCRIPTIVE LANGUAGE INTERPRETER.....	101
R. C. V. Dias, J. R. Oliveira, M. B. Pelosi	
WIRELESS DEEP BRAIN STIMULATION DEVICE WITH INTEGRATED ANTENNAE.....	102
E. Borba, C. Santos, C. Kemere, R.R. Panepucci	
SU-8 NEURAL PROBES ARE OPTIMIZED FOR SINGLE UNIT RECORDINGS IN OPTOGENETIC EXPERIMENTS .....	102
A. H. Malavazi, T. Malfatti, R. M. Covolan, K. E. Leão, R. N. Leão, R. R. Panepucci	
INVESTIGATING THE GENETIC LANDSCAPE OF CHILDHOOD EPILEPTIC ENCEPHALOPATHIES IN LATIN AMERICA .....	103
H. Urquía-Osorio, F. Cendes, I. Lopes-Cende	
A MODEL FOR DIAGNOSTIC DECISION SUPPORT IN MENTAL HEALTH THROUGH THE ANALYSIS OF VARIABLES OF DIFFERENT KINDS.....	103
I. Carvalho, J. L. G. Rosa, C. M. Del-Ben, R. Shuhama, C. M. Loureiro, P. R. Menezes	
VIRTUAL REALITY AS AN ADD ON REHABILITATION THERAPY IN PATIENTS AFTER ISCHEMIC STROKE.....	104
A. F. B. Camargo <sup>12</sup> , L. M. Li <sup>12</sup>	
EFFECTS OF SUB-CONVULSIVE DOSES OF PENTYLENETETRAZOLE DURING ZEBRAFISH BRAIN DEVELOPMENT .....	104
T. G. Parolari, V. Fais, J. E. Cavazos, V. Maurer-Morelli	
FUNCTIONAL STUDIES OF SCN1A MUTATIONS .....	104
Saul, Lindo-Samanamud, A. S. Vieira, F. R. Torres, M. C. Gonsales, F. Cendes, Lopes-Cendes	
PERCEPTIONS OF STIGMA DURING DISCLOSURE AMONG PATIENTS WITH EPILEPSY IN DIFFERENT LIFE SCENARIOS.....	105
C. Y. Tagami, G. S. Spagnol, L. M. Li	
HUMAN-COMPUTER INTERFACE USING FACIAL EXPRESSIONS: A SOLUTION FOR PEOPLE WITH MOTOR DISABILITIES .....	105
Suzana Viana Mota <sup>1</sup> , Eric Rohmer <sup>1</sup>	
HIPPOCAMPAL VOLUME AND FUNCTIONAL CONNECTIVITY PREDICTS FUNCTIONAL DECLINE IN MILD AD AND AMCI .....	105
N. Lecce, C. V. L. Teixeira, T. N. C. Magalhães, A. F. M. K. C. Cassani, M. Weiler, B. Campos, T. J. R. Rezende, L. L. Talib, O. V. Forlenza, F. Cendes, M. L. F. Balthazar	
STUDY OF THE TECHNIQUE OF MAGNETIC RESONANCE SPECTROSCOPIC IMAGING (MRSI) AND APPLICATION TO EVALUATION OF BRAIN METABOLITES OF SYSTEMIC LUPUS ERYTHEMATOSUS PATIENTS .....	106
J. Horvath, D. R. Pereira, L. Rittner, S. Appenzeller, G. Castellano	
HUMAN PROSTHETIC HAND INTERACTION BASED ON ELECTROMYOGRAPHY AND IMAGE RECOGNITION.....	106
A. Ishikawa, A. D. Muñoz, D. T. G. Andrade, E. Rohmer	

# ABSTRACTS PRESENTED AT THE 4<sup>TH</sup> BRAINN CONGRESS BRAZILIAN INSTITUTE OF NEUROSCIENCE AND NEUROTECHNOLOGY (CEDIP-FAPESP)

MARCH 27<sup>th</sup> TO 29<sup>th</sup> 2017 - CAMPINAS, SP, BRAZIL

## PART II

### EVIDENCE OF AGE-RELATED MODULATION OF PARTIAL DIRECTED COHERENCE IN AREAS EXHIBITING CORTICAL THINNING

B. H. Vieira<sup>1</sup>, C. E. G. Salmon<sup>2</sup>

<sup>1</sup>InBrain Lab, Department of Physics, FFCLRP, Universidade de São Paulo, São Paulo, SP, Brazil.

**Introduction:** Partial Directed Coherence (PDC) is a brain connectivity estimator sharing characteristics with Granger causality testing, but instead operating in the frequency domain<sup>1</sup>. It is hypothesized age-related cortical atrophy happens mainly due to neuronal and dendritic architectural reorganization<sup>2</sup>, and not neuronal death. This process might correlate with plasticity, and could have implications on functional dynamics, which are associated to PDC measurements. This work explores the interaction between PDC and age in areas showing age-related thinning. **Materials and Methods:** Resting-state fMRI (TR = 2500 ms, 260 volumes) and anatomical 3D-T<sub>1</sub>-W 3T images of 130 right-handed adult subjects were obtained from a database maintained by the NKI<sup>3</sup>. Anatomical images were processed in FreeSurfer's v5.3.0 default recon-all application. Functional images were preprocessed in CONN v16.b default surface-based preprocessing routine. First-level covariates were regressed out of the timeseries, including the 6-degree rigid body movement parameters and scrubbing. Images were also filtered, detrended and denoised. Three ROIs that exhibited thinning most correlated with aging and their contralateral correspondence were picked for further analysis. PDC was estimated for these ROIs in all subjects using a MVAR(30) model and its spectral energy density was evaluated at six frequencies in the interval between 0.008-0.09 Hz due to preprocessing temporal filtering. Linear regression was performed with PDC against age allowing unique intercept and slope for each sex. Due to the dependence between tests, the heuristic proposed by Li & Ji<sup>4</sup> was used to estimate an effective number of independent tests. **Results:** Contralateral postcentral and precuneus gyri and superior temporal sulci were selected as ROIs. The number of effective independent tests was estimated as 16. The PDC bandlimited spectral energy from the left postcentral gyrus to the right superior temporal sulcus showed positive age coefficient significantly different from zero ( $P_{adj} = 0.0383$ ), with small effect size,  $R^2 = 0.0794$ , 95% bootstrapped CI [0.0187, 0.2263]. Other connections exhibited a moderate effect of age, but no significance was observed. No significant effect of sex was attested. **Discussion:** Postcentral gyri make up the primary somatosensory cortex while superior temporal sulci are multisensory areas implicated in auditory processing, face recognition, and social perception<sup>5</sup>, which are susceptible to aging. Multisensory integration is enhanced in older adults<sup>6,7</sup>. Aging is correlated with increased internetwork connectivity<sup>8</sup>. These observations are convergent with our findings. Moreover, even though no significance was found, some patterns are observable in the coefficients, indicating decreased PDC to the postcentral gyri and increased PDC to the superior temporal sulci. **Conclusion:** Our work implies age modulates functional dynamics as measured by PDC in areas exhibiting cortical thinning. In special, sensory processing and integration areas show altered dynamics with aging, leading to prospective implications in the study of neurodegenerative diseases and neurodevelopmental disorders.

**References:** [1] Baccalá LA, et al. *Biol Cybern*. 2001;84(6): 463-74; [2] Freeman SH, et al. *J Neuropathol Exp Neurol*. 2008;67(12):1205-12; [3] Nooner KB, et al. *Front Neurosci*. 2012;6:152; [4] Li J, Ji L. *Heredity*. 2005;95(3): 221-7; [5] Hein G, Knight RT. *J Cogn Neurosci*. 2008;20(12): 2125-36; [6] Freiherr J, et al. *Front Hum Neurosci*. 2013;7:863; [7] Mozolic JL, et al. *The Neural Bases of Multisensory Processes*. 2012;1-12; [8] Ferreira LK, et al. *Cereb Cortex*. 2016;26(9): 3851-65.

### IMPROVED SISCOM FOR MORE ACCURATE LOCATION OF SEIZURE-ONSET ZONE

L. S. Watanabe<sup>1,3</sup>, S.T. Wu<sup>1</sup>, B. J. Amorim<sup>2</sup>

<sup>1</sup>Computer Engineering and Automation Dept., FEEC, UNICAMP; <sup>2</sup>Division of Nuclear Medicine, FCM, UNICAMP; <sup>3</sup>Clinics Hospital of the University of Campinas.

**Introduction:** Patients with drug resistant epileptic seizures are candidate to surgery resection of the epileptogenic focus. For removing the seizure-producing area from the brain and limiting the spread of seizure activity, its precise localization is essential. SISCOM (Subtraction Ictal SPECT Co-registered to MRI)<sup>1</sup> is a known efficient technique for identifying the epileptogenic focus including cases of nonlesional and extra-temporal MRI-negative epilepsies. This technique takes advantage of transient focal increase in cerebral blood flow during a seizure in comparison with the hypoperfusion or normoperfusion during the interictal state. Both states are captured by SPECT (Single-Photon Emission Computed Tomography) scans. We improved the flow of the algorithm presented in<sup>2</sup> by improving the rigid co-registration and the skull stripping. **Materials and Methods:** The T1-weighted MRI and the ictal and interictal SPECT exams were acquired, respectively, in the Philips Achieva 3T and in the Siemens Symbia T scanners. The original SISCOM algorithm from Mayo Foundation comprises 6 steps, of which two have been improved: 1) noise removal is performed with a brain extraction tool ROBEX<sup>2</sup> rather than threshold-based filtering, therefore original SISCOM brain segmentation and hole filling steps could be bypassed in our approach; 2) ictal SPECT, interictal SPECT and MRI coregistration is performed with an improved mutual information based technique<sup>4</sup> that was validated with the Vanderbilt Database<sup>5</sup>, so the subtraction of the ictal and interictal states becomes more accurate. **Results:** The preoperative T1-weighted MRI-negative exam of a patient with histologically proven Type IIa focal cortical dysplasia is shown in Figure (b). The normalized interictal and the ictal SPECT volumes are presented, respectively, in Figure (c) and (d). They are colored with rainbow palette, where the red color indicates high perfusion and the blue low perfusion. The subtraction of these two volumes is depicted in Figures (e,f) in which the epileptogenic focus in the right mesial frontal lobe becomes visually perceptible. This finding agrees with the medical signs and other exams as electroencefalography. Note that Figure (f) shows the difference volume fused with MRI for anatomical reference. Figure (g) shows the postoperative T1-weighted MRI scan of the resected region which has been submitted to pathological analysis. **Discussion:** Improving the brain extraction and the co-registration of multimodal volumes leads more precise outcome in the difference of SPECT ictal and interictal. When co-registered with an anatomical reference the lesion location can be assessed more accurately. **Conclusion:** This improved subtraction algorithm has shown promising results. However, it is important to assess its clinical value in the detection of subtle lesions.

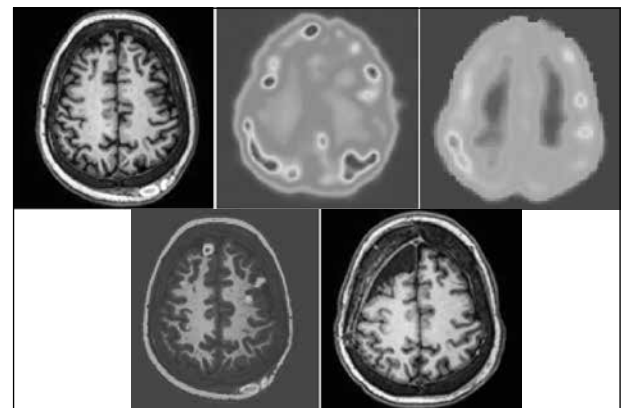


Figure 1.

**References:** [1] O'Brien TJ, et al. *Neurology*. 1998;50(2):445-54; [2] Roy S, et al. 8th ICAPR, Kolkata. 2015;1-6; [3] Available: [http://www.synapticon.net/images/pdf/SISCOM\\_V\\_4.0.pdf](http://www.synapticon.net/images/pdf/SISCOM_V_4.0.pdf); [4] Ting WS, et al. *SIBGRAP*. 2014;41-8; [5] Available: <http://www.insight-journal.org/tire/>



**GRAPH THEORY APPLIED TO A LONGITUDINAL STUDY OF PATIENTS WITH MILD COGNITIVE IMPAIRMENT AND ALZHEIMER'S DISEASE**S. C. Guzmán<sup>1,2</sup>, M. Weiler<sup>1,2</sup>, M. L. Balthazar<sup>2,3</sup>, G. Castellano<sup>1,2</sup><sup>1</sup>Neurophysics Group, IFGW, UNICAMP; <sup>2</sup>Brazilian Institute of Neuroscience and Neurotechnology, BRAINN, Campinas, SP, Brazil; <sup>3</sup>Laboratory of Neuroimaging, FCM, UNICAMP, Campinas, SP, Brazil.

**Introduction:** This study united the capabilities of graph theory, the resting state functional connectivity (RS-fMRI) technique and the abundant need for more longitudinal research of Alzheimer's Disease (AD). Previous studies have generally found AD brain networks with decreased information processing efficiency and more susceptibility to attacks, supporting the notion of AD as a disconnection syndrome<sup>1,2</sup>. The main objective of this study was to track changes in the topological configuration of the functional connectivity of patients with AD and mild cognitive impairment (MCI). **Materials and Methods:** All images were acquired in a 3T scanner (Philips Achieva). Structural images: sagittal T1-weighted, TR 7 ms, TE 3.2 ms, FOV 240×240 mm<sup>2</sup>, and isotropic voxels of 1 mm<sup>3</sup>. Functional images: EPI axial T2\*-weighted, 180 volumes, 40 axial slices, TR 2s, TE 30 ms, same FOV, and isotropic 3 mm<sup>3</sup> voxels. Subjects were instructed to keep their eyes closed, remain awake and avoid initiating goal-directed, attention demanding activity. The participants in the first examination were 15 healthy controls (C) (12 female (f), 69 ± 6 (std. dev.) y.o.), 22 MCI patients (14 f, 70 ± 6 y.o.), and 14 AD (9 f, 73 ± 8 y.o.). For the second examination, as some participants changed diagnosis, 14 C (11 f, 70 ± 6 y.o.), 21 MCI (14 f, 71 ± 6 y.o.), and 16 AD (10 f, 74 ± 8 y.o.). Average time between acquisitions 52 ± 30 weeks. Image preprocessing used the CONN toolbox (www.nitrc.org/projects/conn). Steps were realignment and unwarp, coregistration, normalization, segmentation, smoothing (FWHM 6 mm), and scrubbing of flagged volumes. Later, confound regression, temporal band pass filtering (0.008-0.08 Hz) and a mask of 264 regions of interest [3] were applied. The Pearson correlation was calculated for pairs of the resulting time series. Short distance correlations (<20 mm) were discarded. Using GraphVar (www.nitrc.org/projects/graphvar), degree, characteristic path length, local efficiency, clustering coefficient, betweenness centrality, and small world coefficient were calculated for several correlation thresholds (0.05-0.26). Mixed effects linear models were applied with fixed effects for diagnostic group, education and time between acquisitions; intercepts had the individuals as random effects. Confound variables age and integrated movement parameter were also tested. Multiple comparisons correction for FDR was done with the Benjamini-Hochberg-Yekutieli procedure. **Results:** Global metrics showed no significant differences between the groups; their variances could be further explored but were also not significant. Local efficiency in some nodes at the cingulate cortex could be modeled as a response to the disease stage, but was not significant. **Discussion:** The results found were probably due to the difficulty in global functional connectivity measures to reflect the differences due to AD and MCI. Previous results might have been due to movement artifacts that were not appropriately accounted for. Changes in functional connectivity as the disease progresses seem to follow a localized pattern that is nonetheless hard to track. **Conclusion:** Designs hoping to extract graph metrics useful for longitudinal studies should strive for greater power and more observations if they want to track changes. Other local metrics should be explored and the acquisitions and quality control could be improved to better counter known artifacts.

**References:** [1] Guye M, et al. Magn Reson Mater. Phys Biol Med. 2010;23(5-6):409-21; [2] Tijms BM, et al. Neurobiol Aging. 2013;34(8):2023-36; [3] Power JD, et al. Neuron. 2011;72(4):665-78.

**CAN DIFFERENT DISTRIBUTION OF NORMAL VARIATION IMPACT MOLECULAR TESTING IN THE CLINICAL CONTEXT? A STUDY IN THE BRAZILIAN POPULATION**C. S. Rocha<sup>1</sup>, B. S. Carvalho<sup>2</sup>, I. Lopes-Cendes<sup>1</sup> \*for the BIPMed Collaborative Group<sup>1</sup> Department of Medical Genetics, School of Medical Sciences; <sup>2</sup> Department of Statistics, Institute of Mathematics, Statistics and Scientific Computing; University of Campinas, UNICAMP and the Brazilian Institute of Neuroscience and Neurotechnology, Campinas, SP, Brazil.

**Introduction:** Precision Medicine (PM) has emerged recently as a concept in which scientific knowledge and technology will come together to provide the basis for the 21st century medicine. In order to implement PM it is important to determine the normal genetic profile of a population since genetic distribution of rare and common variants can have a significant impact in determining the

overall effect of a specific mutation in different population. In addition, due to the historic and demographic constitution of the Brazilian population, it is reasonable to assume that one will find a significant source of genomic diversity which is important for studies aiming to disclose the true genomic viability of the human genome, both in normal and disease states. Therefore, we aim to determine the genomic profile of Brazilian individuals and compared it with data available from other population. **Materials and Methods:** We performed Whole Exome Sequencing (WES) in 106 subjects and Affymetrix 6.0 SNP-array in 264 individuals. These are normal/reference individuals from the region of Campinas, SP, Brazil. Genomic data produced was deposited in two public databases (www.bipmed.org) which are part of the Brazilian Initiative on Precision Medicine. We used the Leiden Open Variation Database (LOVD)<sup>1</sup> for data storage and display. Alternative allele frequencies (AAF) were calculated for each variant in both datasets. In the SNP-array study we compared the frequency from 4 populations (CEU - Northern Europeans from Utah; CHB - Han Chinese in Beijing; JPT - Japanese in Tokyo; YRI - Yoruba in Ibadan) which is provide by the array manufacturer. We compared population allele frequencies using PCA. **Results:** In the WES study we found 624,137 different variants (SNVs and INDELs) from 19069 genes, among them 68,149 (10.9%) were not detected in any other studies. Furthermore, 45.51% of the variants detected have AAF of less than 1%, 22.44% of the variants have AAF between 1% and 5%, 7.5% have AAF bigger than 50% and 0.3% have AAF equal to 100%. In the SNP array study the correlation analysis and the PCA showed that our data have a greater proximity to the CEU population and it is more distant from CHB, JPY and has less similarity with YRI. Of the 906600 SNPs present in the array we identified 119 SNPs with a difference of at least 80% in the frequency of the alternative allele compared to any of the 4 populations, which results in a reversal of the allele frequency. As an example, SNP rs5910927 have AAF equals to 0.10 in our data-set, 0.95 in the CEU population, 1.00 in the CHB population, 0.93 in the JPT population and 0.85 in the YRI population. **Discussion and Conclusion:** Because WES and SNP-arrays interrogate different genomic variants; they may reveal different aspects of genomic variability. Our results clearly indicate that there are differences in the genomic distribution of both rare and common variants in Brazilian individuals as compared to other populations, and that none of the 4 reference populations can be used as surrogates for studies in Brazilian individuals. In the WES dataset we found a large number of variants that have never been identified in any other population, including 41 variants with AAF equal to 100% in the 106 Brazilian reference individuals. The SNP array study shows clearly that AAF derived from other populations may not be reliable parameters for studies in Brazilian individuals. In conclusion, our results clearly demonstrate the importance of constructing a larger and geographically diverse panel of reference genomic datasets for both rare and common variants in the Brazilian population. This initiative should be the first step in order to provide the basis for the implementation of Precision Medicine in Brazil.

**References:** [1] Fokkema IF, Taschner PE, Schaafsma GC, Celli J, Laros JF, den Dunnen JT. LOVD v2.0: the next generation in gene variant databases. Hum Mutat. 2011;32(5):557-63.

**THE BRAZILIAN INITIATIVE ON PRECISION MEDICINE (BIPMED): IMPACT AFTER ONE YEAR**I. Lopes-Cendes<sup>1</sup>, C. S. Rocha<sup>1</sup>, W. Souza<sup>1</sup>, B. S. Carvalho<sup>2</sup> \*for the BIPMed Collaborative Group<sup>1</sup> Department of Medical Genetics, School of Medical Sciences; <sup>2</sup> Department of Statistics, Institute of Mathematics, Statistics and Scientific Computing; University of Campinas; UNICAMP and the Brazilian Institute of Neuroscience and Neurotechnology, Campinas, SP, Brazil.

**Introduction:** The BIPMed genomic database is the first product released by our initiative to fulfill the increasing need for publicly available genetic and genomic information about the Brazilian population. It was implemented by following the guidelines and principles of the Global Alliance for Genomics and Health - GA4GH<sup>1</sup> (genomicsandhealth.org/) observing the responsible sharing of genomic and clinical data. It is also part of the Beacon Project of the GA4GH, which is a data discovery engine that allows the user to identify if a mutation has been observed before in the world. One year after launching the database we have been receiving access worldwide and have recently joined the Human Variome Project (www.humanvariomeproject.org). The main goal of BIPMed is to create tools to promote and facilitate the sharing of genomic and clinical

data, thus contributing to the advancement of disease treatment and creating a favorable environment for the implantation of precision medicine in Brazil. **Materials and Methods:** BIPMed is based on a software platform, the Leiden Open Variation Database<sup>2</sup>, it is a fully web-based gene sequence variation database. Two reference databases are already on line, the BIPMed-WES-db, provides information obtained from Whole Exome Sequencing experiments and includes 106 subjects and the BIPMed-Array-db, contemplates 264 individuals and data was obtained from microarray-based experiments (Affymetrix GenomeWide SNP 6.0 array). The beacon was installed and filled with the VCF (Variant Call Format) files with the variants, a process called lighting a beacon. We also developed a Bioconductor package that provides an easy way to access public data servers through GA4GH Genomics API, this package provides an interactive web application and a R command line interface. **Results:** The BIPMed-WES-db reference databases identified 624.137 different variants from 19069 genes. So far our databases received identified access from 90 different countries with an average of 144 daily accesses, with peaks of up to 800 in a single day. Recently, we have also start to include patient data so we will soon launch two additional cohorts, one for Epileptic Encephalopathies and the other for Craniofacial Anomalies. **Discussion and Conclusion:** Data sharing encourages the reuse of data in a number of other studies, favors the reproducibility of research, saving time and resources. However, it is imperative that it is done in a responsible and ethical way; and with appropriate security. It is also essential to follow international naming and terminology standards and to be integrated with other databases. Our biggest challenge now is to expand this database, so it is important to have the participation of additional research groups in order to become a reference for data sharing for different populations in Latin America.

**References:** [1] The Global Alliance for Genomics and Health; Science. 2016;352(6291):1278-80; [2] Fokkema IF, Taschner PE, Schaafsma GC, Celli J, Laros JF, den Dunnen JT. LOVD v2.0: the next generation in gene variant databases. Hum Mutat. 2011;32(5):557-63.

#### COMPARISON BETWEEN THREE DIFFERENT METHODS OF CO-REGISTRATION FOR AN OPEN SOURCE NEURONAVIGATION SYSTEM

F. S. Otsuka<sup>1</sup>, R. H. Matsuda<sup>1</sup>, V. H. Souza<sup>1</sup>, O. Baffa<sup>1</sup>

<sup>1</sup>Laboratório de Biomagnetismo, DF, FFLRP, USP-RP.

**Introduction:** Neuronavigation systems are used in clinical procedures to locate internal structures in human body with real time visualization of tomographic images<sup>1</sup>. In this case, a link between a spatial tracking device space and the medical image space is made by a mathematical equation. This link is called co-registration, and it is highly sensitive to errors due to acquisition of misplaced points and differences in morphology of target objects. Conventional co-registration method is the point-based registration (PBR) that uses three fiducial points to generate a change between two spaces of coordinates<sup>2</sup>. This study proposes three different methods of registration to reduce the registration error (FRE) and thus improve the navigation accuracy of the InVesalius Navigation software developed by our group. **Materials and Methods:** Scripts were written in Python 2.7 and the PATRIOT device (Polhemus, USA) was used for coordinate registration. First method is a modified point-based registration (PBRm) and consists on selecting four fiducial points, test all combinations in groups of three and take the one with the least FRE. The second method, based on the Iterative Closest Points (ICP) algorithm, consists on minimizing the least square distance between two distinct point clouds and then matches them. The third method was based on a rigid transformation (RT) principle, and consists on obtaining a rotation and a translation matrix to take the coordinates from the tracker space to the image space. **Results:** First, four points were used for all three methods resulting in a FRE of 1.70 mm computed in 3.00 ms for the PBRm and in a FRE of 3.93 mm (computed in 4.00 ms) and 4.58 mm (computed in 25.00 ms) for the ICP and RT methods with four points (ICPf and RTf) respectively. Then, the points were combined in groups of three points (Group 1: points 1, 2, 3; Group 2: points 1, 2, 4; Group 3: points 1, 3, 4; Group 4: points 2, 3, 4). The FRE for ICP and RT tested with groups of three points (ICPt and RTt) were displayed on Table 1 (left) so as the time for computing. **Discussion:** The ICPt and RTt methods showed the least FRE, followed by PBRm, ICPf and the RTf. The high value of FRE for the ICPf and RTf can be explained by the fact that all points contribute to the FRE, thus if one

them has a great displacement it may increase the overall error. This may be solved by recollecting the point with great displacement or by using fiducial markers instead anatomical markers to give us more accuracy during points acquisition<sup>3</sup>. As for the ICPt and RTt, each group had a different set of points, thus resulting in the different values of FRE. Besides, the groups with the most displaced point resulted in a higher FRE (around 60% higher than the lower FRE). **Conclusion:** Our study assessed the FRE of three different co-registration methods. ICPt and RTt showed the best FRE and may be suitable for co-registration in neuronavigation. However, alternative methods should be further investigated towards less sensibility to small variations in fiducial selection and sub millimetric registration errors.

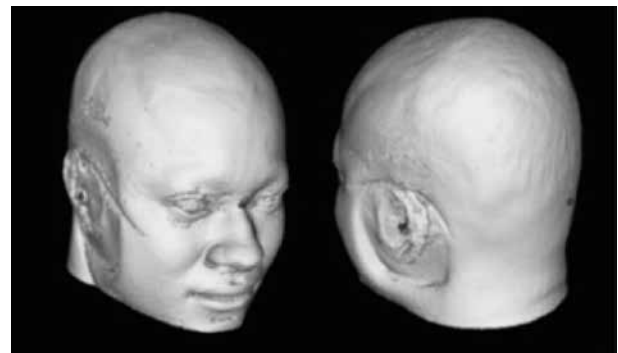


Figure 1. ICP method with 4 fiducials.

Table 1. Values of FRE and time for each method.

		Methods		
		PBR	ICPt	RTt
FRE (mm)	Group 1	2.27	1.77	1.77
	Group 2	2.57	1.51	1.51
	Group 3	1.70	0.93	0.93
	Group 4	3.25	1.58	1.58
Time (ms)		3.00	5.00	60.00
		FRE (mm)		Time (ms)
PBR		1.70		3.00
ICPt		3.93		4.00
RTf		4.58		25.00

**References:** [1] Orringer DA, et al. Expert Review of Medical Devices. 2012; 9:491-500; [2] Grunert P, et al. Neurosurg Rev. 2003;26:73-99; [3] Pfisterer WK, et al. Neurosurgery. 2008;63: 201-7.

#### A VOXEL BASED MORPHOMETRY STUDY OF TREATMENT-RESISTANT PATIENTS WITH GENERALIZED EPILEPSIES

M. S. Polydoro<sup>1</sup>, D. S. Garcia<sup>1</sup>, M. K. Alvim<sup>1</sup>, A. Ishikawa<sup>1</sup>, L. Montanher<sup>1</sup>, M. E. Morita<sup>1</sup>, F. Cendes<sup>1</sup>, C. L. Yasuda<sup>1</sup>

<sup>1</sup>Neuroimaging Laboratory, FCM, UNICAMP, Campinas, São Paulo, SP, Brazil.

**Introduction:** Although structural abnormalities in gray matter (GM) and white matter (WM) have been described in generalized epilepsies (GE)<sup>1,2,3</sup>, the impact of treatment response has not been completely investigated. Therefore, in this study, we compared refractory and seizure-free subjects to differentiate patterns of structural alterations. **Materials and Methods:** Voxel Based Morphometry (VBM) analyses were performed on T1 weighted images with MATLAB2014b/SPM12/CAT12, comparing controls (65 subjects), and two groups of patients (28 seizure-free [SZ-free] and 37 refractory). Individual maps of GM and WM were extracted, modulated, smoothed and normalized. Statistical analyses with CAT12/SPM12 included separate T-tests between patients and matched controls, with contrasts designed to highlight areas of grey and white matter atrophy in patients. **Results:** Refractory patients present a more widespread pattern of atrophy, especially in GM, which included extensive areas in cerebellum. **Discussion:** As expected, atrophy in thalami was observed in both groups, however, a more severe pattern of atrophy was detected in refractory patients, suggesting a negative impact of seizures on the brain integrity. **Con-**

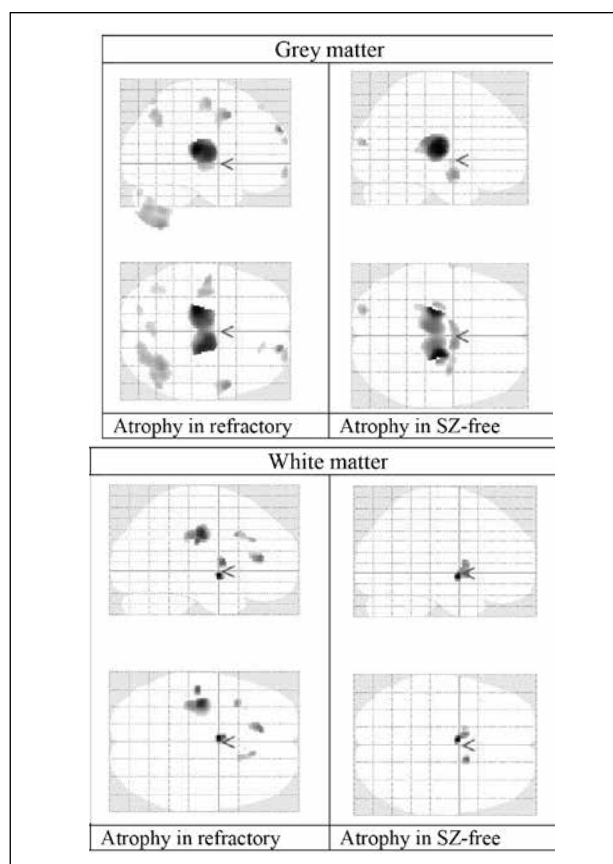


Figure 1.

**Conclusion:** This study showed that treatment-resistant and seizure-free patients have different patterns of brain abnormalities. Further studies are necessary to investigate possible interactions between subtypes of seizures and structural brain abnormalities.

**References:** [1] Bernhardt BC, et al. Thalamo-cortical network pathology in idiopathic generalized epilepsy: insights from MRI-based morphometric correlation analysis. *Neuroimage*. 2009;6:373-81. [2] Betting LE, et al. Voxel-based morphometry in patients with idiopathic generalized epilepsies. *Neuroimage*. 2006a;2:498-502; [3] Betting LE, et al. MRI volumetry shows increased anterior thalamic volumes in patients with absence seizures. *Epilepsy Behav*. 2006b;575-80.

#### DISTINCT FUNCTIONAL AND STRUCTURAL NETWORK ABNORMALITIES IN PATIENTS WITH FOCAL EPILEPSIES

Gonçalves, R.M.<sup>1</sup>, Campos, B.M.<sup>1</sup>, Cendes F.<sup>1</sup>, Coan, A.C.<sup>1</sup>

<sup>1</sup> Department of Neurology, Neuroimaging Laboratory, University of Campinas, Campinas, São Paulo, SP, Brazil.

**Introduction:** Epilepsies are disorders of functionally and anatomically connected neural networks, which can be associated with the variability of ictal phenomena, interictal behavior and prognosis<sup>1</sup>. So far, studies of abnormalities of neural networks in epilepsies were based on the analysis of groups of patients<sup>2</sup>. However, it is known that there is significant inter-individual variation in the clinical characteristics of epilepsies<sup>3</sup>. The aim of this study is to evaluate individual patterns of functional and structural network abnormalities in patients with focal epilepsies and “verify the occurrence the overlap of these networks”. **Materials and Methods:** We selected patients with EEG-fMRI exams and diagnosis of pharmaco-resistant focal epilepsies followed at Clinical Hospital of Unicamp (n=20). They underwent 20-48 minutes echo-planar imaging sequences in a 3T MRI (Phillips Achieva, Netherlands). EEG was acquired using 64 MRI-compatible electrodes. fMRI data was analyzed with SPM8. Interictal epileptiform discharges were visually identified and used to define *blood oxygen level dependent* (BOLD) changes (interictal-related functional changes). Patients with no epileptiform discharges were not selected. The evaluation of the individual patterns of structural brain changes looking for gray matter atrophy

was performed by voxel based morphometry technique, using SPM 8 and SSVBM2 software. T1-weighted volumetric images of 90 healthy subjects were used as control and compared to the image of each patient. Statistical analysis of functional and structural maps consisted of two-sample T-test,  $p < 0.001$ , minimum of 20 contiguous voxels. We evaluated the correlation between structural and functional abnormalities through the co-registration of the maps of each patient using NCA software. **Results:** Eighteen patients (90%) had both interictal-related functional abnormalities and a network of gray matter atrophy including areas outside the epileptogenic zone. The overlap of functional and structural neural network of each patient revealed that 44% (7/16) of patients had overlap of the functional and structural abnormalities, which varied from 0.01% to 2.85% of the areas of the functional maps. **Discussion:** Previous studies consistently demonstrate a network of gray matter abnormalities, as well as a network of interictal-related functional abnormalities in patients with epilepsy. However, the connection between structural and functional abnormalities is not known. One hypothesis is that the occurrence of frequent interictal epileptiform discharges might contribute to the gray matter damage and, therefore, the network of gray matter atrophy should be individually concordant with the functional abnormalities associated with the interictal discharges. We demonstrated, however, that there is no significant overlap of areas of gray matter atrophy and areas of interictal-related functional abnormalities in individual analysis of patients with pharmaco-resistant epilepsies. **Conclusion:** The present work shows that there is no significant overlap of the gray matter structural abnormalities outside the epileptogenic zone and interictal-related functional abnormalities in individuals with pharmaco-resistant epilepsies.

**References:** [1] Spencer SS. *Epilepsia* 2002;43(3):219-27; [2] Morgan VL, et al. *Epilepsia*. 2012; 53(9):1628-35; [3] Laufs H. *Curr Opin Neurol*. 2012;25(2):194-200.

#### HOW A DRUG CAN MAKE YOUR BRAIN FORGET THE WORDS? A LANGUAGE FUNCTIONAL MRI STUDY WITH TOPIRAMATE IN EPILEPSY AND HEADACHE

A. Ishikawa<sup>1</sup>, R. J. Mariano<sup>1</sup>, B. M. Campos<sup>1</sup>, T. M. Lopes<sup>1</sup>, T. A. Zanão<sup>1</sup>, B. Braga<sup>2</sup>, D. S. Garcia<sup>1</sup>, A. L. C. Costa<sup>2</sup>, F. Cendes<sup>1,2</sup>, C. L. Yasuda<sup>1,2</sup>

<sup>1</sup>Neuroimage Laboratory, FCM, UNICAMP; <sup>2</sup>Neurology Dept., FCM, UNICAMP.

**Introduction:** Despite the excellent control of seizures and headache, the antiepileptic drug TOPIRAMATE (TPM) can cause *language* and *memory impairment*. So far, it is unknown how TPM disrupts language function. We hypothesize that TPM disrupts the normal pattern of activations and deactivations, resulting in poor cognitive performance. **Materials and Methods:** 1. **Subjects:** We performed a cross-sectional study, including 39 healthy controls (27 women), 18 patients with migraine/headache taking TPM (HEAD-TPM, 14 women,) and 22 patients with epilepsy using TPM (TLE-TPM, 19 women). Patients were recruited from both Epilepsy and Headache outpatient clinics at UNICAMP Hospital. 2. **fMRI acquisition:** All subjects performed cognitive tests (language performance) and a language fMRI study in a 3T PHILIPS scanner with a blocked-design language paradigm (alternating verbal fluency task and rest every 20 seconds). Groups were balanced for age ( $p=0.94$ ) and gender ( $p=0.3$ ). 4. **Imaging Processing and Statistics:** All images were preprocessed using a MATLAB toolbox UF2C<sup>3</sup>. We used SPM12 (<http://www.fil.ion.ucl.ac.uk/spm/software/spm12/>) to obtain individual contrasts (activation and deactivation). Statistical analyses included group comparisons (full-factorial model) and regression models correlating TPM doses and cognitive tests performance. Statistical analyses of cognitive tests were performed with IBM SPSS22. **Results:** Both HEAD-TPM (21 words) and TLE-TPM (17 words) produced fewer words, compared to controls (31 words) ( $*p < 0.001$ ). On fMRI results both HEAD-TPM and EPI-TPM presented less activations (red) and specially deactivations (blue) compared to controls (Figure and Chart 1). **Discussion:** Our data suggest that TPM prevents normal brain activations and deactivations during language production, which may be associated with poor performance on words generation. **Conclusion:** Despite its efficacy in seizure control and headache, TPM significantly impaired language performance and normal brain function during verbal tasks. Careful attention is necessary to prescribe such drug to avoid excessive cognitive dysfunction.



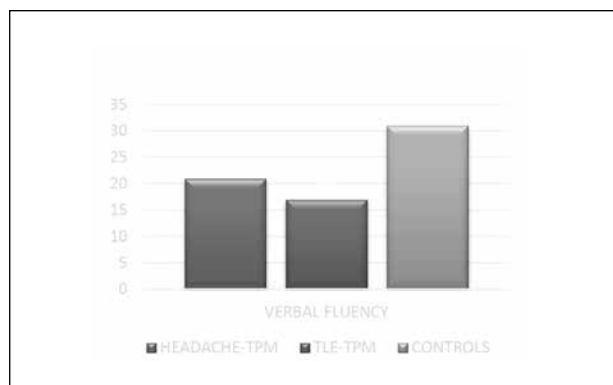


Chart 1. Negative effect of topiramate on language.

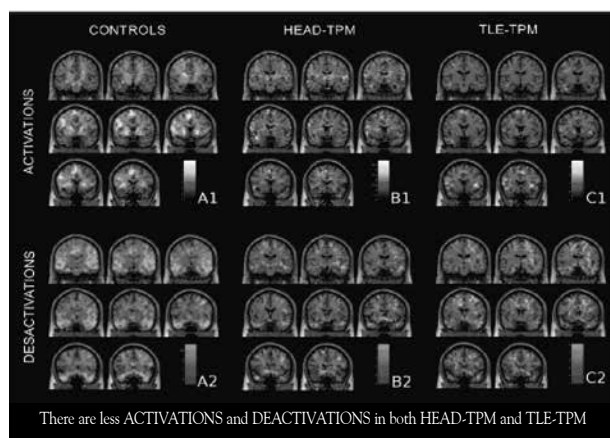


Figure 1. TASK - word generation based on letters (phonemic fluency).

## TRACT INTEGRITY ALTERATIONS THROUGHOUT LIFE SPAN

M. S. Pinto<sup>1</sup>, B. H. Vieira<sup>1</sup>, A. C. Santos<sup>2</sup>, C. E. G. Salmon<sup>1</sup>

<sup>1</sup>InBrain Lab, Physics Dep., FFCLRP, USP; <sup>2</sup>Internal Medicine Dep., FMRP, USP.

**Introduction:** The aging process causes structural and functional alterations in the healthy brain. From Diffusion Tensor Imaging (DTI) data, tractography allows virtual visualization of the architecture of white matter (WM) tracts and the estimation of structural connectivity parameters, as fiber density (FD) and fractional anisotropy (FA). Both parameters are useful quantities to measure WM integrity and reduce in the aging process for specific anatomical brain regions<sup>1,2</sup>. We aim to study which brain tracts are susceptible to specific age-related integrity alteration estimated by FA and FD. **Materials and Methods:** Data from 158 healthy individuals (18-85 y.o.; 81 m.) was used retrospectively. DTI and anatomical T1-weighted images were acquired in a 3T MR scanner. Anatomical images were processed with FreeSurfer v. 5.3.0 software, using recon-all for parcellation information of the brain regions, employing Desikan atlas. Diffusion analysis was performed using FSL software, considering eddy current correction, brain mask creation and estimation of diffusion parameters, including FA maps. Tracts were reconstructed using TrackVis software. Thirteen tracts were manually selected based on anatomical information: Corpus Callosum divided in Genu, Body and Splenium; Corticospinal Tract; Fornix; Inferior Longitudinal Fasciculus; Inferior Occipito frontal Fasciculus and Uncinate Fasciculus<sup>3</sup>. FD was calculated by dividing number of fibers for a specific tract by the WM volume of the whole brain. Statistical analysis to verify the correlations between FA and FD vs age and FD vs FA was performed using R software. Multiple comparisons correction was considered using Benjamini & Hochberg method. **Results:** FA presented significant decrease with age ( $p < 0.001$ ), for all selected tracts, on average 0.001 per year. The Fornix showed significant decrease in FD with age ( $p < 0.001$ ) for Left ( $2.7 \times 10^{-6}$  fibers per  $\text{mm}^3$ /year) and Right ( $2.4 \times 10^{-6}$  fibers per  $\text{mm}^3$ /year) tracts. For the other tracts, FD is

not significantly affected by the aging process. A positive correlation was observed between FA and FC parameters in the Right ( $0.001$  1/fibers per  $\text{mm}^3$ ,  $p = 0.002$ ) and Left ( $0.001$  1/fibers per  $\text{mm}^3$ ,  $p = 0.04$ ) Fornix tracts. **Discussion:** The water diffusion tends to become more isotropic, due to structural alterations on the WM fibers, and FA tends to reduce in the life span [1], this reduction was verified for the analyzed tracts. FD was also expected to reduce with age<sup>2</sup>, however, only the Fornix was susceptible to the alteration with age for this parameter<sup>4</sup>. Regarding both parameters it was verified that, higher FA values correlate with higher FD in the Fornix, however other tracts did not show a strong correlation between them. From these findings, we realize that the aging process affects the brain structural connectivity in a tract specific way, and FD provides complementary information about the age-related WM changes. It leads us to the idea that the fornix is reducing its number of fibers with age and also undergo structural changes in the white matter, as demyelination, and the other tracts only experience the degeneration of fiber integrity without losing fiber number. Fornix tract is a brain structure known for being responsible for memory tasks, that is one of the most affected functions in elderly<sup>5</sup>. **Conclusion:** The present work demonstrated that the Fornix tract, structure related to memory tasks, is one of the most affected brain tracts in the healthy aging, considering the reduction of FD and FA.

**References:** [1] Stadlbauer A, et al. European Journal of Radiology. 2012;81(12):4005-12 [2] Lebel C, et al. NeuroImage. 2012;60(1):340-52; [3] Catani M, et al. Cortex. 2008; 44(8):1105-32; [4] Jang SH, et al. The International Journal of Neuroscience. 2011;121(2):94-100; [5] Metzler-Baddeley C, et al. The Journal of Neuroscience. 2011;31(37):13236-45.

## ASSOCIATIONS BETWEEN ENVIRONMENTAL FACTORS AND DEFAULT MODE NETWORK DEVELOPMENT DURING CHILDHOOD

K. Rebello<sup>1</sup>, J. R. Sato<sup>2</sup>

<sup>1</sup>Neuroscience and Cognition Programm, Federal University of ABC, UFABC;

<sup>2</sup>Neuroscience and Cognition Programm, Federal University of ABC, UFABC.

**Introduction:** Environmental variables might interfere on the maturation of brain functional networks, such as the default mode network. However, studies in the neuroimaging literature investigating the association between environmental conditions and brain connectivity in healthy children are scarce. The findings indicate that abnormal connectivity of default mode network has been associated with a myriad of psychiatric and neurodevelopmental disorders<sup>1</sup>. Our objective is to investigate the effects of socioeconomic and parental relationship variables on the functional connectivity of the default mode of 655 healthy children, evaluated between 7 and 15 years of age, in a trans-sectional study. This may support an identification of the neural basis of abnormal development, as well as foster the elaboration of public policies to promote health and social well-being. **Materials and Methods:** All functional functional magnetic resonance images (fmri) will be acquired in a 1.5T scanner (Philips Achieva) for assessing the connectivity of the default mode network, FES scale to assess parental relationship and ABIPEME questionnaire to assess socioeconomic status. Data pre-processing: for the removal of possible artifacts, the AFNI packages (version 2011 12 21 1014) and FSL (version 5.0) will be used. The statistical maps after the functional scans will be georeferenced and normalized by the Montreal Neurological Institute (NMI) standard, using non-linear transformations. Data analysis: a general linear regression model will be used to investigate if there is any degree of association between the connectivity of the default mode regions (dependent variable) and socioeconomic status and parental relationship (independent variables) after the data preprocessing step. **Expected results:** We expect that environmental and sociodemographic variables be correlated with the development of the default mode network connectivity of children and adolescents probably causing deviations in its trajectory as a function of age, since similar results were detected in children of one year of life<sup>2,3</sup>, as well as in the development of infant structural connectivity<sup>4</sup>, as follows: environmental factors will be associated to changes in connectivity between the main regions of the default mode (especially between the medial pre-fronto and posterior cingulate) and alterations in connectivity will be associated with child environment/parental relationship, as indicative of susceptibility to the development of psychopathologies or developmental disorders.

**References:** [1] Philip NS, et al. European Neuropsychopharmacology. 2013;23(1): 24-32; [2] Graham AM, et al. Child Psychol Psychiatry. 2015; 56:1212-22; [3] Gao W, et al. Cereb Cortex. 2015;25(9):2919-28; [4] Brito NH, Noble KG. Frontiers in neuroscience. 2014;8:276.

### THE IMPACT OF HIPPOCAMPAL ATROPHY ON BRAIN ATROPHY: SIDE MATTERS

J.C.V. Moreira, M.K. Alvim, G. Artoni, A. Ishikawa, D. S. Garcia, B.M. Campos, M. E. Morita, F. Cendes, C. L. Yasuda

<sup>1</sup>Neuroimaging Laboratory, FCM, UNICAMP.

**Introduction:** Atrophy of grey (GM) and white matter (WM) have been extensively analyzed in temporal lobe epilepsy (TLE) patients with either right (RTLE) or left (LTLE) hippocampal atrophy (HA)<sup>1</sup>. However, few studies have investigated patterns of GM and WM atrophy in TLE patients without HA (NEG) and those with bilateral HA (BILATERAL). In this study, we analyzed four groups separately to differentiate patterns of GM and WM atrophy. **Materials and Methods:** We performed Voxel Based Morphometry (VBM) analyses on T1 weighted images with MATLAB2014b/SPM12/CAT12, comparing controls (74 subjects) and four groups of patients (42 RTLE, 49 LTLE, 51 NEG, 23 BILATERAL). Individual maps of GM were extracted and subsequently modulated and smoothed. Posteriorly, CAT12/SPM12 was used to perform statistical analysis with a full factorial design, including all five groups of subjects (comparing controls versus each group of patients) and contrasts designed to highlight areas of GM and WM atrophy in patients. **Results:** Patients and controls were balanced for age ( $p=0.8$ ), however, there were more men in the controls group ( $p<0.05$ ). Despite the difference in gender distribution, we observed specific patterns of GM atrophy, more severe in LTLE (associated with widespread WM atrophy). Thalamic atrophy was observed in all groups with hippocampal atrophy. WM atrophy was observed in all groups, regardless presence or side of HA (Figure 1). **Discussion:** Despite some similarities in clinical presentation, we identified specific patterns of GM atrophy for each group. Interestingly, patients without HA presented minimal abnormalities in GM, but significant WM alterations, possibly associated with seizures. LTLE group presented widespread alterations in both GM and WM, including cerebellum. **Conclusion:** Although unbalanced for gender, we identified more severe abnormalities for LTLE and BILATERAL groups, while RTLE and NEGATIVE presented less widespread alterations. Future studies including balanced groups and more clinical variables may further explore the unique characteristics of each subgroup.

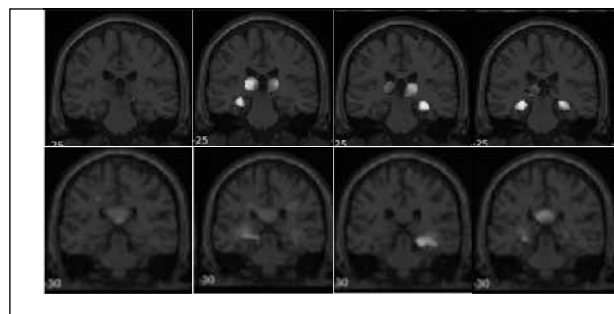


Figure 1. Areas of GM and WM atrophy in different TLE groups, compared to controls.

**References:** [1] Yasuda CL, Betting LE, Cendes F. Voxel-based morphometry and epilepsy. *Expert Rev Neurother*. 2010;10(6):975-84.

### A METHOD FOR EXTRACTION OF CORPUS CALLOSUM'S SHAPE SIGNATURE

W. G. Herrera<sup>1</sup>, A. Costa<sup>1</sup>, L. Rittner<sup>1</sup>

<sup>1</sup>Medical Image Computing Laboratory (MiCLab), School of Electrical and Computer Engineering (FEEC), UNICAMP.

**Introduction:** The Corpus Callosum (CC) is the largest white matter structure in the brain, located under cerebral cortex and allowing communication between both hemispheres. From a clinical point of view, CC alterations are correlated with appearance and evolution of neurodegenerative diseases. Extraction of signature, based on shape, is a novel approach to characterize CC being useful for segmentation evaluation, populations' comparison, alteration inspection and abnormalities identification. In this work, a qualitative study of three automatic and semi-automatic CC segmentations in DWI/DTI is presented, being directly compared with a T1 manual segmentation (ground-truth) using an algorithm for CC's shape signature extraction based on curvature measure. **Materials and Methods:** T1 and DWI images from one subject at

the University of Campinas, were acquired on a Philips scanner Achieva 3T. DTI volumes were obtained after processing DWI data. From each acquired volume, only the midsagittal slice was used. In the T1 image, ground-truth was manually depicted by an expert. Two segmentations were obtained implementing state-of-the-art methods on DTI: segmentation based on Watershed<sup>1</sup> and ROQS [2]. A third segmentation was directly performed on DWI using the voxel-based classification method [3]. A smooth curve was obtained for each segmentation contour using a b-spline implementation. The angle in one point of the contour was obtained positioning a pivot point in the spline curve and measuring the angle between the lines, going from pivot point to anterior and posterior points. These anterior and posterior points were positioned to an SL parametric distance (SL is calculated in percent of the total points conforming the spline) anticlockwise and clockwise from the pivot point, respectively. The signature is extracted measuring curvature (angle in degrees) through the parametric formulation of the spline. **Results:** From splines of four CC segmentations: Manual, Watershed, ROQS and voxel-based method (Figure 1), signatures are obtained (Figure 2) at SL=0.06. **Discussion:** Signature holds CC landmarks enabling a qualitative study. Signature resolution can be changed adjusting SL. **Conclusion:** CC's shape signature allows characterize shape and compares segmentations in different modalities; quantitative evaluation could be done measuring the distance between them.

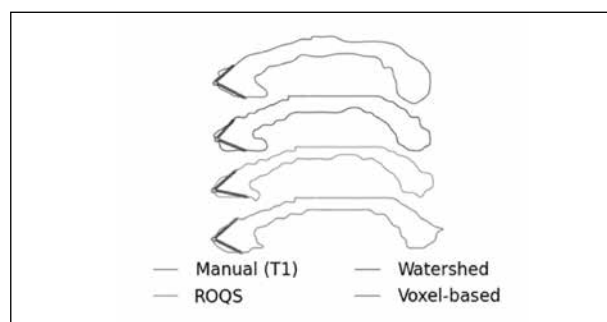


Figure 1. Spline representation of CC segmentations, where angle is measured between lines going from pivot point to anterior and posterior points.

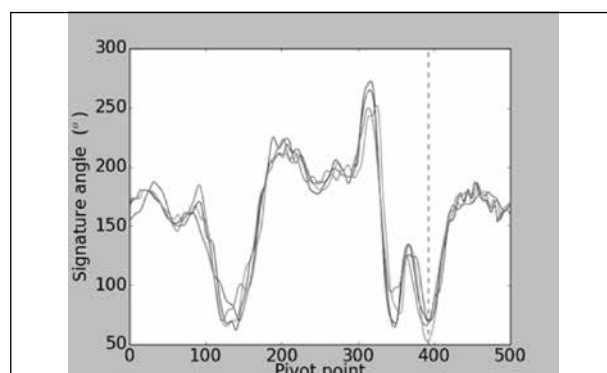


Figure 1. CC signatures (measured in degrees) along spline piv.

**References:** [1] Freitas P, et al. Watershed-based segmentation of the midsagittal section of the corpus callosum in diffusion MRI. *Proceedings - 24th SIBGRAPI Conf. on Graph, Patterns and Images*. (2011): 274-80; [2] Niogi S, et al. Diffusion tensor imaging segmentation of white matter structures using a reproducible objective quantification scheme (ROQS). *NeuroImage*. 2007; 35(1): 166-74; [3] Herrera W, et al. Corpus Callosum Segmentation on DWI through voxel-based Classification. *J Epilepsy Clin Neurophysiol*. 2016;111-2.

### TOPOGRAPHY OF BRAIN ATROPHY IN HUNTINGTON'S DISEASE: A Voxel-BASED MORPHOMETRY STUDY

J. Guitti<sup>1</sup>, P.C. Azevedo<sup>2</sup>, I.Cendes<sup>3</sup>, C.Yasuda<sup>1,2</sup>, F.Cendes<sup>1,2</sup>

<sup>1</sup>Neuroimage laboratory, FCM, UNICAMP; <sup>2</sup>Neurology Dept., HC, UNICAMP <sup>3</sup> Genetics Dept., FCM, UNICAMP.

**Introduction:** Huntington's disease (HD) is an autosomal dominant neurodegenerative disease, yet without curative treatment, clinically characterized by progressive involuntary movements (usually chorea), cognitive impairment



and behavioral disturbances. It affects several brain structures, such as the hippocampus, the cerebellum and the thalamus, but mainly striatum and nucleus accumbens core. Voxel based morphometry (VBM) has proved to be a powerful tool for analyzing changes in gray (GM) or white (WM) matter volume of the brain, especially in HD. The aim of our study is to detail the main alterations in GM and WM in HD using the CAT12 (Computational Anatomy Tool) for VBM on magnetic resonance imaging (MRI). **Materials and Methods:** We analyzed the MRI of 37 patients with molecular confirmation for HD who underwent neurological, cognitive and psychiatric evaluations, and compared with 37 age and gender matched controls. All images were acquired in a 3T scanner (Philips Achieva) and were analyzed through the CAT12 toolbox (<http://www.neuro.uni-jena.de/cat/>) running on Matlab2014/SPM12 (<http://www.fil.ion.ucl.ac.uk/spm/software/spm12/>). After individual maps of GM/WM were extracted, modulated, smoothed and normalized, statistical analysis with T-tests (between patients and matched controls) was performed, with contrasts designed to highlight areas of GM and WM volume atrophy in patients. **Results:** Patients presented widespread atrophy in both WM and GM. The most damaged areas were detected in the striatal regions, indicating the most severe changes throughout the brain. (Figure1). **Discussion:** The results reinforce the devastating brain effects of this disease, given the variety of cerebral structures affected and its functional impact. These areas are responsible for the reward system, movement and behavior control, motor planning, sensorimotor integration, visuospatial function and emotional processing. Further studies are necessary to evaluate the correlation between such alterations and clinical symptoms, including both motor and cognitive. **Conclusion:** The present work confirms that HD is a severe disease, as it extensively disrupts both white and gray matter, including several subcortical areas/structures.

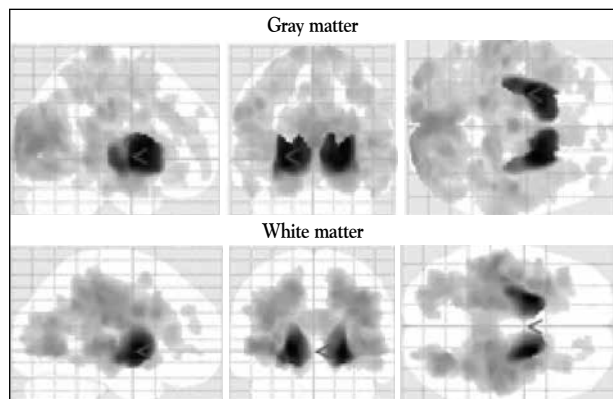


**Figure1.** Areas of atrophy in patients with HD (37 subjects), compared to controls (37 subjects).

**References:** [1] Azevedo PC, et al. *Mov Disord.* 2016;(31):283; [2] Piccinin CC, et al. *Front Neurol.* 2015;(5): 283; [3] Kassubek, et al. *J Neurol Neurosurg Psychiatry.* 2004;(75):213-20.

#### OPERATIONAL AND STRATEGIC MENTAL MODELS REVEAL DIFFERENT BRAIN ACTIVATION

G. S. Spagnol<sup>1</sup>, L. M. Li<sup>2</sup>

<sup>1</sup>PhD student, School of Medical Sciences, UNICAMP; <sup>2</sup>MD, PhD, BBA Professor, School of Medical Sciences, UNICAMP.

**Introduction:** According to Bressan<sup>1</sup>, information from a workplace is received, processed and used differently by people with distinct mental models, which also influences decision making. In this sense, mental models can be divided into: 'operational' - those who receive information and make decisions based in a concrete plan, and 'strategic' - who organize information, identifying new possibilities to support decisions. Yet, there are no references of evidence concerning this classification and the brain response. Within the field of Neuroscience applied to Management, functional Magnetic Resonance Imaging (fMRI) laid the foundation to differentiate entrepreneur's behavior<sup>2</sup>, as well as to understand brain activation in task-based studies<sup>3</sup>. In this research, we applied a psychometric test called Raven, frequently used to estimate IQ, to compare the two groups (operational and strategic) during an fMRI acquisition. **Methods:** fMRI images (TR=2s, voxel=3x3x3 mm<sup>3</sup>, FOV=240x240x117mm<sup>3</sup>) of 25 healthy volunteers classified as operational (na=15) and strategic (nb=10)

were acquired on a 3T MR (Philips Achieva) coupled to InVivo Eloquence stimulation equipment. The MRI protocol was complemented by an anatomical sequence MPAGE (3D high resolution image, weighted by T1), with a total duration of 6 minutes for functional coregistration. During the exam, volunteers were given 20s to mentally solve one of Raven's matrix. Raven's progressive matrix test consists of presenting an array of figures where there is a logical pattern between the figures. One of the casts of the matrix is left blank and the examinee is encouraged to fill the box with the correct figure according to his reasoning. **Results:** According to the t test, areas of activation that present significant differences ( $p < 0.05$ ) between the groups were: left posterior cingulate gyrus (13.9%), thalamus (9.3%) and left hippocampus (3.7%). Raven responses did not present significant difference between groups ( $p < 0.05$ ). **Discussion:** Imaging studies indicate a prominent role for the posterior cingulate cortex in pain and episodic memory retrieval<sup>4</sup>, and thalamus as a hub of information, establishing the connection between different subcortical areas and the cerebral cortex. For the visual system, for example, inputs from the retina are sent to the lateral geniculate nucleus of the thalamus, which in turn projects to the visual cortex in the occipital lobe. The thalamus is functionally connected to the hippocampus as part of the extended hippocampal system at the thalamic anterior nuclei<sup>5</sup> with respect to spatial memory and spatial sensory datum they are crucial for human episodic memory and rodent event memory. These findings indicate a difference in activation patterns related to memory retrieval between operational and strategic mental models. **Conclusion:** This work provides evidence of preliminary differences in brain activation between 'operational' and 'strategic' while making decisions during a test.

**References:** [1] Bressan, et al. *Revista Psicologia: Organizações e Trabalho.* 2013;13(3):309-24; [2] Laureiro-Martinez D, et al. *Strategic Management Journal.* 2014; [3] Desalvo MN, et al. *Brain and Behaviour.* 2014;4(6):877-85; [5] Doll, et al. *Frontiers in Human Neuroscience.* 2013;7:1-13; [4] Nielsen FA, et al. *NeuroImage.* 2005;27(3):520-32; [5] Aggleton JP, et al. *Behavioral and Brain Sciences.* 1999;22(3):425-44.

#### IMU HEAD TRACKING WITH FIXED PAN-TILT LASER FOR WHEELCHAIR NAVIGATION

G. M. Pereira<sup>1</sup>, E. Rohmer<sup>1</sup>

<sup>1</sup>School of Electrical and Computer Engineering, FEEC, UNICAMP.

**Introduction:** This research addresses the topic of a novel driving assistance system of a robotized wheelchair for people paralyzed from down the neck. In<sup>1</sup>, the authors present a navigation strategy, in which an Inertial Measurement Unit (IMU) tracks the user's head posture, to accordingly project a colored spot on the ground ahead, with a pan-tilt mounted laser. The wheelchair is equipped with a low-cost depth camera that models a traversability map in order to define if the desired destination is reachable or not by the chair. The operator can validate the target via an Electromyogram (EMG) device attached to his face, and the system calculates the path to the pointed coordinate, based on the traversability map. Meanwhile, in this work, we present and discuss a simplest navigation strategy focused only on the head posture to actuate on the pan-tilt laser, and a push button to validate the target. **Materials and Methods:** The system composes an IMU, a pan-tilt mounted laser, and one Arduino Mega 2560. The IMU positioned above the operator's head captures its posture and actuates on the pan-tilt laser, which points to the desired location that will be reached autonomously by the wheelchair. By pressing a validation button, the algorithm calculates the target point in relation to the wheelchair frame and send it to the destination. First, the wheelchair performs a rotation of the bearing angle in relation to the target and then dislocate linearly. **Results:** Figure 1 presents an experiment which the user navigates in a corridor with obstacles. The handmade pan-tilt mount and the wheelchair intrinsic parameters introduce errors on the targets calculations and on the wheelchair rotations. In Figure 1(b), the distance between the chosen targets and the wheelchair stop marks are approximately 0.3 meters. **Discussion:** The distance error between the targets and the stop marks are acceptable considering the wheelchair size: 1.30 x 0.6 meters (length x width). Although the system has reached the chosen targets correctly, the locomotion algorithm is not enough safe for the operator either efficient. First of all, the system allows the user to select any target, even if it is not reachable by the chair. And secondly, there is not path planning to calculate a smooth trajectory based on the scene obstacles. **Conclusion:** The driving assistance system of a robotic wheelchair may be an efficient and comfortable mean of navigation for

people paralyzed from down the neck. However, to provide a safe and smooth trajectory toward a reachable target, we will integrate the necessary hardware for the autonomous navigation presented in<sup>1</sup>. Also, buttons will be replaced by an EMG recording of facial muscular contractions and a puff sensor, as the operator can not make use of his arms.

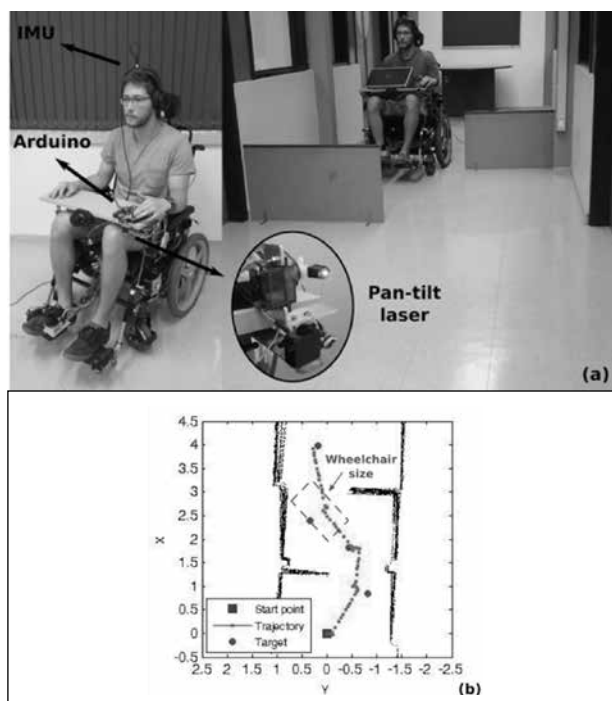


**Figure 1.** Human-robot interface on a scenario with obstacles (a), and the performed trajectory based on the chosen targets (b).

**References:** [1] Rohmer E, et al. Laser based Driving Assistance for Smart Robotic Wheelchairs. In Proc of the 20<sup>th</sup> IEEE Int. Conf. of Emerging Tech. & Factory Automation, 2015.

#### ABNORMAL INTER-INTRANETWORK CONNECTIVITY IN PATIENTS WITH GENERALIZED EPILEPSIES

D. S. Garcia, M. Polydoro, M. K. Alvim, A. Ishikawa, B. M. Campos, L. L. Montanher, M. E. Morita, F. Cendes, C. L. Yasuda

<sup>1</sup>Neuroimaging Laboratory, FCM, UNICAMP.

**Introduction:** Generalized epilepsies (GE) present heterogeneous semiology of seizures and have been considered as a benign disorder. However, several studies have found structural and functional abnormalities such as gray and white matter atrophies/excesses, as well as increased/decreased connectivity in some brain resting state networks (RSNs). Unfortunately, it is not clear how dysfunctional are the interactions among these RSNs. Therefore, the purpose of this study is to compare interactions of 12 RSNs (from resting-state functional-MRIs). **Materials and Methods:** The 12 RSNs were parcellated in 70 regions of interest (ROIs). Sixty-one subjects with generalized epilepsy and sixty-two healthy controls were matched by age and gender. We used UF2C-toolbox (running on MATLAB2014 and SPM12) for image preprocessing, ROI parcellation and statistical analysis, including intranetwork and internetwork connectivity. **Results:** We identified both *decreased* and *opposite correlations* in the GE patients RSNs as presented in Table 1. Figure 1 reveals alterations concentrated predominantly on left side. **Discussion:** These results suggest that Posterior Salience and Visuospatial networks present most of altered interactions in GE patients. Such alterations corroborate with previous findings that revealed abnormalities in frontal, parietal and thalamic regions. **Conclusion:** As an exploratory study, we found extensive alterations in GE functional networking; however, further research is necessary to investigate the impact of seizure controls on dysfunctional networks.

**References:** [1] Zhang Z, et al. Altered functional-structural coupling of large-scale brain networks in idiopathic generalized epilepsy. Brain. 2011;134(Pt 10):2912-28.

#### Reduced Connectivity: (Controls>Patients)

##### Posterior Salience with:

- ✓ Basal Ganglia
- ✓ Visuospatial

##### Visual with:

- ✓ Dorsal DMN

##### Left Executive Control Network with:

- ✓ Visuospatial
- ✓ Ventral DMN

##### Posterior Salience with Posterior Salience

##### Visuospatial with Visuospatial

#### Opposite Connectivity: (Patients ↔ Controls)

##### Visuospatial with:

- ✓ Basal Ganglia
- ✓ Posterior Salience
- ✓ Ventral DMN

**Figure 1.** Key findings from internetwork and intranetwork connectivity analysis between 61 GE subjects and 62 healthy controls.

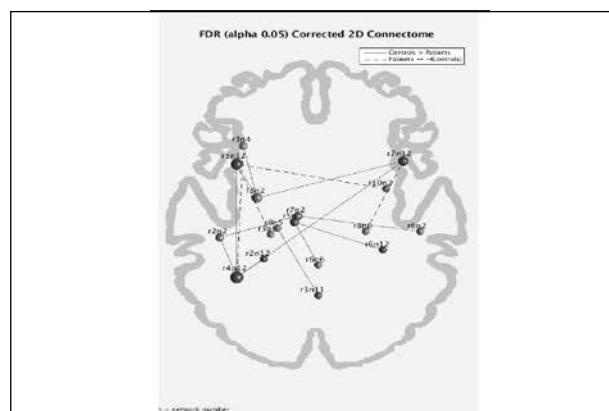


**Figure 1.** Graf with relative decreased and opposite connectivity hubs between patients and controls.

#### CORTICAL SURFACE ANALYSIS IN PATIENTS WITH GENERALIZED EPILEPSIES

D. S. Garcia, M. K. Alvim, M. Polydoro, A. Ishikawa, L. L. Montanher, M. E. Morita, F. Cendes, C. L. Yasuda<sup>1</sup>

<sup>1</sup>Neuroimaging Laboratory, FCM, UNICAMP.

**Introduction:** Volumetric and surfaced based analysis have been extensively used on focal epilepsies to quantify brain alterations. However, in generalized epilepsies (GE) these methods are not commonly utilized and little is known about cortical thickness abnormalities. Thus, the aim of this study is to evaluate the extent of cortical damage in patients with GE using a new variant of computational analysis. **Materials and Methods:** Surface-Based Morphometry (SBM) analyses were performed on T1 weighted images with MATLAB2014b/SPM12/CAT12 (<http://dbm.neuro.uni-jena.de/cat12/>), comparing 67 GE PATIENTS with 68 age and gender matched CONTROLS. This technique is completely automatic and allows measurement of cortical thickness as well as reconstructions of the central surface in one-step. Statistical analyses with CAT12/SPM12 included separate T-tests between Left and Right hemispheres of patients and matched controls, with contrasts designed to highlight areas of atrophy in patients. Reported results have minimum T-statistic of 3, with at least 10 voxels in each cluster. **Results:** Patients with GE presented reduced cortical thickness compared to healthy control, more widespread in the left hemisphere, particularly in the frontal lobe. In addition to alterations in frontal regions (particularly in the precentral gyrus), lower cortical thickness was detected in occipital and mainly in anterior temporal lobe (Figure 1). **Discussion:** This new method revealed significant cortical changes that suggest that generalized seizures might cause significant damage not only to the primary motor cortex area, but also to other regions. Further analyses are necessary to evaluate the

impact of both refractory seizures and valproate on these cortical changes. Besides, how these alterations associate with cognition and mood also need to be investigated. **Conclusion:** Although considered a benign form of epilepsy, our results suggest a negative impact of GE on cerebral cortex.

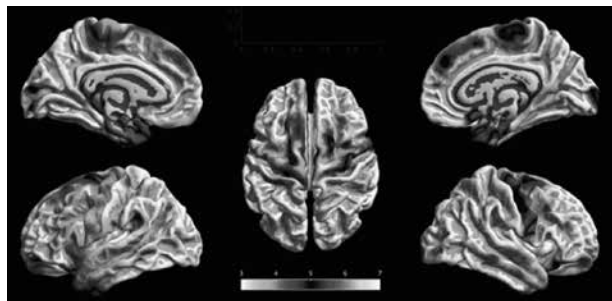


**Figure1.** Surface-based analysis of local cortical thickness. GE patients present widespread, bilateral reduction of cortical thickness.

**References:** [1] Tae WS, et al. Structural brain abnormalities in juvenile myoclonic epilepsy patients: volumetry and voxel-based morphometry. *Korean J Radiol.* 2006;7(3):162-72.

#### CONTRALATERAL HIPPOCAMPAL ATROPHY AFTER TEMPORAL LOBE SURGERY: VOLUMETRIC ANALYSIS OF PREOPERATIVE AND LONG-TERM POSTOPERATIVE MRI

B. F. Silva, A. Ishikawa, I. Amaral, D. S. Garcia, Morita, M. E. Alvim, M.K. Ghizoni, E. Tedeschi, H. F. Cendes, C. L. Yasuda

<sup>1</sup>Neuroimaging Laboratory, FCM, UNICAMP.

**Introduction:** Surgical removal of mesial temporal lobe structures has been the leading treatment for refractory MTLE. This study aimed to evaluate postoperative structural changes, determining the extent and time course of atrophy in contralateral hippocampal volume after surgery. **Materials and Methods:** We performed a longitudinal study of 45 patients (38 *controlled* and 7 *refractory*) with unilateral hippocampal sclerosis, who underwent preoperative (before surgery)/postoperative (after 6 months of surgery) MRI acquired in a 3T scanner (Philips). We included 35 controls who underwent 2 MRIs at long-term intervals. Blinded, manual hippocampal volumetry was performed with free software Display (Montreal Neurological institute). After normalizing individual volumes with individual's intracranial volumes, we used SPSS22 (repeated measures ANOVA) to test the interaction between time (pre-op, post-op) and groups (controls, *controlled* and *refractory*). Statistical analyses were covaried for age (as controls were younger than patients) and multiple comparisons adjusted with SIDAK. **Results:** The paired comparison between pre-op and immediate post-op (first week after surgery) hippocampal volume revealed non-significant volume reduction ( $p > 0.05$ ). However, at long-term evaluation, we observed significant atrophy of contralateral hippocampus in both groups of patients (*controlled*,  $p < 0.001$ , and *refractory* = 0.02), but no volumetric changes in controls ( $p = 0.8$ ). The mean interval of 2 MRIs was 2.6 years. **Discussion:** Significant contralateral hippocampal atrophy occurs following MTLE surgery, however few studies have performed long-term evaluation to investigate this process. A speculative explanation for the mechanisms of this reduction could

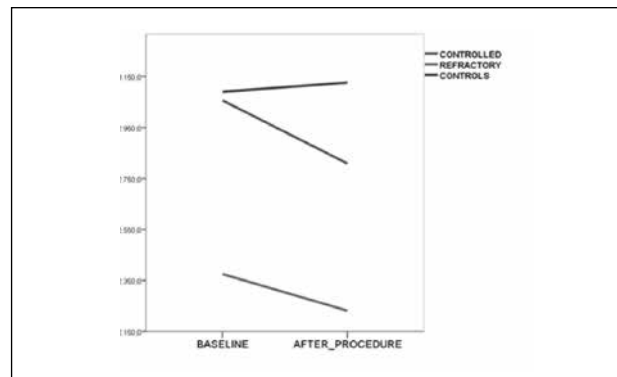


**Figure2.** Evaluation of long-term volumetry in patients (*controlled / refractory*) and controls.

be an association with the deafferentation process triggered after severing the connections between both hippocampi via surgical intervention. **Conclusion:** We demonstrated that manual volumetry can reveal a reduction in contralateral hippocampal volume that could not be detected in visual analysis. These findings suggest that dynamic processes persist after the removal of the hippocampus, and further studies with larger groups may help to understand underlying mechanisms.

**References:** [1] Bonilha L, et al. *Hum Brain Mapp.* 2004;22(2):145-54; [2] Cendes F, et al. *Ann Neurol.* 1993;34(3):795-801; [3] Elliott CA, et al. *Epilepsy Res.* 2016;125:62-71; [4] Fernandes DA, et al. *Epilepsy Behav.* 2014;108-14; [5] Noulhiane M, Samson S, Clemenceau S, Dormont D, Baulac M, Hasboun D. *J Neurosci Methods.* 2006;156(1):293-304; [6] Yasuda CL, et al. 2006;15(1):35-40.

#### POSTOPERATIVE DYNAMIC CHANGES ON CONTRALATERAL HIPPOCAMPUS: MANUAL VOLUMETRY AND RELAXOMETRY ANALYSES

I. Amaral, B. F. Silva, A. Ishikawa, D. S. Garcia, M. E. Morita, M.K. Alvim, E. Ghizoni, H. Tedeschi, F. Cendes, F. C. L. Yasuda

<sup>1</sup>Neuroimaging Laboratory, FCM, UNICAMP.

**Introduction:** Despite good surgical control for approximately 50-60% of operated patients<sup>1</sup>, almost one third persist with seizures. Unfortunately, post-operative dynamic changes on contralateral hippocampus is not entirely known<sup>2,3</sup>, neither its correlation with surgical outcome. Here we investigated alterations in volume and relaxometry time after temporal lobe (TLE) surgery for refractory epilepsy. **Materials and Methods:** We evaluated longitudinally 37 patients with unilateral hippocampal atrophy (31 *controlled* and 6 *refractory*), who underwent preoperative/postoperative MRI in a 3T scanner. Blinded, manual hippocampal volumetry and T2 relaxometry measurements were performed with free software Display (Montreal Neurological institute) and *Aftervoxel*, respectively. Statistical analyses were performed with SPSS22 (repeated measures ANOVA) to investigate deterioration after surgery (groups *controlled* and *refractory*). **Results:** At long-term evaluation, there was significant atrophy of contralateral hippocampus in both groups of patients (*controlled*,  $p < 0.001$ , and *refractory* = 0.002) (Figure 1 A/B). On contrary, relaxometry analyses revealed no significant changes for both groups; however, there was a trend for increase for *refractory* patients (Figure 1 C/D). **Discussion:** We observed significant volumetric reduction of contralateral hippocampus, regardless surgical outcome,

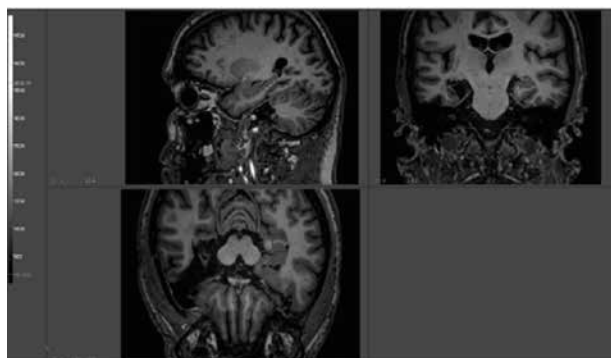


**Figure1.** Software DISPLAY. Manual segmentation of right hippocampus in red.

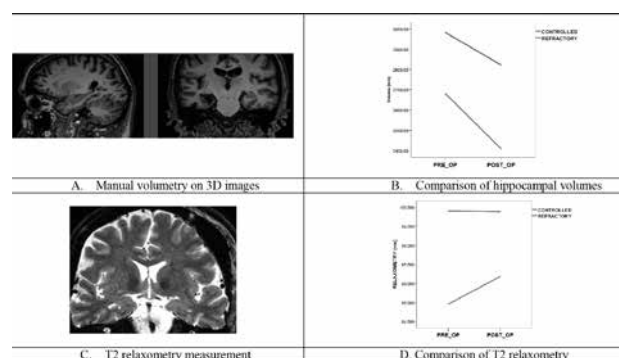


**Figure1.** Longitudinal analyses of hippocampal volume and relaxometry pre and postoperatively.



seen in a previous study<sup>4</sup>. Interestingly, no significant changes were detected on T2 relaxometry of the same subjects as seen in preoperative analyses. These findings suggest that the volumetric reduction may not necessarily impact its function; it is also possible that the small number of refractory patients may have hampered significant increase. These dynamic changes require further investigation and correlations with cognitive assessment. **Conclusion:** Our data suggest that significant volumetric reduction may occur after surgery, however may not be associated with increase of T2 relaxometry.

**References:** [1] Yasuda CL, et al. 2006;15:35-40; [2] Cendes F, et al. Ann Neurol. 1993;34(6):795-801; [3] Elliott CA, et al. Epilepsy Research. 2016;125:62-71; [4] Fernandes DA, et al. Epilepsy Behav. 2014;36:108-14.

#### VIDEO AND KNOWLEDGE STRUCTURE FOR AN AUDIOVISUAL SYSTEM BASED ON ANIMATIONS TO SUPPORT LEARNING ABOUT EPILEPSY

F. N. Akhras<sup>2</sup>, C.S.M. Castro<sup>1</sup>, L. S. M. Pereira<sup>1</sup>, G. S. A. Nascimento<sup>1</sup>, T. E. Hatta<sup>1</sup>  
<sup>1</sup>CTI Renato Archer, <sup>2</sup>IA, UNICAMP

**Introduction:** As a part of the work of the Education and Knowledge Dissemination Group, this BRAINN subproject focuses on providing a means for the population to know more about epilepsy in order to reduce the stigma and the social exclusion that is associated with this disease. In order to do that we are developing an internet system that provides information about epilepsy in the form of video animations which address a broad spectrum of issues. These issues constitute a corpus of knowledge which can help to raise the awareness of the population about epilepsy and about the contexts in which these issues appear in the daily life of people with epilepsy. In this poster we present the video-based knowledge structure that will support the system. **Material and Methods:** The content of the audiovisual system is organized around four main themes that aggregate the issues that are relevant to understand the situations that affect the four main ages of life: childhood, adolescence, adult life and old age. All the content is produced in the form of animations of two kinds: first, *situational animations* that address daily life and work situations that are faced by people with epilepsy, which present challenges due to the limitations that are sometimes imposed by the disease, and second, *informational animations* that are produced from interviews made with healthcare professionals, including: medical doctors and social assistants, which are part of the team of the BRAINN project and work on research and treatment of patients with epilepsy. The general purpose of this content organization is to address the connections between the information and the social contexts in which it becomes relevant and which makes the information meaningful<sup>1</sup>. The situational animations tell a story to introduce the subjects using fictional characters while the informational situations address more deeply the subjects on the basis of theoretical research and interviews with medical doctors. **Results:** A knowledge structure of epilepsy issues composed of video animations constitutes the content of the audiovisual system. Currently, we have produced about twenty videos addressing, for example, issues like: going to school (within the childhood theme), construction of identity (within the adolescence theme), pregnancy (within the adult life theme), among others. Some animations are focused on situations in which the user can make choices of paths to follow (for example, faced to a question of going or not to a party, the user can see what the consequences of each choice are). Other animations are focused on information provided by specialists, which are intended to answer basic questions about how to deal with the conditions of epilepsy. Therefore, the two kinds of animations complement each other. This structure will be the basis for the construction of the system which is designed to provide flexibility to the users to navigate through this structure according to their interests and needs. The resulting video and knowledge structure and its construction will be shown in the poster presentation. **Conclusion:** The need for a system that can support open learning about epilepsy comes from the recognition of the lack of knowledge about epilepsy that exist in the Brazilian population, which can increase the social exclusion that affect people with epilepsy<sup>2</sup>. Working in this direction, we have developed a knowledge structure of epilepsy issues composed of video animations, which constitutes the web-based audiovisual system to support learning about epilepsy that we are constructing within the BRAINN project. Apart from the use of the internet to provide open access to the material, the main features of the system are: the use of videos to organize and disseminate the knowledge about epilepsy in a flexible way, and the addressing of issues of contemporary theories of learning in the way the videos

are produced and organized, emphasizing, for example, the representation of authentic situations of the daily life of people with epilepsy.

**References:** [1] Brown JS, Duguid P. The Social Life of Information. Boston, MA: Harvard Business School Press. 2000; [2] Min LL, et al. Demonstration project on epilepsy in Brazil: situation assessment. Arq Neuro-Psiquiatr. [online], 2007;65(suppl.1):5-13.

#### COMPUTER AIDED DESIGN FOR TRANSPOSING A 2D BRAIN MODEL INTO A 3D EDUCATIONAL OBJECT

C. Rondinoni<sup>1</sup>, J. H. Barbosa<sup>2</sup>, A. C. dos Santos<sup>3</sup>, C. E. G. Salmon<sup>2</sup>, E. Amaro<sup>1</sup>

<sup>1</sup>PISA, InRad, USP; <sup>2</sup>FFCLRP, USP; <sup>3</sup>FMRP, USP

**Introduction:** The transformation of previous knowledge into the specification of a new product is a covert process that develops inside the designer's head and depends on the ability to find the best computational tools for a given task. Here we present the development of a graspable 3D brain model based on the classical Talairach and Tournoux co-planar atlas<sup>1</sup>. The model was transposed from 2D representation into a 3D vacuum formed shape. The application of geometric modeling with the use of B-splines and point registration was proposed to solve the problem of correctly representing the brain surface. **Materials and Methods:** Ten sagittal slices were generated in steps of 7 mm from the mid-line (x=0) to lateral brain slices (x=68) using the visualization of the Talairach model in BrainVoyager QX 2.8 viewport. A collection of 8 control points was arbitrarily defined around the central slice images. A series of straight lines connecting the periphery to an arbitrary mid-point between AC-PC was drawn. Polygon control points were used as a vector of moving points in the non-rigid registration processing<sup>2</sup>. Static points were calculated as if they were equidistant from each other along the guiding line (Figure 1a,b). Registration step was done during figure printing and molding. Instruction manuals and classroom activities are delivered as supplementary materials. **Results:** The information about brain areas, brain curvature, Brodmann areas<sup>1</sup> e cerebellar SUIT atlas<sup>3</sup> is presented as a 3D educational object for anatomy learning and education (Figure 1c). **Discussion:** A proof of concept was developed to include the knowledge about a well-known brain model. The proposed point-based registration did not account for the material deformation during vacuum forming and the original parallel projection showed better compromise between manual intervention and correctness for the location of brain functional areas. **Conclusion:** We aimed to build a model that can be used in the classroom as

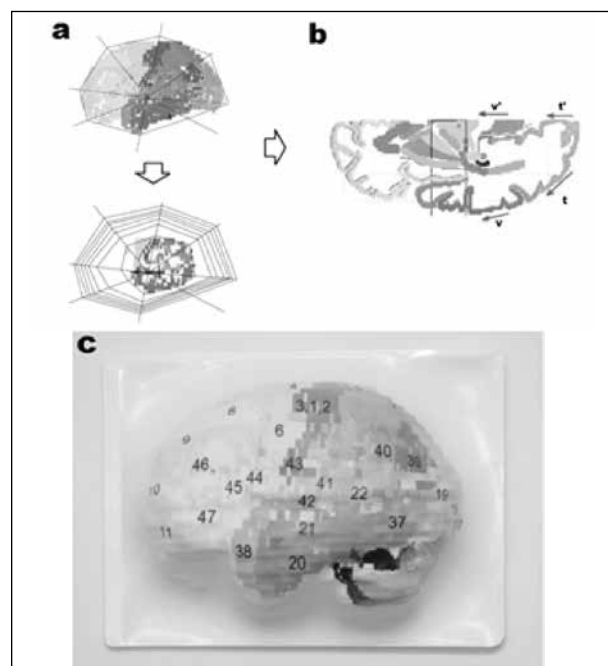


**Figure 1.** Rationale for synthesizing the colored texture to be applied on the Talairach brain surface. a. Each coronal slice was pasted considering the yz location of anterior-posterior commissure line. Moving points were marked around the border of each sagittal slice. b. Axial view of the moving points trajectory from static (v, t) to moving points (v', t'). c. Molded polystyrene sheets after heat transfer of the not-deformed projection image of each Brodmann area.

a material of reference. Further iterations can be useful to refine the texture mapping, improve nervous system representation to include details of Brodmann areas or representations of white matter fascicles.

**References:** [1] Talairach J, Tournoux P. Thieme. New York. 1998; [2] Xie Z, Farin GE. IEEE Transactions on Visualization and Computer Graphics. 2004;10(1):85-94; [3] Diedrichsen J. Neuroimage. 2006;33:127-38.

#### TRANSCRIPTOME PROFILE OF HIPPOCAMPUS CA3 IN THE PILOCARPINE MODEL OF TEMPORAL LOBE EPILEPSY

H. B. Matos<sup>1</sup>, A. S. Vieira<sup>1</sup>, A. M. Canto<sup>1</sup>, S. C. R<sup>1</sup>, B. Carvalho<sup>1</sup>, V. D. B. Pascoal<sup>1,2</sup>, R. Glioli<sup>3</sup>, I. Lopes-Cendes<sup>1</sup>

<sup>1</sup>Department of Medical Genetics, School of Medical Sciences, University of Campinas - UNICAMP, SP, BRAZIL and the Brazilian Institute of Neuroscience and Neurotechnology (BRAINN); <sup>2</sup>Department of Basic Sciences, Fluminense Federal University, UFF, Nova Friburgo, RJ, BRAZIL; <sup>3</sup>Laboratory of Animal Quality Control (CEMIB), University of Campinas, UNICAMP, Campinas, SP, Brazil.

**Background:** It is well known that gene expression profile of specific tissue provides relevant biological information about molecular mechanisms potentially involved in complex biological phenomena. Recently, it has been recognized that due to marked heterogeneity of gene expression in different subset of cells, it is important to take sub-regional specificities when studying gene expression, especially in the CNS. The aim of this study was to analyze gene expression profile using next generation sequencing technology in different sub-regions of the *Comu Ammonis* 3 (CA3) in an animal model of temporal lobe epilepsy induced by pilocarpine. **Methods:** Male Wistar rats were injected with methyl-scopolamine (1 mg/kg) thirty minutes before of the systemic injection of pilocarpine hydrochloride (320 mg/kg) to reduce peripheral cholinergic side effects. Four hours after the administration of pilocarpine diazepam was administrated (4 mg/kg) in order to stop seizures. Control rats were injected with saline after methyl-scopolamine injection. Fifteen days after induction, rats were euthanized (n=4) and brains were processed for laser microdissection. Dorsal, intermediate and ventral CA3 were collected from each rat. RNA sequencing was performed in an Illumina HiSeq® platform. Sequences were aligned and quantified with the TopHat/DESeq2 pipeline for total RNA. Gene ontologies and gene interactions were analyzed with the MetaCore® software. **Results:** We found a total of 2624, 1731 and 1278 genes differentially expressed ( $p < 0.05$ ) when comparing control and pilocarpine rats for the dCA3, iCA3 and vCA3 respectively. Gene ontology analysis indicates genes related to cytoskeleton remodeling and cell cycle upregulate in dCA3. In iCA3 we identified upregulation of genes involved in oligodendrocyte differentiation in adult stem cells. In vCA3 there was downregulation of glutamatergic neurophysiological process, and upregulation of genes related to regulation of G1/S transition. **Conclusion:** Our results indicate region specific molecular mechanisms taking place in the hippocampus sub-regions of an animal model of temporal lobe epilepsy induced by pilocarpine. The transcriptome data suggest an interaction among several molecular components leading to epileptogenesis in this animal model that displays widespread hippocampal damage.

**Financial support:** FAPESP

#### SEGMENTATION OF CORTICAL CYTOARCHITECTONICS FROM IN WHOLE BRAIN THICK NISSL SECTIONS

C. Rondinoni<sup>1</sup>, E. Alho<sup>1</sup>, H. Heinsen<sup>2,3</sup>, L. Grinberg<sup>4</sup>, E. Amaro Jr<sup>1</sup>

<sup>1</sup> Department of Radiology, LIM-44, PISA - FMUSP; <sup>2</sup>Department of Psychiatry, Psychosomatics and Psychotherapy, Center of Mental Health, University Hospital Würzburg, Germany; <sup>3</sup>Ageing Brain Study Group, Department of Pathology, LIM 22, University of São Paulo Medical School, São Paulo, Brazil; <sup>4</sup> Department of Neurology, University of California, San Francisco, USA.

**Introduction:** This study aimed at describing a method to measure densities of cellular bodies on thick sections of healthy *in situ* brains after standard gallocyanin technique (Nissl staining). Covered glass plates from segments of the frontal lobe and whole brain structural MR images from the PISA Project - FMUSP were obtained in high resolution and used here to demonstrate the concept. **Materials and Methods:** High resolution *in situ* images (600  $\mu$ m) from the whole brain of two previously healthy subjects were acquired in a 7T MR system (Siemens). T1-weighted images were submitted to the standard Freesurfer segmentation algorithm. After scanning, the brains were formalin-fixed, dehydrated, celloidin-mounted, cut into 400  $\mu$ m-thick serial

sections and finally stained with gallocyanin (a Nissl stain).. Digital images (resolution 600 dpi) were acquired by scanning the axial brain sections<sup>1,2</sup> of the histological slides. Template regions-of-interest (Freesurfer's aparc+aseg file) including bilateral dorsal anterior cingulate cortices (area 24b<sup>3</sup>) were segmented from histological images, and coregistered with the *in situ* images. Images were segmented using ImageJ and the processing included the following steps: straightening of the cortical layer identified in the axial brain slice; mean brightness across the cortical layer was calculated as a background value in comparison with the darker nuclear layers. The proportion of cell density - area under the curve (AUC) - was used to estimate the density of cells corresponding to each cortical layer; profile plots were used to identify the cortical layers; gray level indices were calculated and used as indicators of neuronal density [3] (Fig 1). **Results:** We were able to identify layers II and V by analyzing segmented images of the inferior frontal cortex. The proportion between the areas under the curve for layers II-III and V-VI was 0,66. Next step in this pipeline includes de definition of a ground truth method, relying upon in-depth segmentation for cell counting. **Discussion:** The results related to the proportion of cells inside each layer are in accordance with a stereological assessment of the dorsal anterior cingulate cortex in schizophrenia<sup>3</sup>. The authors found that there were more glial cells in the deep layers. The values found by Höistad et al. (2013) regarding the relative quantities of glial/neuronal cells in layers II-II and V-VI can be compared to the present results. The proportion of the found ratio (1,5/2,3) is in accordance with our result, thus encouraging further studies. **Conclusion:** The preliminary results show that our method has the potential to allow automatic cytoarchitectonic profiling from whole-brain thick-slice celloidin human samples registered to high-resolution MR images. This relational approach should also provide a basis for the automatic cortical quantification in *in vivo* MR. Further steps will include automatic processing in whole brain slices and calibration of gray values with neuron densities.

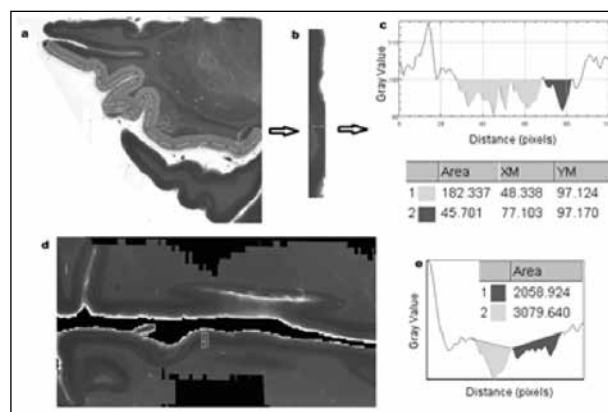


**Figure 2.** Proposed framework for calculating neuronal cell density on one slice of whole-brain microscopy. a) Cortical area is manually selected along the cortical area. b) The selection is straightened to allow batch processing. c) Profile plot indicating the locations of cortical neurons and values under the absorbance curve. d) Profile location inside an axial cut of the area 24b<sup>3</sup> of the left anterior cingulate cortex. e) Area under the absorbance curve for layers II-III (yellow) and V-VI (red).

**References:** [1] Heinsen H, et al. J Histotechnol. 1991;14:167-73; [2] Schleicher A, et al. Neuroimage. 1999;9:165-77; [3] Höistad M, et al. Neuropath and Applied Neurobiol. 2013;39:348-361.

#### MCP-1 IS RELATED WITH FUNCTIONAL CONNECTIVITY AND PHOSPHO-TAU PROTEIN IN AMNESTIC MILD COGNITIVE IMPAIRMENT

T. N. C. Magalhães<sup>1</sup>, C.V. L. Teixeira<sup>1</sup>, M. Weiler<sup>1</sup>, B. M. de Campos<sup>1</sup>, A. Moraes<sup>2</sup>, V. O. Boldrini<sup>2</sup>, L. M. B. Santos<sup>2</sup>, L. Talib<sup>4</sup>, O. Forlenza<sup>4</sup>, F. Cendes<sup>1,3</sup>, M. L. F. Balthazar<sup>1,3</sup>

<sup>1</sup>Neuroimaging Laboratory, Department of Neurology, University of Campinas, UNICAMP, 13083-888 Campinas, SP, Brazil; <sup>2</sup>Institute of Biology - University of Campinas, UNICAMP; <sup>3</sup>Unit for Neuropsychology and Neurolinguistics, Department of Neurology, University of Campinas, UNICAMP, Campinas, SP, Brazil; <sup>4</sup>Laboratory of Neuroscience (LIM-27), Department and Institute of Psychiatry, Faculty of Medicine, University of São Paulo, USP, São Paulo, SP, Brazil.

**Introduction:** Emerging evidence suggests that inflammatory events precede the clinical development of Alzheimer's Disease (AD), as cytokine dysregulation has been observed also in patients with amnesic Mild Cognitive Impairment (aMCI)<sup>1</sup>. Upregulation of a number of chemokines, including monocyte



chemotactic protein-1 (MCP-1), is associated with pathological changes. It has been shown that human monocytes expressing MCP-1 may contribute to the maturation of senile plaques and phosphorylation of protein Tau<sup>2</sup>. Inflammatory processes also play a role in pathological AD cascade, but their relationship with changes in functional connectivity (FC) of Default Mode Network (DMN) is still unknown. **Materials and Methods:** 227 individuals (117 aMCI and 110 mild AD) underwent MRI at 3T to evaluate DMN FC as well as cerebrospinal fluid (CSF) analysis of amyloid-beta, phospho-Tau (p-Tau), total-Tau and MCP-1. A DMN mask was used as a template to extract each patients FC value of the DMN subregions. We used BD CBA Human MCP-1 Flex Set kit to quantify MCP-1. We aimed to verify if MCP-1 levels were associated to DMN FC and AD CSF biomarkers. **Results:** In the aMCI group, MCP-1 was related with DMN left temporal FC ( $p = 0.032$ ,  $R = 0.507$ ); right hippocampal FC ( $p = 0.033$ ,  $R = 0.503$ ) and p-Tau ( $p = 0.023$ ,  $R = 0.354$ ), corrected to age. We did not find significant correlations in patients with mild AD. **Discussion:** This study showed that MCP-1 in our aMCI patients was related with increased FC of DMN and with p-Tau. These findings suggest that inflammation seen in the early phase of the disease is associated with subtle connectivity changes and with a marker of neurodegeneration. **Conclusion:** MCP-1 is related to different pathophysiological aspects of the predementia phase of AD (aMCI). Further studies are needed to evaluate MCP-1 reliability as an AD biomarker.

**References:** [1] Xia MQ, Hyman BT. *J Neurovirol.* 1999;5(1):32-4; [2] Petersen RC, et al. *Arch Neurol.* 1999;56(3):303-8.

#### OPEN SOURCE WEB-BASED TOOL FOR SELECTION OF THE SPECTRA OF INTEREST ON MAGNETIC RESONANCE SPECTROSCOPY IMAGING (MRSI)

D. P. Rodrigues<sup>1</sup>, S. Appenzeller<sup>2</sup>, L. Rittner<sup>1</sup>

<sup>1</sup> MIC Lab., FEEC, UNICAMP; <sup>2</sup> Rheumatology Dept., FCM, UNICAMP, Campinas, SP, Brazil.

**Introduction:** Magnetic resonance spectroscopy (MRS) has been widely used for studying metabolic alterations in diseases of the brain. The MRS uses signal from hydrogen protons to determine the concentrations of metabolites in organic molecules<sup>1</sup>. This paper aims to present a tool to analyze the region in magnetic resonance imaging (MRI) from where the spectra were collected, identifying the types of tissues (GM, WM and CSF) or structures (brain structures, tumors or lesions) and consequently allowing the selection of the spectra of interest. **Materials and Methods:** An open source web-based tool was developed using Python/Numpy in Adessowiki<sup>2</sup>, a collaborative environment for development of scientific computing algorithms. All images and spectra were acquired in a 3T scanner Philips installed at FCM / Unicamp. For each subject were acquired, with VOI's (MRSI) located in the corpus callosum and in the hippocampus. The region in MRI from where the spectra were collected was then analyzed and the percentage of tissues or the intersection with brain structures were computed. **Results:** The open source web-based tool has the following features: spatial location of the volume of interest (VOI) in the image (Figure 1), analysis of VOI content (Figure 2), selection of the spectra of interest and spectra visualization (Figure 3). **Discussion / Conclusion:** Currently, there is no tool that makes the automatic selection of the subset of the spectra of interest, often the selection of the spectra is performed manually. Through the tool will be possible a more precise analysis of the data acquired through the MRSI, grouping spectra from similar regions, such as tissues, brain structures, tumors or lesions.

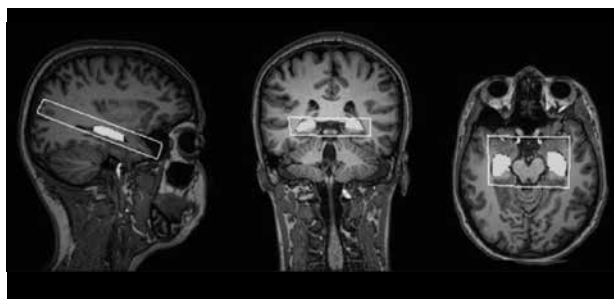


Figure2. Registration of image with the VOI (white) and the binary mask segmentation (yellow).

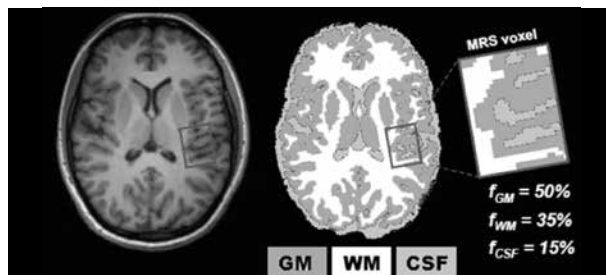


Figure2. Analysis of VOI content<sup>1</sup>.

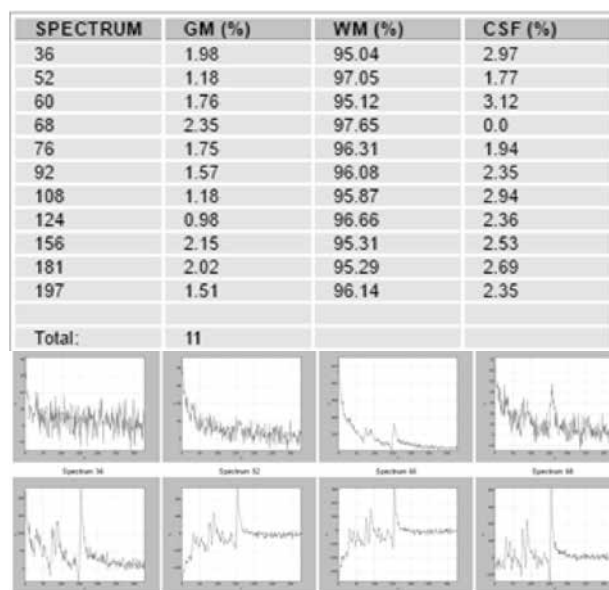


Figure3. Percentage of tissues computed in the VOI's analysis (left) and visualizing spectra (right).

**References:** [1] Salibi N, et al. *Clinical MR Spectroscopy: First Principles*, 1998; [2] Lotufo RA et al. *Proc. International Symposium on Wikis*, 2009, Orlando, Florida, USA; [3] Gussev A. 1H-MR spectroscopic detection of metabolic changes in pain processing brain regions in the presence of non-specific chronic low back pain, *Neuroimage*, 2011.

#### MULTIMODAL VISUALIZATION OF DTI GLYPHS FOR DIFFUSIVITY TENSOR ASSESSMENT

R. Voltoline<sup>1</sup>, C.L.Yasuda<sup>2</sup>, S-T. Wu<sup>1</sup>

<sup>1</sup>School of Electrical and Computer Engineering, UNICAMP; <sup>2</sup>School of Medical Sciences, UNICAMP, Campinas, SP, Brazil.

**Introduction:** Through diffusion of the water molecules, diffusion tensor imaging (DTI) can reveal information about the structure of tissues at a macroscopic level, allowing the assessment of the neural tracts and the connectivity of the brain. DTI has, therefore, emerged as a promising tool for studying some diseases, such as ischemic stroke and neural tract disorder<sup>1</sup>. However, it is an approximate technique and relies strongly on the signal sampled and the sample resolution. When tensors are not well-estimated, it can lead to misinterpretation. Glyphs may be used for quality control of a second order diffusion tensor estimation<sup>2</sup>. Superquadratic glyphs have been shown to outperform with respect to directional ambiguity and spatial perception<sup>3</sup>. Co-localization of the glyphs with the anatomical structure can improve the visual assessment. The goal of this work is to develop a multimodal visualization of superquadratic glyphs and T1-weighted magnetic resonance images (MRI). **Materials and Methods:** For each visible voxel of a DTI volume, we draw the corresponding superquadratic glyph in its center. The glyphs are resized with the smallest dimension of the voxel and colored with a novel colormap we proposed<sup>4</sup>. Each diffusivity tensor is co-located with the cerebral structure through the co-registration<sup>5</sup> of the non-diffusion weighted ( $b=0$ ) and the T1-weighted MRI. The robust estimator with outlier rejection (RESTORE)<sup>6</sup> is used to obtain the second order positive semidefinite tensors from the diffusion-weighted images (DWI). The algorithm

is integrated into the in-house developed VMTK<sup>7</sup>. **Results:** The co-registered axial images of MRI-T1 (in grayscale) and DTI (in colored glyphs) display the diffusivity in the corpus callosum of a healthy control (a) and a patient suffering from subcortical band heterotopia (b). The glyphs of anisotropic DWI voxels are illustrated in the sagittal view of the inferior longitudinal fasciculus (c). Their corresponding regions in MRI-T1 slices are highlighted on the images at the top right corner. Together with the anatomical knowledge, clinicians can visually assess the quality of the estimated tensors. **Discussion:** The procedure is implemented on a GPU, making the images conducive to the visual exploration. Because voxels are mostly anisotropic, the occupancy of the glyphs on the screen is suboptimal (Figure c). This problem can be overcome by resampling either the DWI volumes or the corresponding tensor volume. Nevertheless, superquadric glyphs are not appropriate for visualizing higher order tensors that are promising for representing fiber crossing and fiber kissing. **Conclusion:** We proposed a way to display estimated diffusivity tensors that is useful not only in assessing the estimated tensors but also in evaluating the diffusivity in a larger tensor field as well. Despite limitations, this visualization tool may be helpful in the reconstruction of neural tracts.

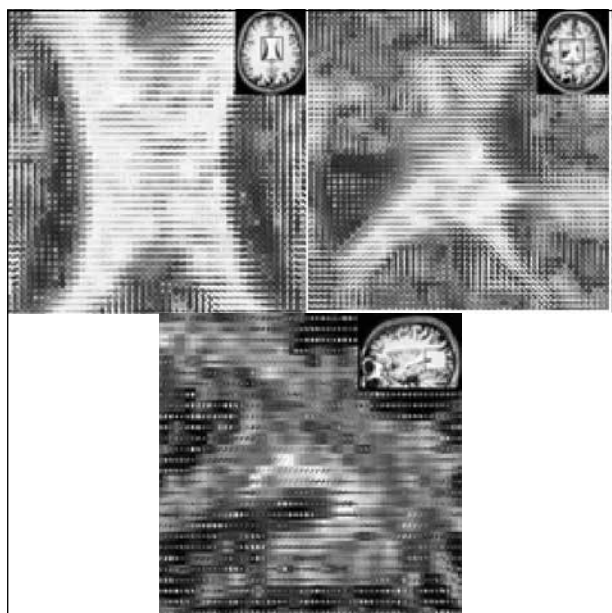


Figure 1.

**References:** [1] Lerner A, et al. *World Neurosurg*. 2014;82(1-2):96-109; [2] Soares JM, et al. *Front Neurosci*. 2013;12:7-31; [3] Kindlmann G. *IEEE VGTC Symposium on Visualization*. 2004;147-54; [4] Wu S-T, Voltoline R, Yasuda CL. *Computers & Graphics*. 2016;60:66-75; [5] Valente AC, S-T Wu. *Siggrapi* 2012;1-6; [6] Chang LC, Jones DK, Pierpaoli C. *Magn Reson Med*. 2005;53(5):1088-95; [7] VMTK. [http://www.dca.fee.unicamp.br/projects/mtk/wu\\_loos\\_voltoline\\_rubianes/index.html](http://www.dca.fee.unicamp.br/projects/mtk/wu_loos_voltoline_rubianes/index.html).

#### SEIZURE CONTROL AND HIPPOCAMPAL SCLEROSIS ARE RELATED TO METABOLIC ALTERATIONS IN MESIAL TEMPORAL LOBE EPILEPSY.

L.R. Pimentel-Silva<sup>1</sup>, R.F. Casseb<sup>1</sup>, M.K.M. Alvim, R. Barbosa<sup>1</sup>, N. Volpato<sup>1</sup>, M.H. Nogueira<sup>1</sup>, C.L. Yasuda<sup>1</sup>, F. Cendes<sup>1</sup>

<sup>1</sup>Neurology Dept., FCM, UNICAMP, <sup>2</sup>Neurophysics Group, IFGW, UNICAMP, Campinas, SP, Brazil.

**Introduction:** Proton magnetic resonance spectroscopy (<sup>1</sup>H-MRS) is able to detect subtle abnormal changes in brain tissue<sup>1</sup>. In mesial Temporal Lobe Epilepsy (mTLE) these abnormalities may be ipsi- or contralateral to the underlying lesion or even bilateral. Moreover, some alterations are biomarkers of poor response to antiepileptic drugs (AED)<sup>2</sup>. However, findings are contradictory: some studies show n-acetylaspartate abnormalities restrict to the hippocampus whilst others show more broad, extrahippocampal alterations. In its turn, glutamate might be increased or decreased in the hippocampus of mTLE patients<sup>1</sup>. Here we investigated whether metabolic alterations are different in patients with left, right or negative MRI mTLE patients (RTLE, LTLE, MRI-neg, respectively) related to two specific characteristics: (1) the presence and side of HS and (2) pharmacoresponse to DAEs. **Materials and Methods:** Our cohort consisted of 101

consecutive unilateral mTLE patients with or without (MRI-neg) visual signs of HS on MRI. They were divided into poor (PSz), good AED response (GSz) and 50 healthy controls. <sup>1</sup>H-MRS data was acquired in a 3T scanner (Philips Achieva) using a single voxel PRESS (Point Resolved Spectroscopy) sequence with repetition time (TR) = 2000msec and echo time (TE) = 35msec. Spectra were then quantified ipsi- and contralateral to the lesion (MRI negative patients were lateralized according to EEG) or considering left and right hippocampi, using LCModel. We used SPSS (IBM, Version 22.0) for statistical analysis. Metabolic data on n-acetylaspartate plus n-acetylglutamate (NAAt) and glutamate plus glutamine (Glx) ratios in terms of creatine in mTLE patients and healthy controls was compared between groups using MANCOVA co-varying for age. No serious violations of the statistical assumptions to perform this test were found. **Results:** MANCOVA showed a statically significant difference regarding seizure control groups on both ipsi- and contralateral measures of NAAt and Glx (F (8, 240) = 4.55, p < .0001). Pairwise analysis with Bonferroni correction for multiple comparisons revealed an ipsilateral reduction of NAAt in PSz compared to GSz (p < .0001) and controls (p = .001). NAAt is also reduced contralaterally in PSz group compared to controls (p = .001). Glx is reduced only ipsilateral to the lesion compared to GSz (p = .04) and control groups (p = .002). Regarding left and right hippocampal quantification of NAAt and Glx, there is a statistically significant difference between the groups studied (F (12, 363) = 2.44, p = .004) but only in the quantification of NAAt. We found a statistically significant NAAt decrease both ipsi and contralateral to HS in LTLE compared to controls (p < .0001 and p = .003, respectively) whilst RTLE showed only ipsilateral reduction when compared to controls (p = .003). There were no left nor right hippocampal Glx alterations between these groups. **Discussion:** We found a ipsilateral reduction of NAAt in PSz patients, corroborating the literature<sup>1,2</sup> and a bilateral decrease in LTLE. We also found an ipsilateral reduction of Glx related to a poorer seizure control. There is only one study addressing the role of HS side in metabolic alterations, which show worse findings for RTLE in the temporal cortex<sup>3</sup>. However, our result might be due to an homogenous cohort, the different region of interest and also a matter of interpretation, since studies on different techniques show evidences on altered results for LTLE<sup>4</sup>. On the same way, our results for Glx might reflect the more appropriated study design. Other studies do not consider systematically the effects of seizure control and presence of HS[1]. **Conclusion:** Our results suggest that abnormalities in NAA might go beyond the lesion and affect both hippocampi, reflecting structural and functional damage whilst Glx alterations might be related to the pattern of AED response rather than the presence of HS, indicating functional damage.

**References:** [1] Pimentel-Silva LR, et al. *Journal of Epilepsy and Clinical Neurophysiology*. 2015; (4):136-43; [2] Campos BAG, et al. *Epilepsia*. 2010;51(5):783-88; [3] Zubler F, et al. *J Neurol Neurosurg Psychiatry*. 2003;74:1240-4; [4] Ahmadi ME, et al. *AJNR Am J Neuroradiol*. 2009;30(9):1740-7.

#### IDENTIFICATION OF THE DISTRIBUTION OF HLA ALLELES IN THE BRAZILIAN POPULATION AND IN NEUROLOGICAL PHENOTYPES POSSIBLY ASSOCIATED WITH AUTOIMMUNITY

T. K. de Araujo<sup>1</sup>, N. Watanabe<sup>2</sup>, R. Barbosa<sup>2</sup>, F. Cendes<sup>2</sup>, I. Lopes-Cendes<sup>1</sup>

<sup>1</sup>Department of Medical Genetics; <sup>2</sup>Department of Neurology; School of Medical Sciences, University of Campinas, UNICAMP, Campinas, São Paulo, SP, Brazil; and the Brazilian Institute of Neuroscience and Neurotechnology, Campinas, SP, Brazil.

**Introduction:** The Human Leucocyte Antigen (HLA) genes, located at chromosome 6p21.3, are involved in susceptibility to more than 100 diseases of inflammatory, infectious and autoimmune nature<sup>1</sup>. With a density of single nucleotide polymorphisms (SNPs) significantly higher than most regions, HLA is among the most polymorphic regions of the human genome and presents considerable diversity among populations. Despite the importance of identifying and linking HLA types to the clinical condition there are very few databases that are dedicated to characterize HLA alleles in various populations. The knowledge about autoimmune encephalitis has undergone a real revolution in recent years, since its recognition as an etiology of several severe acute and chronic neurological conditions has only been widely determined in the last 5 years. Autoimmune encephalitis is an inflammatory disorder characterized by a subacute impairment of short-term memory, psychiatric features and seizures. It is often associated with a variety of other neurological symptoms, and its differential diagnosis is wide, leading to challenges in its recognition. It used to be regarded as a rare disease, usually paraneoplastic and with poor prognosis. However, with the recent recognition of membrane-surface directed

antibodies, it is now known that in a substantial proportion of patients there is no association with any malignancy and there is a good prognosis if treated. Sequencing the HLA region can provide critical insight into various immune disorders. There are no studies investigating the role of HLA in autoimmune encephalitis. Therefore, this study aims to identify HLA alleles distribution in Brazilian population (300 control subjects) and to identify a possible association between HLA alleles and autoimmune encephalitis (300 patients). **Material and Methods:** To date, we have collected 300 samples of the control group and approximately 50 samples of the patients group. The HLA genotyping has been performed through TruSight HLA v2 Sequencing Panel, Illumina. This panel provides an assay to obtain ultrahigh resolution sequencing of 11 HLA Loci (Class I HLA-A, -B, -C; Class II HLA-DRB1/3/4/5, -DQA1, -DQB1, -DPA1, -DPB1) and the prepared libraries are loaded directly onto a MiSeq System for sequencing. The HLA locus is sequenced with paired-end 2 × 150 bp reads and the generated data are analyzed with TruSight HLA Assign 2.0 software. **Results:** This is an ongoing study and currently, we are performing sequencing of the samples already collected and getting good quality data. The Q30 read quality scores are on average above 86.6%. We will evaluate the association of the HLA variants with risk of autoimmune encephalitis using a logistic regression model assuming additive effects of allele dosages on a log-odds scale. **Discussion/Conclusion:** When the works is concluded, we hope to discover specific haplotypes that are predisposing to autoimmune encephalitis. In addition, our data will also be compared to that generated by high density SNP panels in the same sample and in other population, helping to establish a high resolution map of the HLA region in the Brazilian population, which will be made publically available at [www.bipmed.org](http://www.bipmed.org). Overall our study will contribute to a better understanding of the role of HLA variants in health and disease.

**Referências:** [1] Trowsdale J, et al. *Annu Rev Genomics Hum Genet.* 30(1):14-301.

**Supported by:** FAPESP, CNPq.

#### DETERMINING THE BURDEN OF COPY NUMBER VARIATION IN PATIENTS WITH EPILEPSY

T. K. de Araujo<sup>1</sup>, F. R. Torres<sup>1</sup>, R. Secolin<sup>1</sup>, M. K. M. Alvim<sup>2</sup>, C. S. Rocha<sup>3</sup>, M. E. Morita<sup>2</sup>, C. L. Yasuda<sup>2</sup>, B. S. Carvalho<sup>3</sup>, F. Cendes<sup>2</sup>, I. Lopes-Cendes<sup>1</sup>

<sup>1</sup>Department of Medical Genetics; <sup>2</sup>Department of Neurology, School of Medical Sciences; <sup>3</sup>Department of Statistics, Institute of Mathematics, Statistics and Scientific Computing; University of Campinas, UNICAMP; and the Brazilian Institute of Neuroscience and Neurotechnology, BRAINN, Campinas, São Paulo, SP, Brazil.

**Introduction:** Mesial temporal lobe epilepsy (MTLE) and genetic generalized epilepsy (GGE) are the most common epilepsy syndromes. Recently, genomic copy number variations (CNVs) have been identified as a risk factor for some types of epilepsy syndromes. The objective of this study is: i) to investigate the distribution of CNVs in patients with MTLE and GGE, as well as in control subjects; ii) to evaluate recurrence of CNVs in patients; and iii) to identify genes potentially involved in the genetic predisposition to MTLE and GGE within the regions of CNVs found exclusive in patients. **Material and Methods:** To date, we have studied a total of 750 individuals (340 patients with MTLE, 70 patients with GGE and 340 control subjects). CNVs were assessed by the Affymetrix Genome-Wide Human SNP 6.0 array (Affymetrix, Santa Clara, CA, USA). We analyzed CNVs that were > 100kb and that span at least 25 probes for deletions and 50 probes for duplications. **Results:** The analysis of MTLE patients identified 2,246 CNVs (56.4% gains and 43.6% losses). CNV average size was 280 kb, ranging from 100 kb to 2 Mb. Among all CNVs identified, 456 (20.3%) were found only in patients with MTLE and they were absent in controls. A total of 652 RefSeq genes are affected by these CNVs. Using the Metacore software we found an enrichment of genes associated with the following pathways: neurogenesis development and synaptogenesis, learning or memory, cognition, pre-pulse inhibition, ion transport, protein complex assembly involved in synapse maturation, calcium ion transmembrane transport and single-organism behavior. In addition, chromosomal regions more affected by these CNVs were 2q14.2, 2q24.1, 9p24.2, 13q33.3, 14q13.1, 14q23.2, 15q21.2, 16p13.11, 16q22.1, 17q12, 17q25.3, 22q11.21, 22q12.1. In patients with GGE, we identified 340 CNVs (49% gains and 51% losses). CNV average size was 342 kb, ranging from 100 kb to 2Mb. Among all CNVs identified, 59 (17.4%) were found only in patients with GGE and were absent in controls. A total of 59 RefSeq genes are affected by these CNVs. Analysis using Metacore software revealed an enrichment of genes associated with the following pathways: lithium

effect on synaptic transmission and autophagy, glutamic acid regulation of dopamine D1A receptor signaling, mitochondrial dysfunction in neurodegenerative diseases, dopamine D2 receptor transactivation of PDGFR in CNS, GABA-B receptor-mediated regulation of glutamate signaling in Purkinje cells, nicotine signaling in dopaminergic neurons, dopamine D2 receptor signaling in CNS. Chromosomal regions more affected by CNVs were 3p21.2, 6p11.2 and 20p12.3. Finally, analysis of the control group identified 2,100 CNVs (55.1% gains and 44.9% losses). The CNV average size was 327 kb, ranging from 100 kb to 2 Mb. Chromosomal regions more affected by CNVs in controls subjects are: 1q21.1, 1q21.2, 1p36.13, 2q11.2, 3q26.1, 4q13.2, 8p11.22, 8p23.1, 10q11.22, 14q11.2, 15q11.2, 15q11.1, 16p11.2, 17q21.31. **Discussion/Conclusion:** Our results clearly show that there is an increased burden of CNVs in specific chromosomal regions of the genome in patients with epilepsy. These regions are distinct in patients with MTLE as compared to patients with GGE, indicating that the genetic burden, in these two different epilepsy syndromes, is distinct. We identified structural variants that affect neurodevelopmental genes that have a strong impact in crucial neural pathways, leading to epilepsy syndromes. Interestingly, CNVs previously associated with epilepsy syndromes in the literature (1q21.1, 15q11.2, 16p11.2) were also identified in subjects of our control group the significance of which is still unclear.

**Supported by:** FAPESP, SP, Brazil; CNPq.

#### <sup>1</sup>H-MAGNETIC RESONANCE SPECTROSCOPY IN THE RAT MODEL OF TEMPORAL LOBE EPILEPSY INDUCED BY PERFORANT PATHWAY STIMULATION

R. Barbosa<sup>1</sup>, A. H. B. Matos<sup>2</sup>, B. M. Campos<sup>1</sup>, R. F. Casseb<sup>3</sup>, L. R. Pimentel-Silva<sup>1</sup>, J. Francischini<sup>1</sup>, M. M. Cordeiro<sup>1</sup>, R. Gilioli<sup>4</sup>, I. Lopes-Cendes<sup>2,5</sup>, A. S. Vieira<sup>2</sup>, F. Cendes<sup>1,6</sup>

<sup>1</sup>Neuroimaging Laboratory, UNICAMP; <sup>2</sup>Molecular Genetics Laboratory, FCM, UNICAMP; <sup>3</sup>Medical Physics Laboratory, UNICAMP; <sup>4</sup>Multidisciplinary Center for Biological Investigation on Laboratory Animal Science, UNICAMP; <sup>5</sup>Department of Medical Genetics, FCM, UNICAMP; <sup>6</sup>Department of Neurology, FCM, UNICAMP, Campinas, São Paulo, SP, Brazil.

**Introduction:** <sup>1</sup>H-magnetic resonance spectroscopy (<sup>1</sup>H-MRS) is a non-invasive neuroimaging modality able to quantify the variability of metabolic injury usually found in humans and animal models in temporal lobe epilepsy. Quantification of the different metabolic levels may help in the identification of the epileptic focus, optimization of clinical diagnosis, drug treatment and to determine the patient clinical prognosis. This study aimed to evaluate <sup>1</sup>H-MRS in a rat model of temporal lobe epilepsy, which does not show *status epilepticus*, induced by perforant pathway stimulation. **Materials and Methods:** 6 male *Wistar* rats *in vivo* at 12 weeks old were studied and divided into 2 groups: Sham control group (4) and Electrical stimulation group (n=2). A 3-T Philips scanner was used with an 8 integrated channels volumetric coil (Rapid Biomedical GmbH, Würzburg, Germany). Spectra from all animals were obtained in the hippocampus using a single voxel with point-resolved spectroscopy (PRESS) at TE/TR: 135/2000ms and size of the VOI (Voxel of Interest): 5 × 8.5 × 9 mm<sup>3</sup>. We performed a <sup>1</sup>H-MRS acquisition before the electrical stimulation using the perforant pathway to have a baseline data from the animals. New spectra acquisitions were obtained after 48 hours, 15 days, and 30 days after the electrical stimulation. According to this electrical stimulation model, bilateral bipolar electrodes were implanted in all rats' brains and one week after the surgery a recovery sequence of stimulation was performed with a Grass Astro-Med S88 stimulus generator (paired pulses, 0.1-ms pulse duration, interpulse interval of 40ms, and pulse amplitude of 20V). In the first two days a 30 min. stimulation sequence was performed and followed by 8 hours stimulation on the thirtieth day. The same procedures were used for the Sham control group, however they were not stimulated. The automatic quantification of metabolic levels from <sup>1</sup>H-MRS was performed using the LCModel software. Only good quality spectra with <15% of error using Cramér-Rao lower bounds were included. Metabolites were expressed in terms of their ratio to Creatine+Phosphocreatine. **Results:** Our results are preliminary from a longitudinal research which is currently being developed. There are no studies published in literature regarding the description of <sup>1</sup>H-MRS with this experimental model of temporal lobe epilepsy. This protocol has been shown to be efficient for metabolic quantification; however we will include more animals in our future analysis in an attempt to achieve a sample with significant statistical power. **Discussion:** Changes in chemical compounds in epilepsy are common and may reflect glial and neuronal impair-



ment. Abnormalities in N-Acetyl aspartate (NAA) concentration may evidence neuronal loss or dysfunction in mitochondrial metabolism, and they are related to the epileptogenic zone in mesial temporal sclerosis. **Conclusion:** <sup>1</sup>H-MRS could help to identify biomarkers linked to mechanisms of the epileptogenesis and follow the efficiency of antiepileptic drug therapy and epilepsy progression.

**References:** [1] Norwood BA, et al. *J Comp Neurol*. 2010;18(16):3381-407; [2] Gülin Öz, et al. *Radiology*. 2014;270(3):658-79; [3] Pearce PS, et al. *Epilepsia*. 2016;57(12):1978-1986.

#### AEROBIC PHYSICAL EXERCISE PROGRAM CAN IMPROVE QUALITY OF LIFE IN PATIENTS WITH TEMPORAL LOBE EPILEPSY

N. Volpato<sup>1</sup>, J. Kobashigawa<sup>1</sup>, C.L. Yasuda<sup>1</sup>, F. Cendes<sup>1</sup>

<sup>1</sup>Laboratory of Neuroimaging, FCM, UNICAMP, Campinas, São Paulo, SP, Brazil.

**Introduction:** Epilepsy is a frequent neurologic disorder, with variable clinical manifestations. Temporal Lobe Epilepsy (TLE) is the most common epileptic syndrome in adults, and one of the most refractory to antiepileptic drugs. The diagnosis of TLE leads to changes in how patients picture themselves in their social and economic circles, and usually affects their future plans. Therefore, this diagnosis endangers not only their physical health but also compromises their quality of life (QOL). Ideally, the treatment of epilepsy should go beyond the seizure control, and include complementary actions to improve both well being and emotional state. Despite the scientific evidences showing that physical exercise (PE) contributes to QOL of subjects with different pathologies, there are still controversies related to the benefits of PE to people with epilepsy. The objective of the present study was to evaluate the effect of 16 weeks of an aerobic physical exercise program in the aerobic capacity, and QOL of patients with TLE. **Materials and Methods:** We recruited 25 TLE patients, divided in two groups: the training group (T), which practiced the aerobic physical exercise program, and the control group (C), which was instructed to maintain their normal daily habits. Both groups underwent all procedures before and after period of intervention. Quality of life: was evaluated with QOLIE31 (it evaluates the total score of QOL, along with seven sub-items). Maximal effort cardiopulmonary test in treadmill: A graded protocol was used to determine the individual VO<sub>2</sub>max. Aerobic physical exercise program: The PE program was based on sessions of walking exercise, twice a week, during 16 weeks. Each session lasted 60 minutes, with the intensity based on the individual aerobic threshold identified during the maximal effort test. Statistical Analysis: Using the software SYSTAT 9 (SPSS Inc., Chicago, IL), we conducted paired t-tests and Wilcoxon tests to compare variables before and after exercise. **Results:** Before the intervention: we didn't observe significant group differences, regarding QOL, the sub-items, and aerobic physical capacity (VO<sub>2</sub>max). After the period of intervention: group T presented significant improvement of 31% in total score of QOL, and the sub-items: Seizure Worry, Overall Quality of Life, Well-Being, Energy/Fatigue, Cognitive and Social Function. In addition, there was an improvement of 6% in aerobic physical capacity. Although the group C presented a significant decrease of 11% in total score of QOL (p=0.03), and in the sub-items (Well-Being, Cognitive and Social Function), the aerobic physical capacity was maintained. After all, there were differences between groups, with better QOL, well being and cognitive function for Group T. **Discussion:** People with epilepsy, especially refractory to treatment, are prone to an inactive lifestyle; therefore, these patients should be counseled by doctors, physical educators and health professionals about the health risks over the sedentary lifestyle and the fear of risk of injury during a PE session. Taking into account the low risk and the benefits of PE for this population, strong efforts should be directed to stimulate PE. Ideally, we hope that in the future such actions can be offered as part of a more global approach for all subjects with epilepsy. **Conclusion:** The intervention of 16 weeks of aerobic PE was effective to increase the TLE patient's QOL and physical capacity, showing that it can be a complementary action to the conventional treatment, improving the general health as the well being.

**References:** [1] De Oliveira GNM, et al. *Seizure*. 2010;19(8):479-84; [2] Arida RM, et al. *Annals of Indian Academy of Neurology*. 2012;15(2):167. [3] De Lima C, et al. *Epilepsy & Behavior*. 2013;28(1):47-51.

#### EFFECTS OF AEROBIC EXERCISE ON PROGRESSION OF HIPPOCAMPAL VOLUME AND COGNITION IN AMNESTIC MILD COGNITIVE IMPAIRMENT DUE TO AD

B. V. L. Teixeira<sup>1</sup>, T. J. Rezende<sup>2</sup>, T. N. Magalhães<sup>1</sup>, M. Weiler<sup>3</sup>, A. F. M. K. C. Cassani<sup>4</sup>, D. Q. de Almeida<sup>5</sup>, T. Q. A. C. Silva<sup>6</sup>, H. P. G. Joaquim<sup>5</sup>, L. L. Talib<sup>5</sup>, O. V. Forlenza<sup>5</sup>, M. P. Franco<sup>6</sup>, P. E. Nechio<sup>7</sup>, P. T. Fernandes<sup>6</sup>, F. Cendes<sup>1,7</sup>, M. L. F. Balthazar<sup>1,7</sup>

<sup>1</sup>NeuroImage laboratory, FCM-UNICAMP, Campinas, Brazil; <sup>2</sup>Medical Physics laboratory, IFGW-UNICAMP, Campinas, Brazil; <sup>3</sup>National Institute of Health, Baltimore, MD, USA; <sup>4</sup> Department of Cardiology, UNICAMP, Campinas, Brazil; <sup>5</sup>Laboratory of Neuroscience, Institut of Psychiatry-USP, São Paulo, Brazil; <sup>6</sup> Physical Education Faculty, UNICAMP, Campinas, São Paulo, SP, Brazil; <sup>7</sup> Neurology Dept, FCM-UNICAMP, Campinas, São Paulo, SP, Brazil.

**Introduction:** Increasing evidence demonstrates that physical exercise is an important modifiable factor not only for cardiovascular fitness, but also for brain health and dementia prevention. However, it is not clear how supervised physical exercise can affect cognition and biomarkers in patients with amnesic mild cognitive impairment (aMCI) due to Alzheimer's disease (AD). In this study, we aimed to evaluate six months of supervised aerobic training on hippocampus volume in aMCI subjects with CSF positive AD biomarkers (low A $\beta_{1-42}$  and/or low A $\beta_{1-42}$ /p-tau). **Materials and Methods:** 19 aMCI (mean age of 70,6  $\pm$  7,6 years old) subjects were diagnosed using the core criteria of the NIA/AA for MCI and presented positive CSF AD biomarkers. All patients underwent neurocognitive tests, which included Mini Mental State Examination (MMSE) and Rey Auditory-Verbal Learning Test, and a structural MRI at 3.0T. Hippocampal volume was analyzed using FreeSurfer software (<https://surfer.nmr.mgh.harvard.edu/>). A graded maximal exercise test on a motor-driven treadmill assessed aerobic fitness (measured by VO<sub>2</sub>maximum). Participants were divided into Aerobic group (AG, 9 patients with supervised exercise 3 times per week for 6 months) and control group (CG, 10 patients with non-supervised exercise). The groups were controlled for age, sex, and education. **Results:** General Linear Model for repetitive measures showed a significant improvement in aerobic fitness, indicating that while AG improved VO<sub>2</sub>maximum, CG decreased (p<0.009). CG presented a significant decrease in the MMSE, Right hippocampus volume and a tendency in left hippocampus volume (p<0.033, p<0.05, p<0.082, respectively), while these variables did not change in the AG over time. **Discussion:** The present results show that physical exercise may play an important role on changes in synaptic interconnections, axonal integrity and capillary bed growth, which could be explained with changes in growth factors such as Brain-derived neurotrophic factor<sup>1</sup>. Some studies with healthy cognitive elderly have shown an improvement in cognitive functions and increase in brain volume<sup>2,3</sup>. Even though our studied presented patients with high-risk to develop AD, they benefited from aerobic exercise. **Conclusion:** Six months of supervised aerobic exercise seems to be effective, not only for improving aerobic fitness, but also in maintaining global cognitive functions and hippocampus volume in aMCI subjects due to AD.

**References:** [1] Voss MW, et al. Neurobiological markers of exercise-related brain plasticity in older adults. *Brain Behav Immun*. 2013;28:90-9. [2] Colcombe SJ, et al. Aerobic fitness reduces brain tissue loss in aging humans. *J Gerontol A Biol Sci Med Sci*. 2003;58(2):176-80. [3] Colcombe SJ, et al. Aerobic exercise training increases brain volume in aging humans. *J Gerontol A Biol Sci Med Sci*. United States. 2006;61:1166-70.

#### EFFECT OF ORTHOGRAPHIC NEIGHBORHOOD DENSITY IN READING

K. Lukasova<sup>1,3</sup>, T. Vasconcelos<sup>2</sup>, D. Gomes<sup>2</sup>, E. Amaro<sup>3</sup>

<sup>1</sup>CMCC, UFABC, São Paulo; <sup>2</sup>Faculty of Psychology, CRUZEIRO DO SUL, São Paulo; <sup>3</sup>NIF/LIM44, FMUSP, São Paulo, SP, Brazil.

**Introduction:** Reading can be facilitated in words with high orthographic neighborhood density (N), that refers to the number of new real words that can be made by one letter substitutions in the target (eg. well, sell). High N words are recognized faster than low N words and this effect is believed to be due to parallel activation of lexical and sublexical units (Braun et al., 2015). The aim of this study was to assess the feasibility of identifying neural circuits in healthy adults for N manipulated words/pseudowords and transposed pseudowords. **Materials and Methods:** 10 healthy university students participated in the study and all signed the informed consent approved by the Ethics Committee of the university (FMUSP 089/11). All participants were screened for reading and general cognitive functioning. Silent reading was assessed in MR scanner by a block procedure composed of 100 words and 100 pseudowords. 50 stimuli of each group were words and pseudowords with low orthographic neighborhood density (N0) and 50 stimuli with high density (N3+). The pseudowords N0 were created by letter inversion and N3+ by letter substitution. The compliance with the task was verified by integrated eye tracking. Images were acquired in a 3T scanner (Philips Achieva). Single shot echo planar imaging with sensitivity-encoded was used with parameters repetition time (TR)=2000ms, echo time (TE)=30ms, flip angle=90°, slice thickness=3.0mm, gap=0, matrix=80

x 77 pixels. The total duration was approximately 8 minutes. **Results:** Reading non-familiar words compared to familiar words ( $N0 < N3+$ ) activated the right angular gyrus. Comparison of high-density pseudowords and words activated bilaterally fusiform gyrus, superior parietal cortex and postcentral gyrus. Left hemisphere activation was found in middle and inferior frontal gyrus and temporal gyrus. Reading of transposed pseudowords (pseudowords  $N0 >$  words  $N0$ ) activated the same regions but in a much larger extension especially in the parietal cortex extending into the inferior portion, left temporal cortex and frontal eye fields in the frontal cortex (Figure 1A-1C). **Discussion:** The results showed that the activation of reading circuitry changed due to the orthographic density effect. The most interesting finding was the activation of right angular gyrus in the low-density real words that indicate right hemisphere participation in lexical access. The activated regions related to transposed pseudowords showed lexico-semantic activity but also fronto-parietal activation related to attentional and visual analyses. **Conclusion:** The present work confirmed that paradigms manipulating words/pseudowords orthographic neighborhood density proved to identify subjacent neural activation and can be used in clinical population such as Developmental dyslexia.

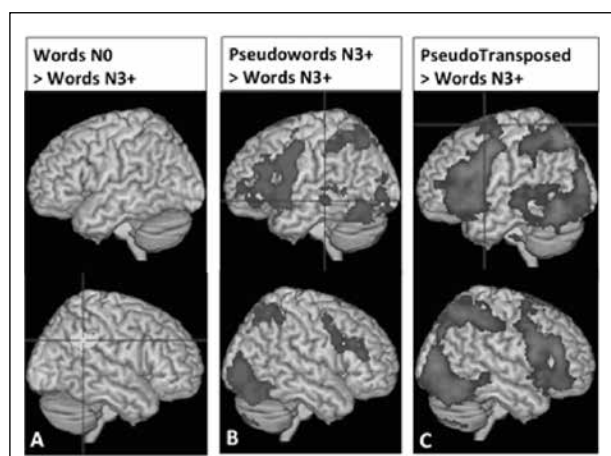


**Figure 1.** Left and right hemisphere representation of activation during reading task in healthy adults ( $N=10$ ). A) Low ( $N0$ ) and high ( $N3+$ ) orthographic neighborhood density words contrast with activation in right angular gyrus. B) Pseudowords  $N3+ >$  Words  $N3+$  activated in left middle temporal gyrus (cross) and inferior frontal gyrus, bilateral superior parietal and fusiform gyrus. C) PseudoTransposed  $>$  Words  $N3+$  contrast shows bilateral frontal eye field activation (cross), middle and inferior frontal gyrus, middle and inferior temporal gyrus, superior and inferior parietal cortex and occipital cortex [cluster  $Z > 2.3$ ;  $p < 0.05$ ; the scale depicted in the figure  $Z = 2.3$  to  $4.0$ ; brain template MNI152].

**References:** [1] Braun M, et al., *Frontiers in Human Neuroscience*. 2015;9(423):1-13.

#### PREDICTION OF TEMPORAL DECISION BASED ON ELECTROPHYSIOLOGICAL ACTIVITY OF RATS PRE-FRONTAL CORTEX

G. C. Tunes<sup>1</sup>, M. B. Reyes<sup>1</sup>, D. C. Soriano<sup>2,3</sup>

<sup>1</sup>CMCC; UFABC; <sup>2</sup>CECS, UFABC; <sup>3</sup>Brazilian Institute of Neuroscience and Neurotechnology, BRAINN.

**Introduction:** Time is an intrinsic variable in animal behavior. It is important for surviving. For instance, when a predator is hunting, it has to estimate precisely the prey time reaction, so it will have its dinner. The neural basis of time perception has been a target of several studies<sup>1</sup>. The involvement in several regions and some types of neurons was found in animals trained in tasks that require some temporal organizations learning. Neurons that seem to encode a time interval were described on the hippocampus, thalamus, and prefrontal cortex. Furthermore, cells that present several types of electrophysiologic behavior were identified, for instance, some neurons increase (or decrease) their spike rate linearly, or some neurons that fire in specific time instants after a start cue<sup>2,3</sup>. By developing a classification algorithm for temporal decision it is possible to study and extract information and features from neurons, and to determine the population that is correlated to time perception. **Materials and Methods:** We recorded 165 neurons from the prefrontal cortex of 3 implanted rats. The data was recorded while the animal was performing a temporal perception task named DRRD (Differential Reinforcement Response Duration). At this task,

the rats should hold his nose at the nose poke through an interval time equal or larger than 1500 ms to win a reinforcement (glucose solution). The data was recorded and processed by TDT (Tucker-Davis Technologies) hardware and software. In order to develop the classification algorithm, we selected the intervals that the rats held on his response through at least 1000 ms up to 2000 ms. By considering a 1 ms bin interval we constructed an adjacency matrix of the delays between spikes of two different neurons. The algorithm developed compared an adjacency matrix of each trial, with a template of trials corrects and incorrect, to classify this as a correct or incorrect trial. To compare the trials with the template we used the mean square error between the adjacency matrixes. To evaluate the algorithm efficacy we constructed a confusion matrix. **Results:** After repeating the classification procedure one hundred times for each rat, we get the mean and median of the confusion matrixes. The results suggest an aleatory classification algorithm since the percentage of correct judged trials was fifty percent or around this value. Below, we present the mean  $\pm$  standard deviation confusion matrix of one rat. **Discussion:** The results show that the classification algorithm was not able to distinguish correct from incorrect trials. There are two possible explanations for these results. First, there is no correlation between time perception and firing rate of neuron pairs. Second, the classification algorithm needs to be refined in order to select neurons and bins that are important to distinguish the groups of the trials considered. **Conclusion:** The classification algorithm developed until now was not able to classify trials correct and incorrect. We intend to implement different types of classification algorithm in the future, to select the relevant features of the data.

**Table 1.** Mean Confusion Matrix of one rat.

Mean $\pm$ STD	
25 $\pm$ 25.10	26 $\pm$ 25.10
24 $\pm$ 25.10	26 $\pm$ 25.10

**References:** [1] Buhusi CV, et al. *Nature Reviews Neuroscience*. 2005;6(10):755-655; [2] Komura, Y, et al. *Nature*. 2001;412(6846):546; [3] Eichenbaum H. *Nature Reviews Neuroscience*. 2014;15(11):732-44.

#### COMPUTATION OF BRAIN MIDSAGITTAL PLANE THROUGH DTI-BASED DIVERGENCE MAP

G. R. Pinheiro, G. S. Cover, L. Rittner

<sup>1</sup>Medical Image Computing Laboratory (MICLab), School of Electrical and Computer Engineering (FEEC), UNICAMP, Campinas, São Paulo, SP, Brazil.

**Introduction:** The Corpus Callosum (CC) is a white matter structure that interconnects both brain hemispheres. Many studies have shown the correlation between CC alterations and neurodegenerative diseases. In order to properly analyze the CC structure in 2D studies, the midsagittal slice selection of the brain is required, and it is usually identified by the diffusion properties<sup>1</sup> observed in the interhemispheric fissure, being applied to the midsagittal plane (MSP) of the whole brain<sup>2</sup>. This work proposes the CC midsagittal plane computation directly on Diffusion Tensor Imaging (DTI) through the divergence map, a scalar map that represents the quantity of a vector field's source or sink at each point. The method explores the well-organized white matter in the CC and finds the plane with maximum fibers divergence, differently from MSP, which is based on structural characteristics of the brain, such as symmetry and inter-hemispheric fissure localization. Experiments have shown that the computed plane is invariant to CC misalignment relative to the image acquisition plane, and low sensitivity to the parameters selection. **Materials and Methods:** Our image dataset was composed by DTI from two subjects obtained in the axial plane (2.0 mm thickness, 1.0 x 1.0 mm, 32 directions) at Hospital de Clínicas of UNICAMP. Initially, a manually cropped volume of (18x83x36) voxels around the CC is loaded and a divergence map is computed over many directions. For divergence map computation, we apply the algorithm described in<sup>3</sup>. The plane computation is done using an iterative fitting of least squares method and removing 10% of the points placed far away from the computed plane. This step is re-executed until all points are in 2 voxels range from the plane. In the end, the desired plane is the plane where the direction of interest is the one perpendicularly closest to the plane normal vector. **Results:** The proposed method for midsagittal plane computation was tested over two subjects with similar and satisfactory qualitative results (Fig. 1). In one of them, the MSP was aligned with the vector [0.999805x, -0.019226y, 0.004409z], while the other



was aligned with the vector  $[0.99628x, 0.068077y, 0.052832z]$ . **Discussion:** The method finds the plane of maximal divergence (inflexion) of the CC fibers. As this plane lies in the CC symmetry plane, this method is an option for the brain midsagittal slice selection. **Conclusion:** This work implements a mid-sagittal plane computation method, showing that the plane is invariant to CC misalignment relative to the image acquisition plane, and low sensitivity to the parameters selection.

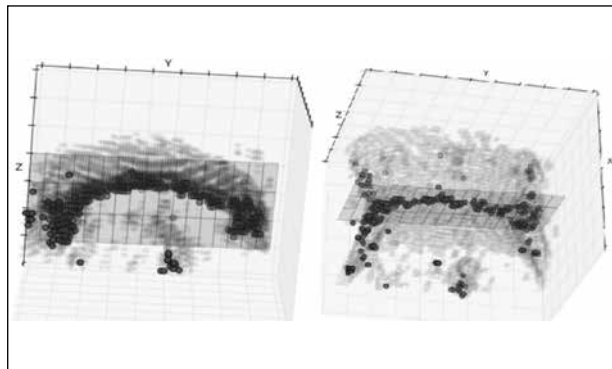


**Figure 1.** Computed midsagittal plane seen in two different perspectives. Red dots are points with maximum absolute divergence, blue region is a rough segmentation of the white matter, and red surface is the obtained plane.

**References:** [1] Rittner L, et al. *Rev Bras Eng Biom.* 2014;30(2):132-43; [2] Bassar P, et al. *J. Magnetic Resonance, Series B.* 1996;111(3):209-19, 1996. [3] Pinheiro GR, et al. *Conf Proc IEEE Eng Med Biol Soc (EMBC), IEEE 38th Annual International Conference,* 2016.

#### APPLICATION AND CHARACTERIZATION OF NEURAL PROBES

E. V. Dias<sup>1</sup>, A. S. Vieira<sup>2</sup>, R. Panepucci<sup>3</sup>, R. Covolani<sup>4</sup>, I. T. L. Cendes<sup>2</sup>, F. Cendes<sup>4</sup>

<sup>1</sup>Neurology Dept, FCM, UNICAMP, <sup>2</sup>Genetics Dept., FCM, UNICAMP, <sup>3</sup>CTI Renato Archer, <sup>4</sup>Neurophysics Group, IFGW, UNICAMP, Campinas, São Paulo, SP, Brazil.

**Introduction:** Brain probes constitute the only available tool for examining the link between the electrical activity of single neurons and subject behavior. Because the electrodes contained in the neural probes need to be positioned within tens of micrometers of the neurons of interest, these are necessarily invasive devices. As such they incur the damage of neural tissue, therefore unleashing the chain of events that characterizes inflammation. As it happens with any foreign material that is implanted in the body, the process starts with the unspecific adsorption of proteins and the recruitment of defense cells that attempt to clean up the site and eliminate the threat of the invader. If the threat persists, a chronic inflammatory process ensues, with the attempt to shield the affected area from the surrounding tissue. The common perception is that this shielding, which in the brain consists of a capsule formed predominantly by astrocytes, gradually decreases the quality of the recorded neuronal signals. This project will focus on the application and characterization of neural probes already designed and fabricated by the BRAINN research groups. Furthermore, this project will also have the objective of producing new probe configurations and materials for the improvement of neural recordings in experimental animal models. **Materials and Methods:** Stereotaxic surgery for implantation of recording neural probes will be performed in Fischer 344 male rats (aged 12 weeks) acquired from Cemib, State University of Campinas (Unicamp). Rats will either receive recording neural probes developed previously in Brainn projects, or commercial silicon probes (Neuronexus), or stainless steel micro wires. Recording probes will be implanted into the dentate gyrus of the hippocampus (AP -3.0; L  $\pm$ 2.0; V -3.5) and bipolar stimulating electrodes will be implanted into the perforant pathway (AP -8.0; L  $\pm$ 4.5; V -3.0). After a period of 7 or 28 days, neural electrical activity will be recorded. Subsequently, rats will be euthanized and the nervous tissue of rats that received chronic probe implants will be analyzed with immunofluorescence labeling for markers for foreign body reaction such as the astrogliosis markers GFAP and microglia activation marker CD68. Gene expression analysis of tissue reactivity markers will also be performed in laser microdissected regions proximal to probe implantation and will be subjected to transcriptome analysis by RNA-seq. All procedures were approved by the Ethics Committee for Animal Research at the Unicamp (protocol 4438-1). **Results:**

In this project, we will explore the use of neural probes developed in previous Brainn projects for nervous tissue electrical activity recording. Furthermore, we will explore and characterize tissue reaction to different neural probe materials and design. **Discussion:** Recent evidence suggests the neurotoxic effect of the signaling cytokines that are released by nervous tissue in contact with implanted probes. It is noteworthy that such inflammatory process may result in the loss of the ability to record single action potentials. Consequentially, exploring tissue reaction is crucial for the development of more efficient implantable neural probes. **Conclusion:** The present work will permit to evaluate the biocompatibility and efficacy of the neural probes designed and developed by BRAINN team researchers for application in animal models researches and with potential for application in humans.

**References:** [1] Kozai TDY, et al. *ACS Chem Neurosc.* 2015;6:48-67.

#### MOTOR ADAPTATION THROUGH THE PREDICTIVE SACCADIC: FMRI STUDY OF THE EYE MOVEMENTS

T. Vasconcelos<sup>1</sup>, D. Gomes<sup>1</sup>, E. Amaro<sup>2</sup>, K. Lukasova<sup>2,3</sup>

<sup>1</sup>Faculty of Psychology, CRUZEIRO DO SUL, São Paulo; <sup>2</sup>NIF/LIM44, FMUSP, São Paulo, <sup>3</sup>CMCC, UFABC, São Paulo, SP, Brazil.

**Introduction:** Saccades are rapid eye movements and its properties can be altered by advanced knowledge of target position. These kinds of saccades are called the predictive saccade and are characterized by the reduction of the time between the target appearance and the triggering of the saccades to almost 0ms. In predictive saccade task, the target appears alternating in constant frequency and speed on the left/right side in a square wave like manner that allows for the anticipation of the eye movement and functional adaptation to the task. The aim of this study was to access the brain activation during predictive tracking to investigate the motor adaptation circuitry. **Materials and Methods:** 10 healthy university students participated in the study and all signed the informed consent approved by the Ethics Committee of the university (FMUSP 089/11). All participants were screened for general cognitive functioning. The task consisted in the appearance of a black point on the gray background that induces predictive saccade motion in fast speed target movement. In the block design, for 40 seconds the participant followed the movement of the point alternating in 500 milliseconds intervals, followed by 20 seconds rest cross fixation and 40 seconds slow alternation of 1667 milliseconds for reflexive saccades. The compliance with the task was verified by integrated eye tracking. Images were

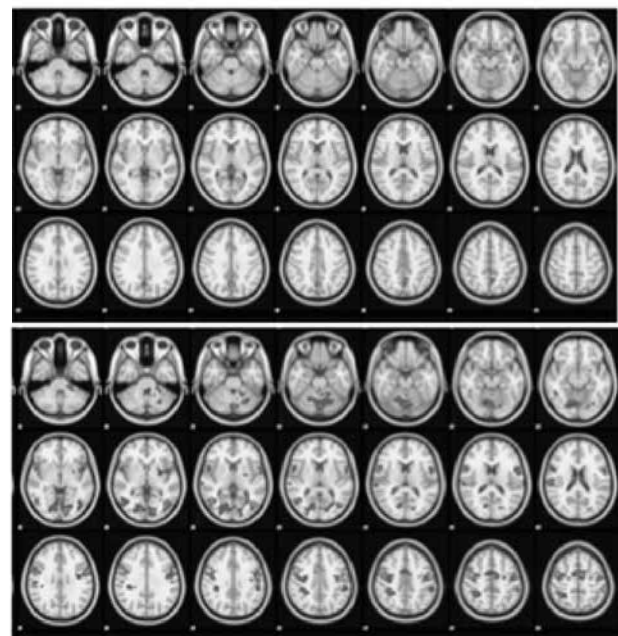


**Figure 1.** Representation of activation during predictive saccades task in healthy adults (N=10). On the left reflexive saccades > predictive saccades comparison showed activation in posterior cingulate gyrus and left inferior temporal gyrus. On the right, predictive saccades > reflexive saccades activation [cluster  $Z > 2.3$ ;  $p < 0.05$ ; the scale depicted in the figure  $Z = 2.3$  to 4.0; brain template MNI152].

acquired in a 3T scanner (Philips Achieva). Single shot echo planar imaging was used with parameters: repetition time (TR) of 2000 ms, echo time (TE) 30 ms, flip angle 90°, slice thickness 3.0 mm, gap 0, matrix size of 80 x 77 pixels. The total duration was approximately 9 minutes and the total of 240 volumes were acquired. **Results:** Predictive compared to reflexive saccades showed activation in fronto-parietal regions, mainly in the bilateral frontal eye fields, supplemental eye field, intraparietal sulcus anterior part, bilateral inferior temporal gyrus and cerebellum. The comparison of reflexive to predictive saccades showed activation in posterior cingulate gyrus and left inferior temporal gyrus. **Discussion:** Studies in monkeys have largely reported on spatial tuning of the lateral intraparietal cortex (LIP), but have only recently shown a specific role of the supplementary eye field (SEF) and the neurons within this area in sequential state representation and timing. Our results showed that the direction of upcoming saccade can be coded by intraparietal regions with the SEF providing detailed information on upcoming motor intention and the timing of the saccade sequence. **Conclusions:** Successful execution of predictive saccades is supported by an internal estimation of the stimulus timing together with the feedback of previous saccade monitored by fronto-parietal system.

#### E-STREET: VIRTUAL REALITY FOR SPATIAL ORIENTATION IN URBAN ENVIRONMENT

A. F. Brandão<sup>1,2,3</sup>, D. R. C. Dias<sup>4</sup>, G. G. Paiva<sup>5</sup>, M. P. Guimarães<sup>2</sup>, L. C. Trevelin<sup>5</sup>, G. Castellano<sup>1,3</sup>

<sup>1</sup>Neurophysics Group, IFGW, UNICAMP; <sup>2</sup>Health Informatics, UNIFESP; <sup>3</sup>Brazilian Institute of Neuroscience and Neurotechnology (BRAINN), Campinas; <sup>4</sup>Computer Science Dept, UFJF; <sup>5</sup>LaViC, Computer Science Dept, UFSCar.

**Introduction:** Human-Computer Interaction (HCI) allows communication between people and computer systems in a variety of ways, including body movements (or gesture interaction). HCI based in body movements can occur in a physically active manner and therefore achieve benefits related to physical activity and health promotion. The main objective of this work was to develop a body movement/gesture interaction HCI, namely, a virtual reality (VR) solution for the exploration of a three-dimensional (3D) city, through movement of the lower limbs. The idea is to use this software for spatial orientation training, motor rehabilitation of gait and fall prevention. **Materials and Methods:** The Unity3D<sup>1</sup> game engine (development platform) and the Natural User Interface (NUI)<sup>2</sup> concept were used, which allow natural means of interacting with digital systems, including interaction through physical activity, inherent to the human behavior. Ultrasound sensors controlled by an Arduino were also used. **Results:** A software, called e-Street, was modeled (3D), in order to simulate an urban environment oriented for navigation from movements that reproduce the stationary gait and that require spatial orientation from the user. E-Street runs on a smartphone within Google Cardboard<sup>3</sup>. System control is performed from ultrasound sensors attached to the distal position of the lower limb (near the ankle joint), which are physically connected (wired) to an Arduino. The Arduino interacts with the software by means of Bluetooth. Every time the user performs the movement of raising the feet from the floor alternately, simulating a walk (without spatial displacement), a forward shift is assigned within the e-Street environment. Thus, it is possible to explore the VR environment from real body movements. **Discussion:** NUI has the following characteristics<sup>4</sup>: 1. User-centered design: provides the changing needs of the interface for different users; 2. Multichannel: captures multiple channels of user input to perform the interaction with the computer. The considered user input channels are the body parts, such as the ankle. 3. Interaction based on behavior: recognizes the user's body language, that is, movements that express some meaning (gestural interaction). These NUI characteristics can be used to simulate real situations and benefit motor and neurofunctional therapies through multisensory stimuli<sup>5</sup>, which is what is proposed by e-Street. **Conclusion:** E-Street can be used to reproduce activities of daily living (ADLs) from immersive virtual experiences with the user assisted by trained professionals (specialist) and in a safe and controlled environment. It can therefore be used for motor rehabilitation of gait, fall prevention and neurofunctional therapies, as proposed. The next steps are usability tests with healthy people and gait impaired or disoriented patients.

**References:** [1] Unity – Game Engine, <https://unity3d.com/pt>, [accessed feb 2017]; [2] Wigdor D, et al. Brave Nui World. San Francisco: MKP Inc. 2011; [3] Google Cardboard, <https://vr.google.com/cardboard/>, [accessed feb 2017]; [4] Lui W. IEEE 11th Int Conf Comp Aided Industrial Design & Conceptual Design 1. 2010; 2:20-205; [5] Rose FD, et al. Cyberpsychol Behav. 2005;8(3):241-62. Lui W, IEEE 11th Int Conf Comp Aided Industrial Design & Conceptual Design 1 2:203-205, 2010.

#### FUNCTIONAL CONNECTIVITY OF DEFAULT MODE NETWORK IN ISCHEMIC STROKE: A PROSPECTIVE STUDY

J. E. Vicentini<sup>1</sup>, S.R.M. de Almeida, B.M. de Campos, L. Valler, L. M. Li<sup>1</sup>

<sup>1</sup> Neurology Dept., FCM, UNICAMP, Campinas, São Paulo, SP, Brazil.

**Introduction:** Brain reorganization is a fundamental mechanism during patient recovery after a stroke, since it involves the capacity of brain to restore itself or compensate for damage caused by the lesion. Resting-state functional connectivity is defined as a temporal correlation between spatially remote regions of brain [1]. The Default Mode Network (DMN) is one of most prominent resting-state functional network of the brain and it has been associated to self-referential processing, as cognitive and emotional skills [2]. We aimed to explore the mechanism of DMN functional connectivity recovery in ischemic stroke through a longitudinal study. **Materials and Methods:** This study was approved by the Ethics Committee and all individuals provided written consent to participate. Twenty stroke patients aged between 45-80 years old who had experienced their first-ever ischemia, without previous neurological history, were submitted to functional Magnetic Resonance Imaging (fMRI) acquisition using a 3T scanner (Philips Achieva®) on their first and sixth month after stroke. Image processing based on realignment, segmentation, normalization (MNI-152) and smoothing used UF<sup>2</sup>C (User Friendly Functional Connectivity) toolbox. Paired t-test performed in SPM12 for MATLAB followed the parameters of  $p < 0.001$  uncorrected and cluster size with at least 50 voxels. **Results:** We found an increased connectivity of DMN functional connectivity in posterior cingulate cortex (PCC) (table 1 and figure 1) in first month post stroke, when compared to six months after ictus. **Discussion:** Increased DMN functional connectivity on the first month after ictus suggests failure to suppress activity in some of the core region of DMN, which is associated with self-referential processing [3]. However, six months after stroke, there is a functional improvement in this network, suggesting that the first six months are a critical period for neural reorganization [4]. **Conclusion:** Abnormal DMN was found following stroke in sub acute stage. There was a natural recovery of this network six months post stroke. Our findings are exploratory, and further research may facilitate the understanding of potential mechanisms underlying self-referential processing in stroke recovery.

**Table 1.** Coordinates and cluster size of increased DMN functional connectivity on the first month after stroke in comparison with the sixth month ( $p < 0.001$ , uncorrected).

Cluster size	Region	Stereotaxic coordinates (mm)			
		X	Y	Z	T value
212	Posterior Cingulate Cortex	-2	-48	24	4.35

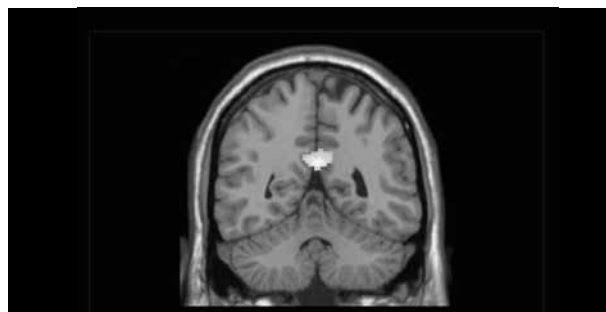


**Figure 1.** Paired t-test results showed increased DMN functional connectivity in the sub acute stage, which was restored after six months ( $p < 0.001$ , uncorrected).

**References:** [1] Raichle ME, et al. PNAS.2001;98:676-82; [2] Greicius, et al. PNAS. 2004;101:4637-4642; [3] Grady CL, et al. Cogn Neurosci. 2006;8:227-41, 2006; [4] Park JY, et al. Eur J Neurosci. 2014;40(4):2715-22.

#### COMMON CAROTID LUMEN SEGMENTATION USING CINE FAST SPIN ECHO MAGNETIC RESONANCE IMAGING

L. Rodrigues<sup>1</sup>, R. Souza<sup>1</sup>, L. Rittner<sup>1</sup>, Richard Frayne<sup>2</sup>, R. Lotufo<sup>1</sup>

<sup>1</sup>University of Campinas, Campinas, SP, Brazil; <sup>2</sup>University of Calgary, Calgary, Canada

**Introduction:** Stroke is the most common cause of death in the world. It is

estimated that 4.4 million people die every year due to stroke and 5000 in every million are victims of stroke disabilities<sup>1</sup>. Aiming to prevent stroke caused by atherosclerosis, it is desired to use a non-invasive method to quantify stenosis and plaque morphology. Magnetic resonance (MR) imaging permits the evaluation of plaque and analysis of its composition. In the present work, we focus on segmenting the lumen, this is, the interior of the common carotid artery (CCA), applying morphological techniques to Cine Fast Spin Echo (FSE) time-series of MR images. By segmenting the lumen during a cardiac cycle, we can analyze its cross-section area and shape variation, which correlates with atherosclerotic disease<sup>2</sup>. Our method uses the max-tree area signature analysis combined with the watershed transform from markers to get accurate segmentations. **Materials and Methods:** Our method was developed based on three assumptions about the CCA and one assumption about Cine FSE images: (1) We have previous knowledge about the diameter of the carotid lumen and trachea. (2) We have anatomical knowledge of right and left CCAs relative position. (3) Twoimages corresponding to the same axial position at consecutive time points have similar gray-level intensities. The method developed has four main steps: CCA centroid estimation, Internal marker selection, External marker selection and Watershed transform.

**Results:** For a numerical analyses we compared the resulting segmentation from the automatic method with the ground truth, represented here by the manual segmentation. Table<sup>1</sup> shows the results of the methods for both volumes for right and left CCA on the three positions before the bifurcation. **Discussion:** Analyzing some results from the literature, we can see that<sup>3</sup> used 3T static MR image, achieving a dice coefficient of  $0.93 \pm 0.019$ . Our method achieved a smaller global dice, however we use dynamic low resolution images. **Conclusion:** This case of study differs from other carotid segmentation studies due the nature of the image. Although there are many contributions on carotid MRI field, there are no studies using a time-series type of imaging for carotid segmentation. This can be seen as a introductory study, since many improvements can still be done in order to find better outcomes. For future work, we pretend to extend the automatic code for slices after carotid bifurcation.

**Table 1.** Metrics for both volumes, left carotid and right carotid.

	Left carotid	Right carotid	Total
Dice	$0.902 \pm 0.063$	$0.907 \pm 0.058$	$0.905 \pm 0.060$
Sensitivity	$0.892 \pm 0.090$	$0.931 \pm 0.059$	$0.912 \pm 0.074$

**References:** [1] Yuan C, Mitsumori L, Beach K, Maravilla K. Carotid atherosclerotic plaque: Non-invasive MR characterization and identification of vulnerable lesions. *Radiology*. 2001;221(2):285-99. [2] M.Naghavi, et al. From vulnerable plaque to vulnerable patient, *Circulation*. 2003;108(14):1664-72. [3] Ukwatta E, Yuan J, Rajchl M, Qiu W, Tessier D, Fenster A. "3-D Carotid Multi-Region MRI Segmentation by Globally Optimal Evolution of Coupled Surfaces". *IEEE Transactions on Medical Imaging*. 2013;32:770-85.

#### A FEASIBILITY EVALUATION OF EEG DATA ACQUIRED USING A NEUROFEEDBACK TRAINING INTERFACE: PRELIMINARY RESULTS

L. T. Menezes<sup>1,2</sup>, C. A. Stefano Filho<sup>1,2</sup>, G. Castellano<sup>1,2</sup>

<sup>1</sup>Neurophysics Group, IFGW, UNICAMP; <sup>2</sup>Brazilian Institute of Neuroscience and Neurotechnology, BRAINN.

**Introduction:** Neurofeedback training (NFBt) has been used as a complementary or alternative treatment for disorders such as ADHD and epilepsy<sup>1</sup>. However, it is still a controversial topic<sup>2</sup>. Our group aims to understand how NFBt can affect the brain in order to assert its efficacy. In this work, we performed basic initial analyses of electroencephalography (EEG) data acquired via our NFBt interface, in order to determine whether the recorded signal differs significantly from simple EEG fluctuations, to assess the feasibility of using it for NFBt sessions. **Materials and Methods:** Two subjects participated in this initial study (mean age  $24 \pm 1$  years). Data from 16 dry electrodes were acquired using the g.tec amplifier g.USBamp at 256 Hz. Input for the interface consisted of the Welch's power spectral density (PSD) ratio of the signal between the two bands of interest – theta (4-7 Hz) and lowbeta (12-20 Hz) – decrease of this ratio is associated to concentration gain<sup>3</sup>. Two runs were made for each subject. For each run, subjects had a 50 s resting period, followed by a 150 s task in which they should develop a mental strategy, aiming at modulating their PSDs in the referred bands, to maintain a vertical bar above a threshold value. If the subject did not perform the task successfully, they should adapt their strategy on their

own accordingly. The threshold value was updated in real-time using the mean value of the last 10 s of data. All these calculations were performed from signals from the C3 electrode. Signals from each participant were averaged across both runs, and within runs, using 10 s epochs, and the PSD ratio between theta and beta bands was calculated and compared for each situation (rest and task periods). A T-test comparing rest and task epochs was also performed. **Results:** The bar plot in Figure 1 shows values of the PSD ratios between theta and beta bands for the rest (blue) and task (yellow) periods, for each of the subjects, and the respective p-value, found with the t-test. **Discussion and Conclusion:** The results show that values of the PSD ratio of the theta and beta bands were significantly different for both subjects when rest and task periods were compared, being smaller for task periods, as expected (both below a significance level of 0.05). Our initial analysis suggests that, indeed, our recordings consist of more than pure fluctuations of EEG data and, therefore, our interface seems ready to be used in our investigation of NFBt, after a proper protocol is designed.

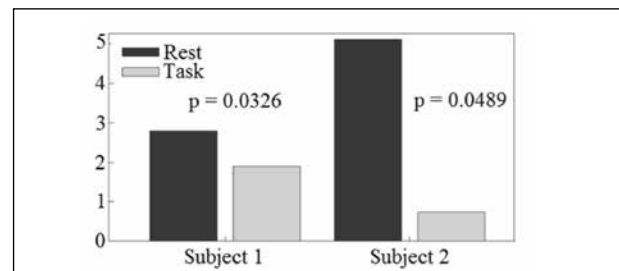


**Figure 1.** Difference between theta-beta ratio during resting state and task performance for each subject. P-values were obtained by a t-test.

**References:** [1] Egner T, Gruzeller JH. *Neuroreport*. 2001;12(18):4155-9. [2] van Dongen-Boomsma, et al. *The Journal of Clinical Psychiatry*. 2013;74(8):821-7. [3] Lubar JF, et al. *Biofeedback and Self-Regulation*. 1995;20(1):83-99.

#### DEFAULT MODE NETWORK IN TLE PATIENTS WITH AND WITHOUT HIPPOCAMPAL ATROPHY

T. A. Zanão, T. M. Lopes, B. M. Campos, M. H. Nogueira, C. L. Yasuda, F. Cendes  
Neuroimaging Lab, FCM, UNICAMP, Campinas, São Paulo, SP, Brazil.

**Introduction:** Temporal Lobe Epilepsy (TLE) has been traditionally associated with memory impairment, however, it is also notable that TLE patients frequently present more extensive cognitive damages not easily explained by temporal seizures focus<sup>1</sup>. The Default Mode Network (DMN) has a controversial recruitment of mesial structures as hippocampus. Regardless of controversies, several evidences indicate impairment of DMN in TLE<sup>2</sup>. Our main hypothesis is that DMN will be severely disrupted in patients with atrophy, followed by a more coherent network in non lesional group. **Materials and Methods:** We included 122 TLE patients (age range 21-70, 78 female, mean age 46) divided into right hippocampal atrophy (HA) (RTLE, 42 subjects) and left HA (LTLE, 49 subjects) temporal lobe epilepsy and MR-Neg (31 patients without HA). Also, 69 healthy controls (age range 23-66, 44 female, mean age 44) were enrolled. All subjects included are literate Brazilian Portuguese native speakers and were submitted to structural and functional brain imaging. **Results:**

**Table 1.** comparison between patients (RTLE, LTLE and MR-Neg) and controls. Similar patterns were highlighted with same colors (blue and red).

	Ipsilateral	Contralateral
RTLE>CONT	Frontal Lobe	Frontal Lobe + Temporal Lobe + Parietal Lobe + Cerebellum
RTLE<CONT	Temporal Lobe + Caudate + Hippocampus	Temporal Lobe + Limbic Lobe
LTLE>CONT	Frontal Lobe	Parietal Lobe + Pallidum
LTLE<CONT	Temporal Lobe + Caudate + Hippocampus	Frontal Lobe + Temporal Lobe + Insula
	<b>Right hemisphere</b>	<b>Left hemisphere</b>
MR-Neg>CONT	Frontal Lobe + Basal Ganglia + Cerebellum	Frontal Lobe + Temporal Lobe + Parietal Lobe + Basal Ganglia + Occipital
MR-Neg<CONT	Temporal lobe + Caudate + Hippocampus	--No activations--



**Discussion:** Relating to patients with HA, the results shown may indicate that the presence or localization of atrophy is little or non-determinant for the ipsilateral hemisphere's DMN connectivity. Our results indicate some similarities between MR-Neg and RTLE groups connectivity, but the non-lesion group presented more connections in both hemispheres when compared to others groups.

**Conclusion:** Our data suggest that TLE disrupts normal pattern of DMN, as we observed reduction of temporal lobe recruitment in patients, especially in LTLE. The absence of HA (MR-Neg) seems to yield a less prominent disruption in functional connectivity. We can also relate the participation of temporal lobe in DMN.

**References:** [1] Cataliti M, et al. *Epilepsia*. 2013;54(12):2048-59; [2] Raichle ME, et al. 2001;98(2):676-82.

#### CORTICAL SURFACE ANALYSIS IN PARKINSON DISEASE PATIENTS

R. Guimarães<sup>1</sup>, L. Campos<sup>2</sup>, L. Piovesana<sup>2</sup>, P. Azevedo<sup>2</sup>, C. Yasuda<sup>1,2</sup>, J. C. Moreira<sup>1</sup>, D. Garcia<sup>1</sup>, A. D'Abreu<sup>1,2</sup>, F. Cendes<sup>1,2</sup>

<sup>1</sup>Laboratory of Neuroimaging, UNICAMP, <sup>2</sup>Neurology Dept., FCM, UNICAMP, Campinas, São Paulo, SP, Brazil.

**Introduction:** Parkinson's disease (PD) is a neurodegenerative chronic disease. The pathophysiology is still unknown, and many symptoms can't be explained by corticostriatal lesions<sup>1</sup>. We assessed cortical thickness in order to find pathological brain regions that could be associated with the heterogeneous symptoms of PD. **Materials and Methods:** We included 110 patients (73 men, mean age 59.48, SD 9.7; mean disease duration 8.2, SD 6.2) and 76 healthy controls. Patients and controls underwent the same protocol for MRI acquisition. Patients were assessed by a complete neurological examination. Surface-Based Morphometry (SBM) analyses were performed on T1 weighted images with MATLAB2014b/SPM12/CAT12. This is a fully automated technique and allows measurement of cortical thickness as well as reconstructions of the central surface in one-step. Statistical analyses with CAT12/SPM12 included T-tests to compare patients and controls. Contrasts were designed to highlight areas of atrophy in patients. Reported results have minimum T-statistic of 3, with at least 10 voxels in each cluster. **Results:** We found reduced cortical thickness in PD patients when compared to controls in cingulum, superior temporal gyrus, angular gyrus, gyrus rectus, olfactory cortex, splenium of corpus callosum, calcarine gyrus and parietal lobule. **Discussion:** We found significant cortical changes showing that brain abnormalities go beyond the substantia nigra and basal ganglia. Interestingly, we found reduced cortical thickness in the olfactory cortex, region that receives sensory information from the olfactory bulb, and is already affected in early disease stages, even before the motor symptoms<sup>2</sup>. **Conclusion:** There is widespread cortical brain impairment in PD, which might be responsible for the great variability of PD symptoms, however, future studies correlating these areas with clinical scales are necessary to corroborate this hypothesis.

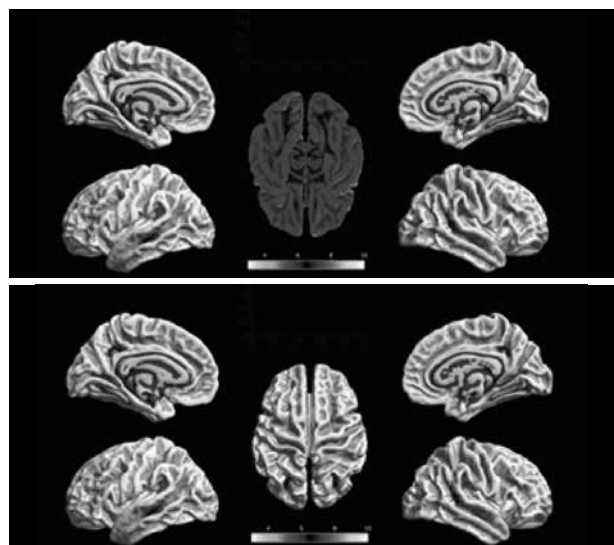


**Figure 1.** Surface-based analysis of local cortical thickness. PD patients present widespread, bilateral reduction of cortical thickness.

**References:** [1] Uribe C, et al. *Mov Disord*. 2016;31(5):699-708. [2] Guimarães R, et al. *Front Neurol*. 2017;13(7):7-243.

#### BICLUSTERING IN THE ANALYSIS AND IDENTIFICATION OF BIOMARKERS

R. Veroneze, F. J. Von Zuben

<sup>1</sup>Laboratory of Bioinformatics and Bio-inspired Computing (LBiC/DCA/FEEC/Unicamp).

**Introduction:** Veroneze et al.<sup>5</sup> proposed algorithms to mine all maximal biclusters<sup>2</sup> in numerical datasets, named RIn-Close algorithms. The great potential of the RIn-Close algorithms is explored here to (i) test the discriminatory capability of proposed biomarkers in the literature of neuroscience; and (ii) propose biomarkers from scratch. In genetics, biomarkers are defined as a set of genes that are associated with a disease or are associated with the susceptibility to develop a specific disease. Remarkably, the smaller the set of genes, the easier it is to be assessed in real scenarios. However, few genes may not be sufficient to produce a proper identification. **Materials and Methods:** The identification of biomarkers from available data is a recurrent demand in several research areas, such as ecology and medicine. Computationally speaking, they are equivalent problems and here we have decided to conduct experiments in a public cancer dataset, having samples of the small, round blue cell tumors (SRBCTs) of childhood, which include neuroblastoma (NB), rhabdomyosarcoma (RMS), non-Hodgkin lymphoma (NHL) and the Ewing family of tumors (EWS). Biomarkers here are the subset of genes capable of discriminating those class labels. This dataset consists of expression levels of 2,308 genes, which were obtained from glass-slide cDNA microarrays using the standard protocol of the National Human Genome Research Institute<sup>3</sup>. It has 88 samples, being 29 EWS, 11 NHL, 18 NB, 25 RMS, and 5 non-SRBCT samples. Khan et al.<sup>1</sup> proposed a set of 96 genes as biomarkers, and Pal et al. [3] proposed a set of only 7 genes, with only 4 of them in common with the 96-genes proposal, thus revealing that they are very different in size and composition. Given this scenario, we used RIn-Close to analyze the group of genes proposed by Khan et al.<sup>1</sup> and by Pal et al.<sup>3</sup>. We also used RIn-Close to analyze all genes of the dataset, aiming at indicating a new group of genes as biomarkers. Our analysis considers only the biclusters composed of samples from the same class, named here *pure biclusters*. For more details see<sup>4</sup>. **Results:** Our analysis indicated that the 96 genes proposed by Khan et al. [1] are sufficient to discriminate all types of SRBCTs. However, with less than 30 of these 96 genes, RIn-Close was able to find pure biclusters covering all SRBCT samples. The 7 genes proposed by Pal et al.<sup>3</sup> were not sufficient to discriminate between all class labels. However, with the addition of only one more gene, RIn-Close was able to find pure biclusters covering all SRBCT samples. When applying RIn-Close to the entire dataset, we were able to select 62 genes as biomarkers. It has 31 genes in common with the biomarker proposed by Khan et al.<sup>1</sup>, and 1 gene in common with the biomarker proposed by Pal et al.<sup>3</sup> (this gene is also part of the biomarkers proposed by Khan et al.<sup>1</sup>). **Discussion:** RIn-Close demonstrated to be a valid and complementary tool to detect biomarkers. The fact that multiple and possibly very distinct subsets of genes may be identified as biomarkers in this public cancer dataset may be explained by the co-occurrence of multiple dominant molecular processes, which should be further investigated by the domain experts. **Conclusion:** The present work confirmed that, by means of RIn-Close biclustering, we can test the discriminatory capability of proposed biomarkers, pointing to minimum sets that still act as biomarkers. Moreover, it is possible to use RIn-Close to directly find biomarkers from scratch.

**References:** [1] Khan J, et al. *Nature Medicine*. 2001;7(6):673-9; [2] Madeira SC, et al. *IEEE/ACM Transactions on Computational Biology and Bioinformatics*. 2004;1(1):24-45; [3] Pal NR, et al. *BMC Bioinformatics*. 2007;8(1):5; [4] Veroneze R. 2016. [5] Veroneze R, et al. *Information Sciences*. 2017;379:288-309.

#### MOTION ARTIFACTS AND SLICE TIMING CORRECTION CAN INFLUENCE BOLD RESTING STATE RESULTS

W. A. A. Rocha<sup>1,2,3</sup>, A. C. Carvalho<sup>1,2</sup>, S. L. Novil<sup>1,2</sup>, R. M. Forti<sup>1,2</sup>, A. Quiroga<sup>1,2</sup>, M. M. Cordeiro<sup>2,4</sup>, C. L. Yasuda<sup>2,4</sup>, R. C. Mesquita<sup>1,2</sup>, A. Saa<sup>3</sup>

<sup>1</sup>Neurophysics Group, IFGW, UNICAMP; <sup>2</sup>Brazilian Institute of Neuroscience and Neurotechnology; <sup>3</sup>Institute of Mathematics, Statistics and Computing Science, IMECC, UNICAMP; <sup>4</sup>Neuroimaging Group, FCM, UNICAMP, Campinas, São Paulo, SP, Brazil.

**Introduction:** There are several options in the pre-processing of resting state (RS) data obtained with blood-oxygen-level dependent (BOLD) signals of functional magnetic resonance imaging (fMRI), but there is no consensus in the literature about the appropriate use of some of these features. In this work,

we evaluated how slice timing correction (STC) and dynamic removal of motion artifacts (DRMA) significantly affect graph analysis of fMRI data. **Materials and Methods:** We performed resting-state fMRI in 44 healthy adults (23  $\pm$  5 years old). For each subject, 5-minute baseline runs were performed from 2 to 5 times. All subjects underwent 3T MRI (Philips Achieva) according to the following protocol: Structural images: T1 weighted sagittal 3D FEE, voxels of 1x1x1 mm, TE = 3.2 s, TR = 7 ms, TI = 900 ms, flip angle = 8°. Functional images: T2 weighted gradient echo EPI sequence for BOLD imaging, voxels 3x3x3 mm, TE = 30 ms, TR = 2 s, flip angle = 90°. For pre-processing, we followed standard SPM routines gathered in UF2C to align, smooth and band-pass filter (0.009-0.08 Hz) data. We also additionally performed an algorithm, DRMA, to identify motion artefacts and remove highly contaminated volumes<sup>1,2</sup>. Since this additional process reduced the number of volumes in each run, runs with less than 50 remaining volumes were deleted. Therefore, the number of subjects was decreased to 28 and the number of total runs (across all subjects) to 106 after the DRMA process. To perform graph-theoretical analysis, we first divided the cerebral cortex onto 90 regions, using an atlas described in detail elsewhere [3]. For the network construction, each region was treated as a node, and the link between two nodes were based on the Pearson correlation coefficient across the BOLD time series of each region. To create binary graphs, we defined a correlation threshold and varied it from 0.0 to 1.0. For each threshold, standard network parameters were computed such as the average degree, the clustering coefficient, and the global efficiency<sup>4,5</sup>. **Results and Discussion:** We contrasted three different pre-processing procedures: (1) DRMA vs no DRMA; (2) DRMA and STC vs no DRMA and STC and; (3) DRMA and STC vs DRMA and no STC. In most of the cases, the DRMA improved the reliability of the network parameters. To this improvement, we calculated the maximum discrepancy (MD) in the network parameters by measuring the standard deviation across runs. For the preprocess (1), we observed reductions of 56  $\pm$  22 % in the MD from the average degree in 78% of all cases, 29  $\pm$  17 % in the clustering coefficient in 63% of all subjects, and 33  $\pm$  25 % in the global efficiency in 56% of all volunteers. For (2), we verified reductions of 55  $\pm$  22 % in the MD from the average degree in 85% of all cases, 40  $\pm$  17 % in the clustering coefficient in 63% of all subjects, and 32  $\pm$  21 % in the global efficiency in 78% of all volunteers. For the last one (3), we did not find significant differences, suggesting that STC has no effects on data that DRMA was previously applied. **Conclusion:** Overall, our results open new directions to the investigation of the human brain connectivity at rest, reinforcing the impact of the data pre-processing in the results. We investigated three different types of pre-processing and evaluated the differences of each one of them with graph analysis. We found that removal of motion artefacts is crucial to construct reliable networks with stable topological organization over time. Last, by applying slice timing correction in our data cohort after the removal of motion artefacts, we found that the STC has no significant impact in the connectivity patterns as measured by the global network parameters. This work appoints to the importance of a better understanding of the pre-process stage for BOLD data from the resting state.

**References:** [1] Power, et al. *NeuroImage*. 2012;59:2142-54; [2] Power, et al. *NeuroImage*. 2014; 84:320-41; [3] Tzourio-Mazoyer N, et al. *NeuroImage*. 2002;15:1053-8119; [4] Novi, et al. *Biomed OptExpress*. 2016;7(7): 2524-37, 2016; [5] Rubinov N, Sporns O. *NeuroImage*. 2010;52: (3):1059-69.

## ORTHOSTATIC TREMOR: A CASE REPORT

A.R. Coimbra Neto<sup>1</sup>, P. C. Azevedo<sup>1</sup>, L. G. Piovesana<sup>1</sup>

<sup>1</sup>Movement Disorders Clinic, Neurology Department, FCM, UNICAMP, Campinas, São Paulo, SP, Brazil.

**Introduction:** Orthostatic tremor is an uncommon disease and a rare form of tremor, characterized by tremor of the lower limbs activated on standing, absent while seated or lying and improved by walking or leaning. Patients report leg shaking, unsteadiness and imbalance. Electrophysiologically it is characterized by an orthostatic-induced 13 to 18-Hz tremor of the lower limbs and trunk. It may evolve as an isolated progressive disorder or a combined neurodegenerative diseases such as Parkinson's disease<sup>1</sup>. **Materials and Methods:** C.T.B., 66 years old, female, confectioner, complaints for 10 years of symmetrical lower limb tremor when assuming the orthostatic position that disappears during ambulation, decubitus and sitting. Five years ago there was worsening of the condition, with involvement of the upper limbs (Figure 1). Because of the tremor, she began to work on the seated position. On neurological examination, tremor in the lower limbs was discrete and only palpable, with high frequency and small amplitude.

After a few minutes in the orthostatic position, there was a progressive increase in the amplitude and appearance of distal tremor in the upper limbs (Figure 2). Surface electromyography revealed tremor with a frequency of 16 Hz in orthostasis (Figure 2). **Results:** Once the diagnosis was made, treatment with clonazepam, primidone, propranolol and baclofen were tried elsewhere, but without improvement. As a result, topiramate was introduced but the patient presented rosacea. We exchange it for mirtazapine, which in turn triggered a significant worsening of the condition. A new therapeutic attempt was made with biperidene, whose effects will still be evaluated. **Discussion:** Our patient's symptoms began in the sixth decade, similar to reported by<sup>1</sup>, who found an average age of symptom onset of 59,3 years. The time required for diagnosis was 10 years, while<sup>1</sup> reported 7.2 years in a series of 184 patients. This could be attributable to patients' use of nontremor descriptors and, moreover, this tremor may be difficult to visualize. The reported tremor frequency was 16 Hz, consistent with the literature on diagnostic criteria. Medications used to alleviate complaints include benzodiazepines, anticonvulsants, beta-blockers, antiparkinsonian drugs, antispasmodics, anticholinergics and antidepressants, but almost 70% of times it failed to improve symptoms<sup>1</sup>. Our patient presented poor response as well. **Conclusion:** Orthostatic tremor is a rare and poorly understood condition which requires a great diagnostic suspicion. Usually, its medical response to treatment is weak. We believe better treatment will come from pathophysiology studies and more clinical trials on this topic to establish new therapeutic options, such as functional neurosurgery.

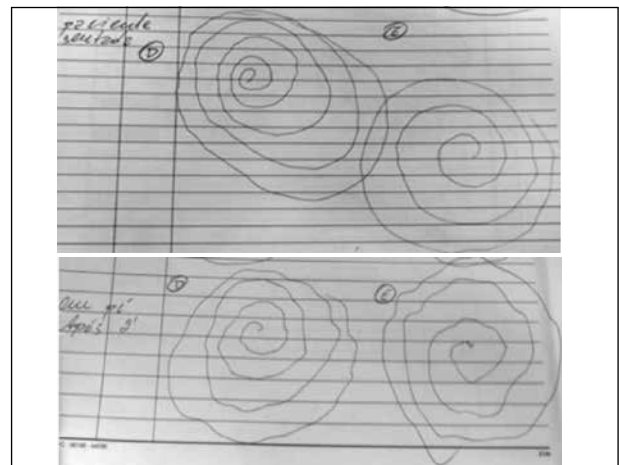


Figure 1. Archimedes spiral in seated position on the left and in standing position on the right.

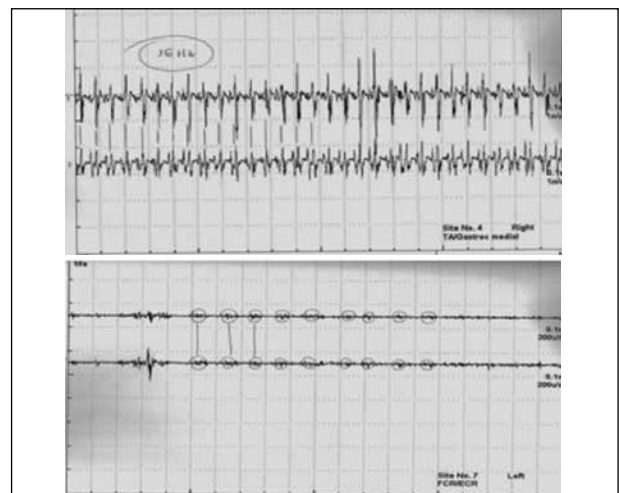


Figure 1. Motor unit action potential (MUP) of the right tibialis anterior and right medial gastrocnemius muscle on the left and MUP of the left flexor carpi radialis and left extensor carpi radialis on the right.

**Reference:** [1] Hassan A, et al. *Neurology*. 2016;86(5):458-64.



### MULTIELECTRODE ARRAYS FOR CELL POTENTIAL MEASUREMENTS: TESTING NOVEL INSULATING LAYER BETWEEN ELECTRODES AND CULTURE

V. P. Gomes<sup>1,2</sup>, A. D. Barros<sup>2</sup>, J. B. Destro-Filho<sup>3</sup>, J. W. Swart<sup>1,2</sup>

<sup>1</sup>School of Electr. & Comput. Eng., UNICAMP; <sup>2</sup>Center of Semiconductor Components and Nanotechnologies, UNICAMP; <sup>3</sup>School of Electr. Eng., UFU.

**Introduction:** This paper reports the fabrication of planar sixty channels Mutielectrode Arrays (MEAs) in order to investigate the use of TiO<sub>2</sub> as insulating layer between electrodes and cell culture. Among its advantages, we can highlight the high mechanical and chemical stability, high dielectric constant, low cost, optical transmittance (about 90% in the visible range), good adhesion to the glass substrates, and biocompatibility<sup>1-4</sup>. The goal is to measure cell potentials and obtain images from neural cell cultures, specifically from dorsal root ganglion (DRG) neurons. We have successfully developed all fabrication steps in order to generate MEAs with 100% national technology. Testing results point out that the device yields very good performance, close to standard commercial MEAs, and is biocompatible. **Materials and Methods:** MEAs' fabrication was made through conventional silicon microfabrication processing using glass as substrate. The device consists of sixty round, flat electrodes, connected to square contact pads by the tracks. Fabrication steps can be subdivided into 4 basic parts, after the cleaning of the substrates: (1) deposition of an insulator interlayer between glass and conductor, which will form the (2) electrodes/tracks/contact pads through lift-off technique, (3) formation of the insulation layer, also using lift-off, and (4) placement of a glass ring that surrounds the active region of MEA. **Results:** The electrical characterization of the noise level from the TiN electrodes showed good sensitivity to noise, compatible with commercial systems. Most of the working TiN electrodes have showed low noise, with amplitudes ranging from -8 to 10  $\mu$ V, i.e. 20  $\mu$ V<sub>p-p</sub> (peak-to-peak potential). In addition, we have performed electrode tests: Cyclic Voltammetry (CV) and Impedance Spectroscopy (IS), which showed good responses. Finally, we have performed the biocompatibility test to evaluate the TiO<sub>2</sub> insulator interlayer. **Discussion:** Regarding the CV test, resulting curves of our MEA presented similar shapes to commercial device, but with higher current density, as well as IS test. Moreover, due to the qualities of the conductor used (such as high charge injection safe limit and low impedance), TiN may be considered an interesting option for extracellular stimulation and neural activity recording. The biocompatibility test to evaluate the TiO<sub>2</sub> insulator interlayer with cell culture using DRG neurons showed that the neurons developed themselves and there was proliferation of non-neuronal cells. **Conclusion:** The present work confirmed that, based on all tests and considerations, we have successfully developed process steps, as in the implementation of MEAs with functional microelectrodes. Results arising from testing the device reported in this work are within the expected range and compatible to standard commercial MEAs, so they are suitable for MEA applications.

**References:** [1] Hashimoto K, Irie H, Fujishima A. *Jpn J Appl Phys.* 2005;44(12):8269-85; [2] Dhar A, Alford TL, Mater APL. 2013;1(1):012102; [3] Carballo-Villa M, et al. *J Biomed Mater Res A.* 90(1):2009;94:105; [4] López-Huerta Et al. *Materials (Basel).* 2014;(6):4105-17.

### HIERARCHICAL OBSERVATION MODELING IN FMRI: SLIDING WINDOW 2.0

R. F. Casseb<sup>1</sup>, A. Sojoudi<sup>2</sup>, G. Castellano<sup>1</sup>, M. C. França Jr<sup>1</sup>, B. Goodyear<sup>2</sup>

<sup>1</sup>Brazilian Institute of Neuroscience and Neurotechnology (BRAINN), Campinas, SP, Brazil; <sup>2</sup>Seaman Family MR Research Centre, University of Calgary, Calgary, Alberta, Canada.

**Introduction:** The first analyses of Resting state fMRI data considered the relationship of brain regions signal as static. Later on, other approaches such as the sliding window strategy allowed more dynamic investigations, in which smaller segments (windows) of the signal were used to determine the functional connectivity (FC). However, due to the reduced amount of time points and also to noise intensity (and fluctuation) during scans<sup>1</sup>, the potential of the sliding window approach is probably diminished. To address these issues, Sojoudi and Goodyear introduced a two-level hierarchical model method<sup>2</sup> (HOMME), and now we implemented an optimization of the noise parameters used in the model. Moreover, we created a graphical user interface (GUI) to make the method available to the scientific community. **Materials and Methods:** HOMME is a Matlab toolbox that uses GLM to model one time-series as a set of windowed segments of another time-series. In this first level, the model

also includes parameters for noise intensity and for the noise autocorrelation. In the second level, another parameter establishes that changes in FC values between adjacent windows must not be abrupt, since there is a great overlap of their content. Figure 1A illustrates the HOMME GUI exploring interface. We ran HOMME and improved HOMME on the data of one subject to evaluate differences in the t-values for each FC value (Figure 1B). **Results:** Enhanced noise parameters do change t-values as can be seen in Figure 1B, even though the fluctuation of the values follows the same curve. **Discussion:** As we do not know the ground truth about FC values, it is difficult to point out which HOMME version produces value is more correct. Nevertheless, as the model bases itself on noise parameters, it is reasonable to speculate that realistic values would yield more precise results. **Conclusion:** The benefits of HOMME over the conventional sliding window approach have already been discussed elsewhere<sup>2</sup>. Here we tried to contribute to its improvement by enhancing the values of the noise parameters and also to make the method easily usable to the scientific community.

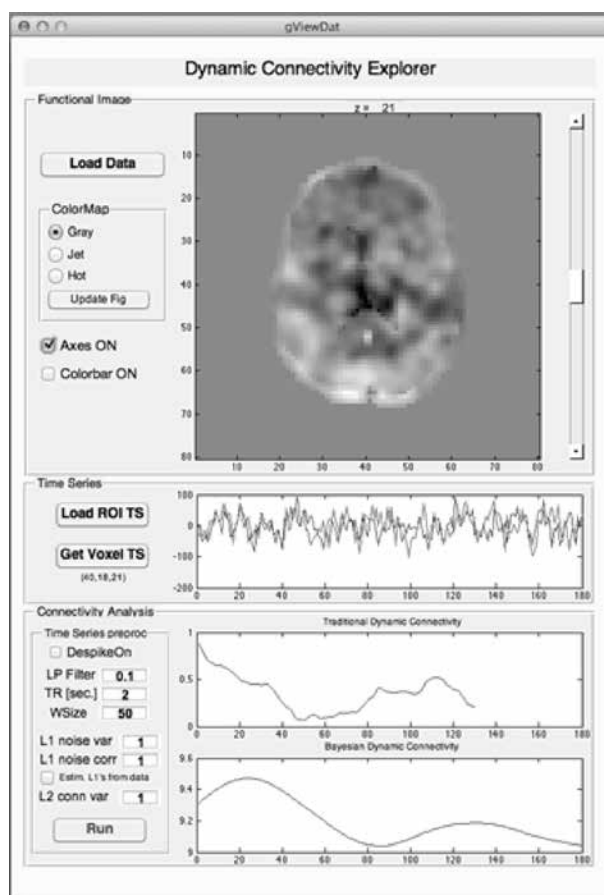


Figure 1.

**References:** [1] Hutchison RM, et al. *Neuroimage* 2013;80:360-78; [2] Sojoudi A. *Hum Brain Mapp.* 2016;37(12):4566-80; [3] Friston KJ, et al. *Neuroimage.* 2002;16(2):465-83.

### PYTHON-BASED VIRTUAL KEYBOARD DESCRIPTIVE LANGUAGE INTERPRETER

R. C. V. Dias<sup>1</sup>, J. R. Oliveira<sup>1</sup>, M. B. Pelosi<sup>2</sup>

<sup>1</sup>DCA/FEEC, UNICAMP; <sup>2</sup>FCM, UFRJ.

**Introduction:** This study proposes the use of brain signals for alternative communication by interfacing it to virtual keyboards, making possible not only to express words, phrases and texts but also enabling transparent end integration with other daily-use computer programs. In alternative communication context virtual keyboards make a set of options available to the user, normally related to communication context (letter, words, and sentences) but not limited to, and these options can be accessed in many ways, and with different types of

input. In most restricted scenario, a virtual keyboard with N options can be used and controlled only with a binary signal input, using scan techniques. The objective of this study is to implement a Python<sup>2</sup> based interpreter that can be used to instantiate different virtual keyboards and at the same time has its inputs connected to the output of processed brain signals, enabling effective end-user communication. **Materials and Methods:** As shown in the work “Descriptive language for virtual keyboards with focus on augmentative and alternative communication”<sup>1</sup>, virtual keyboards can be described and defined using data structures based on ontologies. That work also defines a description language supporting main virtual keyboards features, which will be used in this work as the format for defining and inputting virtual keyboards into the interpreter. Also, this interpreter will have an interface for inputting the brain output data, enabling the control of this virtual keyboard. Tests will be made in simulated environment, since the interpreter expects processed brain signals outputs, and with some basic virtual keyboard options. **Results:** The interpreter was developed in Python<sup>2</sup> and expects input in XML format defined by the virtual keyboard descriptive language<sup>1</sup>. Two basic keyboards were proposed: Basic Words. Options (buttons): “Yes”, “No”, “Maybe”, “Stop”, “Pain”. Free Writing Keyboard. Options (buttons): all letters of the alphabet (“A”, “B”, “C”, “D”, “E”, “F”, etc). The interpreter implemented two options for input:

- Binary Signal: the interpreter makes a time-based scan of all options, so the signal must be inputted when the desired option is on focus.
- Direct Mapping: each input is mapped directly to one option of the keyboard.

**Discussion:** The results have shown that virtual keyboards can be used for effective end-user communication from brain signal when these signals are already processed in order to give a more clean output. The developed interpreter based on the virtual keyboard descriptive language makes possible to adapt it to specific needs without any change in computer code, since only the high-level description of the keyboard must be changed. Also, as this description of the keyboard is very close to the characteristics of the keyboard itself, it's easy to researches make changes to fit it to their needs. **Conclusion:** The present work confirmed that virtual keyboards can be used to write and express feelings, words and sentences with minimal – for example only one binary signal - from brain. But virtual keyboards can also be used to interact with other programs or systems, as its options can be structured as control panels or even “cockpits”. So, this interpreter can be evolved in order to make integration with other systems possible.

**References:** [1] Dias RCV. Descriptive language for virtual keyboards with focus on augmentative and alternative communication, MA thesis. 2016; [2] Python [www.python.org](http://www.python.org)

## WIRELESS DEEP BRAIN STIMULATION DEVICE WITH INTEGRATED ANTENNAE

E. Borba<sup>1</sup>, C. Santos<sup>3</sup>, C. Kemere<sup>2</sup>, R.R. Panepucci<sup>3</sup>

<sup>1</sup>FACTI/CTI Renato Archer; <sup>2</sup>Rice University; <sup>3</sup>CTI Renato Archer

**Introduction:** Deep Brain Stimulation (DBS) is an enables stimulation of brain areas involved in neurodegenerative diseases leading to new knowledge. It has been shown to be a valid treatment for diseases such as Parkinson's, with ongoing clinical trials towards its use in epilepsy. We are working within the scope of an open science initiative with Rice University to develop next generation wireless DBS devices for use in experimental neuroscience<sup>1,2</sup>. Our aims are to contribute to the body of knowledge by developing improved circuit designs enabling lower power consumption, lower weight, and lower dimensions in the wireless module, while providing the needed electric stimuli in the experimental conditions required. In this first re-design we have proposed the addition of the radiofrequency antenna for near-field communication (NFC) into the printed circuit board (PCB). **Materials and Methods:** The project is based on the initial design available in the open science project by Rice University's Kemere Lab available in Github<sup>3</sup>. We used AUTODESK Eagle version 8.0.0 to design the circuit. The PCB was prototyped with a LKPF ProtoMat S103 circuit board plotter. The device was tested in the development environment, with a functional DBS board (Rev2016), by verifying communication with an Android-based NFC cellphone. A comparison of the manufactured antenna was made with a commercial NFC antenna model ANFCA-2515-A02 from ABRACON (Figure a). **Results:** Figure (a) shows two setups, one with a commercial antenna, and the PCB with antenna, both connected to the current DBS board. Figure (b) shows the proposed complete PCB designed with inte-

grated antenna and DBS electronics. At this stage of the testing, the PCB has a dummy metal filler. The results achieved with both antennas are comparable, with the minimal distance for NFC communication from antennas to the cellphone, of approximately 20 mm. **Discussion:** The NFC transmitter energized both circuits and showed that the PCB with integrated antenna and device was detected with a sensitivity similar to the commercial antenna. Further tests with a PCB with antenna and populated with the electronic components are needed. We expected that the greater extension of the antenna, since this covers the whole perimeter of the area, would lead to an improved sensitivity; however that improvement was not observed. **Conclusion:** The present work reduces the number of devices and the cost of the device without loss of performance. Further work will redesign the actual circuit and explore the use of new components for the radio using alternative technologies: Bluetooth Low Energy and 6lowPAN; which allow greater range and optimize the consumption of the battery by modifying the stimulus circuit.

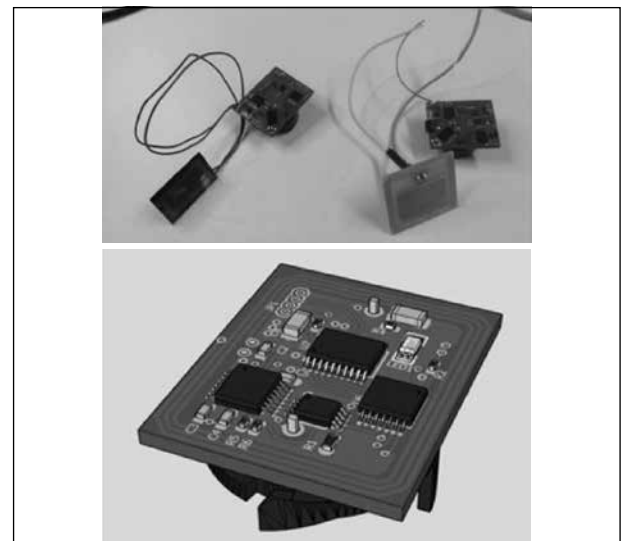


Figure 1. (a) Right: PCB antenna in this study, Left: commercial antenna; (b) Proposed PCB with antenna.

**References:** [1] Lewis E, Kemere C. Soc Neurosci. Abstract #415.12, 2016. [2] Summerson S, Aazhang B, Kemere C. IEEE Trans Neural Sys; Rehab Eng. 2014;22(6):1218; [3] <https://github.com/kemerelab/RodentDBS>

## SU-8 NEURAL PROBES ARE OPTIMIZED FOR SINGLE UNIT RECORDINGS IN OPTOGENETIC EXPERIMENTS

A. H. Malavazi<sup>1</sup>, T. Malfatti<sup>2</sup>, R. M. Covolani<sup>1</sup>, K. E. Leão<sup>2</sup>, R. R. Leão<sup>2</sup>, R. R. Panepucci<sup>3</sup>

<sup>1</sup>Neurophysics Group, IFGW, UNICAMP; <sup>2</sup>Instituto do Cérebro, UFRN; <sup>3</sup>CTI Renato Archer.

**Introduction:** The ability to control with temporal and spatial precision brain function with optogenetics has revolutionized neuroscience. However, it has been difficult to record brain activity using electrodes in experiments that involve light stimulation (due to the optoelectric effect). Here we show that probes constructed with the SU-8 polymer withstands optical stimulation and are less prone to the optoelectric effect than classical Si-based probes. **Materials and Methods:** We used neural probes designed and fabricated with SU8 and Au electrodes, as reported previously<sup>1</sup>. To validate the application of the fabricated neural probes, an experiment was carried out with in vivo registration of the neuronal activity of mice expressing channelrhodopsin (ChR2). We then compared the performance of SU-8 probes with a commercial Si neural probe (Neuronexus) with similar channel count in anesthetized ChR2-expressing mice. We also implanted a 200µm-thick fiber to stimulate ChR2+ neurons with 473nm light. **Results:** The figure below shows spike sorting of a signal obtained with the SU-8 probe. The algorithm separates the spikes in clusters which refer to the signature electrical activity of individual neurons. It is possible to observe the separation into three different clusters, indicating detection of 3 distinct neurons in the range of the microelectrode in the probe. However, the SU-8 probe shows a significantly smaller electrical artifact in response to light

stimulation. **Discussion:** As expected the two devices were capable of recording the biological signal optically stimulated. While SU-8 probes had performance comparable to that of commercial Si probes in recording single units, the latter suffered significantly less interference from the light stimulation. **Conclusion:** This test suggests the use of polymer based neural probes, in particular SU-8, as a promising tool to record neuronal activity allied to optogenetics.

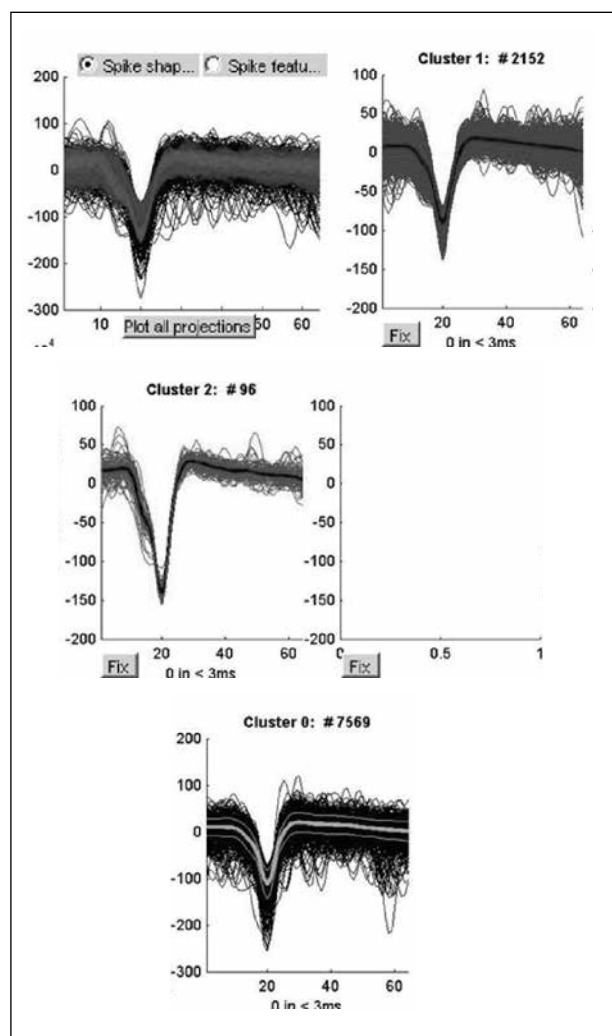


Figure 1. (a) Right: PCB antenna in this study, Left: commercial antenna; (b) Proposed PCB with antenna.

**References:** [1] Malavazi AHA, et al. 2nd BRAINN Congress: "Development of Polymer-based Neural Probes".

#### INVESTIGATING THE GENETIC LANDSCAPE OF CHILDHOOD EPILEPTIC ENCEPHALOPATHIES IN LATIN AMERICA

H. Urquia-Orsorio<sup>1</sup>, F. Cendes<sup>1</sup>, I. Lopes-Cende<sup>2</sup>

<sup>1</sup> Department of Neurology; <sup>2</sup> Department of Medical Genetics; School of Medical Sciences, University of Campinas, UNICAMP, Campinas, São Paulo, SP, Brazil; and the Brazilian Institute of Neuroscience and Neurotechnology, BRAINN, Campinas, São Paulo, SP, Brazil.

**Introduction and Hypothesis:** Childhood epileptic encephalopathies (CEEs) are severe cerebral disorder in which the epileptic activity itself may contribute to progressive development of psychomotor dysfunction. Recent advances in molecular genetics have led to the discovery of several genes for CEEs. However, the etiology in most patients remains unknown, and important population groups such as Latin American have not yet been well studied, which increases the possibility of the identification of new candidate genes for different forms of CEEs. **Objective:** This study aims to characterize the genetic bases of CEEs in patients from Latin America. **Methods:** This is an effort done in conjunction

with the International League Against Epilepsy (ILAE) by means of the Commission on Latin American Affairs. Data will be obtained from patients with CEEs (West, Lennox-Gastaut, Otahara, Dosse, Dravet syndrome and others), from neurology services of each collaborative center in different Latin American countries. A common clinical protocol has been defined to determine inclusion and exclusion criteria for patient enrolment. Initially, patients will be evaluated for mutations on *SCN1A*, for both sequence variants and structural alterations, and if negative whole exome sequence will be performed. **Relevance:** The presence of genetic heterogeneity and clinical variability represents a major challenge when assessing the impact of genetic discoveries in clinical practice; nevertheless, the specific diagnosis can influence treatment decisions in some patients. A systematic evaluation of CEEs has never been performed in Latin America, since it is well known that allele frequency for rare variants may significantly vary across populations from different ethnic backgrounds, it is possible that frequency of mutations in CEE patients in Latin America differ from previously described in the literature. In addition, because genetic variability, due to admixture, is high in Latin America one will have the opportunity to describe additional mutations/candidate genes.

**References:** [1] Gonsales MC, et al. *Arq Neuropsiquiatr*. 2015;73(11): 946-58; [2] Casals F, et al. *Science*. 2012;337(6090):39-402.

Supported by: FAPESP, SP, Brazil

#### A MODEL FOR DIAGNOSTIC DECISION SUPPORT IN MENTAL HEALTH THROUGH THE ANALYSIS OF VARIABLES OF DIFFERENT KINDS

I. Carvalho<sup>1</sup>, J. L. G. Rosa<sup>1</sup>, C. M. Del-Ben<sup>2</sup>, R. Shuhama<sup>2</sup>, C. M. Loureiro<sup>2</sup>, P. R. Menezes<sup>3</sup>

<sup>1</sup>ICMC, USP, São Carlos; <sup>2</sup>FMRP, USP-Ribeirão Preto; <sup>3</sup>FMUSP, USP, São Paulo, SP, Brazil.

**Introduction / Hypothesis:** The diagnosis involves not only deciding what is true about a patient, but also the data needed to determine what is true. The requirements for decision-making cover accurate data, relevant professional knowledge and skills for solving problems. In psychiatry, the patient presents subjective complaints and the trained doctor categorizes the complaints based on operational criteria. However, few definitive objective measures can be used as additional tests to confirm the diagnosis. Thus, the lack of biological markers leads many investigators to conclude that there is no "gold standard" for diagnosis process in this area<sup>1</sup>. The computational tools allow data to be manipulated for an easier knowledge management<sup>2</sup>. The hypothesis is that the construction of a decision model based on mathematical representation of the context is able to organize the characteristics of the problem, to acquire knowledge through the relationships among the characteristics and then improve the diagnostic accuracy of psychotic disorders studied. **Objective:** The aim of this study is to propose and evaluate decision models that incorporate, in addition to information on signs and symptoms of patients, imaging aspects and risk factors, such as support for the psychiatric diagnosis of schizophrenia, bipolar disorder and depressive disorder. **Method:** Three groups (patient at first psychotic episode, brothers, and control) compose the universe of study with approximately 600 people. When considering the first episode of the psychotic disorder for diagnosis, it is possible to reach a more secure detection of the causes of the disorder, excluding the effects of chronicity and medicines on the result<sup>3</sup>. The data about signs and symptoms of patients were obtained through the Structured Clinical Interview for DSM-IV intended for the process of psychiatric diagnosis. The set of environmental and social risk factors were collected in a detailed evaluation, mainly through interviews and semi-structured assessment tools applied in all study participants. The variables representing the biological markers is based on information about the family history of psychosis and some analyses of specific polymorphisms with the collection of biological material in all study participants for genetic and immunological analyzes. Imaging exams are represented by the set of variables that describes the characteristics of the analysis of white and gray matter by magnetic resonance of the participants. The method will be based on exploring the models of decision by means of the study variables. Techniques that involve Bayesian networks and complex networks should be applied with the purpose of outlining the sets of variables relevant to the problem and their principal correlations. Then, the evaluation of the models found will be made with the help of medical experts with support of the Kappa statistical method. **Relevance:** This work aims to contribute to the accuracy of diagnosis in mental health. The study of the medical model



in psychiatry directly affects: (i) the quality of life of patients, who have their prognoses increasingly effective and will undergo the most effective treatments and (ii) the health system, by proposing public policies based on better decisions to support these patients and families.

**References:** [1] Aboraya A, et al. *Psychiatry*. 2006;3(1):41-50; [2] Musen MA, et al. *Biomedical Informatics*. 2014;643-74; [3] Peruzzo D, et al. *Journal of Neural Transmission*. 2015;897-905, 2015.

#### VIRTUAL REALITY AS AN ADD ON REHABILITATION THERAPY IN PATIENTS AFTER ISCHEMIC STROKE

A. F. B. Camargo<sup>1,2</sup>, L. M. Li<sup>1,2</sup>

<sup>1</sup>Laboratory of Neuroimaging, Department of Neurology, FCM-UNICAMP; <sup>2</sup>Brazilian Institute of Neuroscience and Neurotechnology, BRAINN, Campinas, São Paulo, SP, Brazil.

**Introduction / Hypothesis:** Stroke is the leading cause of functional disability in adults. Muscular weakness of hemiparesis is the most prevalent functional consequence for the post-stroke patient<sup>1</sup>. Neuroimaging studies show that post-stroke patients with motor symptoms have a decrease in motor connectivity and reduction in the number of functional brain networks, affecting their independence, daily living activities, quality of life and behavior<sup>2</sup>. Thus, the treatment for these patients is multidisciplinary and global, seeking their return to functionality and restoration of their autonomy. The Virtual Rehabilitation (VR) demonstrates promising results as an add on to conventional rehabilitation, allowing the performance of natural movement patterns in varied environments and enabling activation of neural networks<sup>3</sup>. In our experience through a research project with 4 post-stroke patients with conventional physiotherapy plus VR during 4 weeks, improvements were observed in quality of life, Fugl-Meyer Assessment and Time Up and Go Test before and after intervention when compared to a control group of 4 subjects with similar characteristics only with conventional physiotherapy<sup>4</sup>. Our hypothesis is that patients who respond positively to functional recovery after a VR program show distinct patterns of functional connectivity observed in magnetic resonance imaging (MRI). **Objective:** The main aim of this study is to analyze the effects of Virtual Rehabilitation in post-ischemic stroke patients, besides the conventional physiotherapy. **Method:** Thirty post-stroke symptomatic patients will be included in the study, randomized in control and experimental group. Patients will be evaluated before and after intervention by a blinded evaluator. Structural and functional MRI will be acquired before and after intervention. All patients will receive conventional physiotherapy protocol twice weekly for six weeks, and the experimental group will receive the VR at the same frequency. The clinical data obtained will be tabulated and the differences will be analyzed using the ANOVA and a value of  $P \leq 0.05$  will be adopted as significant. MRI will be analyzed with SPM12. We hope to identify a positive influence on the application of VR and establishment of neural connectivity patterns – a prove of its effectiveness from the data obtained. **Relevance:** This research assists in the diffusion of knowledge about the performance of VR in symptomatic patients post chronic stroke, enabling the later implementation of this appliance in the functional recovery of these patients if its efficacy is proven as an add-on therapy for rehabilitation.

**References:** [1] Silva JM, et al. *Rev Neurocienc*. 2015;23(1):48-54; [2] Almeida S, et al. *J Neuroimaging*. 2016;27(1):65-70; [3] Lee SJ, et al. *Archives of Physical Medicine and Rehabilitation*. 2014;95(3):431-8; [4] Camargo AFB, et al. Presented in III Encontro Científico do Curso de Fisioterapia da Universidade de Sorocaba 2016.

#### EFFECTS OF SUB-CONVULSIVE DOSES OF PENTYLENETETRAZOLE DURING ZEBRAFISH BRAIN DEVELOPMENT

T. G. Parolari<sup>1</sup>, V. Fais<sup>1</sup>, JE Cavazos<sup>2</sup>, V. Maurer-Morelli<sup>1</sup>

<sup>1</sup>Zebrafish Laboratory, Department of Medical Genetics, FCM, UNICAMP; <sup>2</sup>The University of Texas Health Science Center at San Antonio.

**Introduction / Hypothesis:** Experimental animal models play an important role to investigate basic mechanisms underlying human diseases, including epilepsy. In the last decade, *Danio rerio*, popularly known as zebrafish, has been used as a model of acute seizures; even so, there is no indicative in the literature that the zebrafish can become chronically epileptic. In order to understand the epileptogenic process, electrical or chemical kindling have been used in animal models, mainly in rodents. Given the advantages of zebrafish for genetic, cellular and drug screening studies, it is important to investigate whether zebrafish is able to become chronically epileptic. **Objective:** The main aim of this study is to investigate the effect of sub-convulsive doses of pentylenetetrazole on molecular

and behavioural patterns during brain development in the zebrafish. **Methods:** This study was approved by the Ethics Committee on Animal Use (CEUA) of UNICAMP #4426-1. Wild-type zebrafish embryos, larvae and adult will be maintained according to standard patterns. Larvae at 5days post-fertilization (dpf) will be divided in Control Group (CG) and Kindling Group (KG). Animals from KG will be exposed to sub-convulsive doses of the pentylenetetrazole (PTZ) at 7.5 mM for a period of 20 minutes, during four weeks (once a day, Monday to Friday). Behaviour and molecular profiles will be assessed immediately after the first exposition to the PTZ (5dpf) and later with animals at 9, 16, 23 and 30 dpf (n= 25, each group). Animals from CG will be handled in the same way but in PTZ-free water. Another batch of animals at 5dpf (named as KG60) will receive the following treatment: four weeks of PTZ-treatment, as early described, followed by a break of four weeks (no PTZ-treatment). At the end of this break period, adult animals (at 60 dpf) will be exposed to PTZ 15 mM (seizure-induced dose) in order to evaluate the latency to reach a complete seizure, indicating the convulsing brain sensitization. Control animals (CG60) will be handled in the same way but in PTZ-free water. Behavioural analysis will be recorded by the Danio Vision equipment and analysed with EthoVision software for swimming activity and distance travelled quantification. Real-time PCR will be applied to assess the brain mRNA expression of *il1b*, *cox-1*, *bdnf*, and *c-fos* genes using TaqMan™ system (Applied Biosystems, Foster City, CA, USA). **Relevance:** Today there are no data in the literature showing that the immature zebrafish brain can become chronically epileptic. By attempting to reproduce the kindling phenomena in zebrafish brain we hope to bring new insights into the basic mechanisms that transform a normal neuronal network into an overexcited network. In addition, because zebrafish is a suitable model for drug screening, we expect to provide an alternative model for studying compounds for seizure suppression or to prevent the events underlying the epileptogenesis.

**References:** [1] Baraban, SC, et al. *Neuroscience*. 2005;131(3):759-68.

#### FUNCTIONAL STUDIES OF SCN1A MUTATIONS

Saul, Lindo-Samanamud<sup>1</sup>, A. S. Vieira<sup>1</sup>, F. R. Torres<sup>1</sup>, M. C. Gonsales<sup>1</sup>, F. Cendes<sup>1,2</sup>, Lopes-Cendes<sup>1</sup>

<sup>1</sup>Department of Medical Genetics, School of Medical Sciences, University of Campinas, UNICAMP, Campinas, São Paulo, SP, Brazil.

**Introduction:** Mutations in *SCN1A*, a gene that encodes the  $\alpha$ -subunit of the sodium channel voltage-dependent (Nav1.1), impair the flow control of sodium ions, resulting in abnormal sodium influx into neurons that causes a disruption in the channel activity, neuronal hyper excitability and epilepsy (1). Previous studies carried out by our group found that 81% of patients with Dravet syndrome (DS) have de novo mutations in *SCN1A* (2). Interpretation of the mutation impact in protein function is usually performed using pathogenicity prediction software's. Therefore, functional studies are important both to confirm results from *in silico* analysis and to better characterize the deleterious effects of mutations. **Objective:** To evaluate the molecular pathogenesis of *SCN1A* gene mutation in a Tsa 201 cell line using electrophysiology techniques. **Method:** Mutation c.5329delG was selected following two parameters: 1) mutations that are not described in literature and 2) scores obtained by bioinformatics tools as SIFT and Polyphen2 showing that variations are damaging to protein function. The wild forms of *SCN1A* and the genes encoding auxiliary  $\beta$ -subunits *SCN1B*, *SCN2B* (wild-type genes) were cloned by recombinant DNA technology. Recombinant plasmids were isolated, purified and submitted to sequencing on a Miseq (Illumina) in order to assure that sequences were properly cloned. Primers for Site-Directed Mutagenesis were designed using the PrimerX software. Site-Directed Mutagenesis was performed using GeneArt PLUS Kit @Site-Directed (Thermo Fisher Scientific) to obtain the mutant plasmid (pSCN1A-mut). The pSCN1A-mut was submitted to sequencing on a Miseq to confirm if mutation c.5329delG was properly inserted. Thereafter, the wild type *SCN1A*, *SCN1B* and *SCN2B* recombinant plasmids were co-transfected into the TSA201 cell line. In addition, pSCN1A-mut was co-transfected with wild type *SCN1B* and *SCN2B* plasmids into the TSA201 cell line. **Relevance:** Nav1.1 functional studies (as well as of other ion channels) are important both to confirm results that were previously predicted exclusively by *in silico* analysis and to characterize mutations which could not be classified by bioinformatics tools. We expect that our results will not only help to improve molecular diagnosis of patients with DS an, but



will also help us to better understand the repercussion of genetic variability (both normal and pathological) in the functional aspects of Nav1.1 sodium channels and other epilepsy-related ion channels.

**References:** [1] Meng H, et al. Hum Mutat. 2015;6(6):573-80; [2] McA G, et al. J Epilepsy. 2012;18(2):60-2.

#### PERCEPTIONS OF STIGMA DURING DISCLOSURE AMONG PATIENTS WITH EPILEPSY IN DIFFERENT LIFE SCENARIOS

C. Y. Tagami<sup>1,4</sup>, G. S. Spagnol<sup>1,2,3</sup>, L. M. Li<sup>1,2,3</sup>

<sup>1</sup>Brazilian Research Institute of Neuroscience and Neurotechnology, UNICAMP; <sup>2</sup>School of Medical Sciences, UNICAMP; <sup>3</sup>ASPE, a non-governmental organization to assist the patient with epilepsy; <sup>4</sup>Faculty of Psychology at UNISO.

**Introduction / Hypothesis:** Epilepsy imposes a great psychosocial burden not only to the patient, but also to the family and society. Concealing diagnosis is often the case, as disclosing the condition can lead to discrimination and social isolation. Stigma, as defined by Goffman is "the situation of the individual who is disqualified from full social acceptance", related to the gap between virtual social identity (assumptions of others regarding an individual) and actual social identity (attributes the individual could in fact be proved to possess)<sup>1</sup>. These concepts influence construction of personal identity. For patients with epilepsy, disclosing or not information about epilepsy is related to probability of how much this modify their personal identity in time and space. Quantity and quality of social interaction are directly related to quality of life of patients with epilepsy, which may be reduced due to stigma<sup>2</sup>. Yet, it is not clear whether the social interactions take place in a total openness about one having epilepsy, or the patients conceal their diagnosis. In this sense, it is important to understand situations that patients with epilepsy are more at ease or not about their willingness to disclose about their epilepsy. Our hypothesis is that the patients disclose about epilepsy depending on the social situation they are in. **Objective:** The aim of this study is to evaluate in which social situations the person with epilepsy would feel comfortable to disclose their condition or would rather conceal it. **Method:** We will perform a quali and quantitative survey through application of a questionnaire adapted from Troster (1997) survey<sup>3</sup>. This questionnaire describes six different scenarios for a possible disclosure: "(a) a random contact with a stranger on a bus, (b) a pleasant evening with an old friend, (c) a social evening during which new members of a sports association get to know each other, (d) a family gathering at which one gets to know one's future in-laws; (e) a job interview with a superior, and (f) a visit of several days from a close relative"<sup>3</sup>. In these scenarios, patients will be questioned regarding the probability that they would disclose their condition to their specific interaction partner; classifying in a 6-point scale: "in no way" (O), "most probably not" (I), "probably not" (2), "probably yes" (3), "most probably yes" (4), and "certainly yes" (5). This research will take place at the Neurology Outpatients Clinic of a University Hospital. **Relevance:** Situations that bring discomfort in talking about epilepsy may also be related to felt or enacted stigma. Understanding about situation related stigma can lead to development of strategies to minimize the impact of stigma that could result in social isolation.

**References:** [1] Goffman E. Stigma: Notes on the Management of Spoiled Identity. Prentice-Hall. 1963; [2] Smezer E, Jokic H. Seizure. 2015;26(1):12-21; [3] Troster. Epilepsia. 1997;38(11): 1227-37.

#### HUMAN-COMPUTER INTERFACE USING FACIAL EXPRESSIONS: A SOLUTION FOR PEOPLE WITH MOTOR DISABILITIES

Suzana Viana Mota<sup>1</sup>, Eric Rohmer<sup>1</sup>

<sup>1</sup>FEEC, DCA, UNICAMP, Campinas, São Paulo, SP, Brazil.

**Introduction / Hypothesis:** Brazil has 13.2 million people with some sort of motor disability<sup>1</sup>. The technology improvement dedicated to this theme originated a study area called Assistive Technologies<sup>2</sup>. Rodrigues e Teixeira claim that technology products become support, contents and ways of inclusion processes<sup>3</sup>. It is possible to see that people with motor disabilities have difficulty to control their mobile devices, since in most cases they do not have enough skills to touch the screen as a form of interaction. This paper presents a proposal of mobile interaction using facial expressions. **Objective:** This work proposes the development of a human-computer interaction for mobile devices based on computer vision. It features a solution for people with motor disabilities such as: cerebral palsy, muscular dystrophy, amyotrophic lateral sclerosis, cerebrovascular accident among others. It allows using a front camera already existing in most devices and controlling them through expressions or facial movements. People with disabilities can also control a robotic wheelchair or even a smart home, equipped with sensors that interact with their

mobile device. In addition, an Intel RealSense 3D camera-based solution will be implemented to compare the benefits of their approaches. **Method:** In performing this work, it is first necessary to define which facial expressions should be used in the proposed human-computer interaction. We should analyze a range of possible facial expressions and observe which are frequently used involuntarily and those that are used voluntarily. This phase is important because it prevents us from adopting an interaction that generates false negatives or false positives throughout its use. From this point will be implemented computer vision techniques through the OpenCV library in the Android environment using the front camera of low cost smartphones and tablets and a RealSense 3D camera with Raspberry Pi. These applied techniques should identify the different facial expressions already defined in the previous step and associate each one with the computer human interaction functions available in the Android environment and later interact with other devices such as a robotic wheelchair or a smart home equipped with sensors. **Relevance:** This work proposes a solution that will offer to the person with motor disability, independence and autonomy of locomotion, in addition to the control of the environment where it is inserted, thus, improving its quality of life and social inclusion.

**References:** [1] Instituto Brasileiro de Geografia e Estatística. (2010) Censo Demográfico; [2] BRASIL. Decreto 6.949 de 25 de agosto de 2009. Convenção sobre os direitos das pessoas com deficiência. Diário Oficial, Brasília, DF, 25 de agosto de 2009; [3] Rodrigues, CA, Teixeira, RA. Tecnologias em Processos de Inclusão. Rev Inter Ação. 2007;31(2):261-76.

#### HIPPOCAMPAL VOLUME AND FUNCTIONAL CONNECTIVITY PREDICTS FUNCTIONAL DECLINE IN MILD AD AND aMCI

N. Lecce<sup>1</sup>, C. V. L. Teixeira<sup>1</sup>, T. N. C. Magalhães<sup>1</sup>, A. F. M. K. C. Cassani<sup>1</sup>, M. Weiler<sup>1</sup>, B. Campos<sup>1</sup>, T. J. R. Rezende<sup>1</sup>, L. L. Talib<sup>2</sup>, O. V. Forlenza<sup>2</sup>, F. Cendes<sup>1</sup>, M. L. F. Balthazar<sup>1</sup>

<sup>1</sup>NeuroImage Laboratory, Department of Neurology, Medical Science School, UNICAMP, Campinas, São Paulo, SP, Brazil, <sup>2</sup>Laboratory of Neuroscience (LIM-27), Department and Institute of Psychiatry, Faculty of Medicine, University of São Paulo, São Paulo, SP, Brazil.

**Introduction / Hypothesis:** The study of biomarkers in mild Alzheimer's disease dementia (AD) and amnesic mild cognitive impairment (aMCI) is essential for the improvement of early diagnosis. However, it is not completely known the usefulness of different biomarkers for tracking the progression of the disease. The aim of this study is to evaluate if cerebrospinal fluid (CSF) biomarkers (A $\beta$ 42, ptau and tau), hippocampal volumes (HV) and Default Mode Network (DMN) functional connectivity (FC) could predict the cognitive and functional evolution of mild Alzheimer's disease dementia and amnesic mild cognitive impairment patients.

**Objective:** Compare the dosage of beta-amyloid, total tau and phosphorylated tau proteins in patients with AD and aMCI at the onset of the disease; Compare the hippocampal volume in patients with AD and aMCI at the onset of the disease; Compare the Default Mode Network (DMN) functional connectivity (FC) in patients with AD and aMCI at the onset of the disease; Verify if the biomarkers described are correlated with the progression of cognitive (MMSE) and functional (Pfeffer Questionnaire and CDR sum of boxes) measures. **Method:** We evaluated 32 mild AD and aMCI due to AD during 9 months. All subjects underwent neuropsychological assessment, MRI at 3 Tesla for structural and FC evaluation, and CSF biomarkers. All aMCI subjects had evidence of AD pathophysiology (hippocampal atrophy and/or low CSF A $\beta$ 42 and/or low A $\beta$ 42/ptau). HV was obtained by FreeSurfer software. We performed the FC analysis using the UF2C toolbox (<http://www.lni.hc.unicamp.br/app/uf2c/>). We estimated an average DMN map that was divided in eight DMN subparts: the prefrontal cortex; medial parietal cortex; left and right parietal lobe, left and right temporal lobe, left and right hippocampus. The average values were converted to z-scores that were used for statistical analysis. Dosages of A $\beta$ 42, tTau and pTau were obtained from INNOTEST® kits (Fujirebio). We performed multiple regressions considering changes ( $\Delta$ ) in cognition (Mini Mental Status Examination MMSE) and in functional status (Pfeffer's Questionnaire of daily living) as dependent variables and, age, sex, education, CSF biomarkers, HV and DMN subparts FC as independent variables. **Preliminary Results:** We did not find any significant result concerning these variables and changes in MMSE over time. However, we found that hippocampal volume and FC predicted changes in Pfeffer's Questionnaire: left HV (adjusted R<sup>2</sup> = 0.79, F = 5.75; t = 5.73, p = 0.029); right hippocampal FC: (adjusted R<sup>2</sup> = 0.84, F = 12.06; t = 5.13, p = 0.004). All tests were corrected for multiple comparisons. **Relevance:** Hippocampal structure and functional connectivity (but not CSF biomarkers) predict changes over time in functional activities in patients with mild AD and aMCI. Interestingly, we found a direct relationship between hippocampal FC and the worsening of our patients, what could mean that initial high connectivity might be compensatory.

# STUDY OF THE TECHNIQUE OF MAGNETIC RESONANCE SPECTROSCOPIC IMAGING (MRSI) AND APPLICATION TO EVALUATION OF BRAIN METABOLITES OF SYSTEMIC LUPUS ERYTHEMATOSUS PATIENTS

J. Horvath<sup>1,4</sup>, D. R. Pereira<sup>2,4</sup>, L. Rittner<sup>2,4</sup>, S. Appenzeller<sup>3</sup>, G. Castellano<sup>1,4</sup>

<sup>1</sup>Neurophysics Group, IFGW, UNICAMP; <sup>2</sup>Computer Engineering and Industrial Automation Dept., FEEC, UNICAMP; <sup>3</sup>Dept. of Medical Clinics, FCM, UNICAMP; <sup>4</sup>Brazilian Institute of Neuroscience and Neurotechnology, BRAINN, Campinas, São Paulo, SP, Brazil.

**Introduction / Hypothesis:** Patients with systemic lupus erythematosus (SLE) have a decrease of the ratio between N-acetylaspartate (NAA) and creatine compounds (Cr), and an increase of choline compounds/Cr, compared to healthy subjects<sup>1</sup>. These findings have been achieved using the magnetic resonance spectroscopy (MRS) technique, with a single-voxel acquisition. In this project, we will use multivoxel spectroscopy (MRSI, magnetic resonance spectroscopy imaging) to evaluate metabolite levels in SLE patients and compare them to those of healthy subjects. We will also test a software, developed by the group of Prof. Leticia Rittner (FEEC – UNICAMP), which automatically matches MRSI data to corresponding anatomical MR images, which is something that was previously only possible to perform at the scanner console. This project is part of a larger project, coordinated by Prof. Simone Appenzeller (FCM – UNICAMP), which has as one of its objectives to establish possible associations between cytokine levels and metabolic changes measured via MRS in SLE patients. **Objective:** The main aim of this project is to study the <sup>1</sup>H-MRSI technique, apply it to the evaluation of brain metabolites from patients with systemic lupus erythematosus (SLE) and compare the results with those of healthy volunteers. Specifically, we aim to: 1) study the MRSI technique, from its physical principles and pulse sequence used, up to pre-processing and analysis (or quantification) of resulting data; 2) test the software developed by the group of Prof. Leticia Rittner, applying it to MRSI data of the corpus callosum of SLE patients and healthy controls; 3) compare corpus callosum metabolite levels of SLE patients and controls. **Methods:** We will use the software created by the group of Prof. Leticia Rittner to combine the MR images with the MRSI grids and thus verify the positioning of the spectra grids, which are, in this case, in the upper region of the corpus callosum to avoid cerebrospinal fluid. Besides that, the software, through the use of a segmentation mask, allows the selection of only a part of the acquired spectra<sup>2</sup>, belonging only to the desired region of interest (corpus callosum). After this, the software LCMoDe<sup>3</sup> will be studied and used to quantify the selected MRSI spectra. **Relevance:** Through this project, we expect to find the same results of the literature<sup>1</sup>, but with the use of multivoxel MRS instead of single voxel MRS. Besides that, the software created by the Prof. Leticia's group is being tested for the first time.

**References:** [1] Appenzeller S, et al. Arthritis Rheum. 2006;55(5):807-11; [2] Pereira DR, Fritolli RB, Lapa AT, Appenzeller S, Lotufo RA, Rittner L. Metodologia para seleção de espectros de interesse em espectroscopia multi-voxel por ressonância magnética. XXV Congresso Brasileiro de Engenharia Biomédica – CBEB, Foz do Iguaçu-PR, 2016; [3] Provencher SW. Magn Reson Med30: 1993;672-679.

# HUMAN PROSTHETIC HAND INTERACTION BASED ON ELECTROMYOGRAPHY AND IMAGE RECOGNITION

A. Ishikawa<sup>1</sup>, A. D. Muñoz<sup>1</sup>, D. T. G. Andrade<sup>1</sup>, E. Rohmer<sup>1</sup>

<sup>1</sup>School of Electrical and Computer Engineering, FEEC, UNICAMP.

**Introduction / Hypothesis:** The World Health Organization appointed a demand of 30 million prostheses in low-income countries by 2011. Hand prostheses available on the market have high prices and besides their cost, they also rely on an intensive and tiring muscular training to learn how to trigger one of their predefined grasping sequences, without the guarantee the user is going adapt. We hypothesize that the proposed interface can make an easier use of the prosthesis at a much lower production price. **Objective:** Develop a hybrid Human-Machine Interface for prosthetic hand using electromyography (EMG) and image recognition technologies as an alternative to the ones that require a great set of electrodes. The hybrid innovating solution will allow the user to easily select one of the predefined grasping pattern to interact with an object based on a picture taken of this object. **Materials and Methods:** As shown in Figure 1, the system architecture is composed by two parallel processing fluxes, being EMG the input for the first and an object image for the second. The EMG based contraction detector system, that is always running, starts the camera processing flux when the user executes an arm contraction. It then activates the Raspberry Pi 3.0 camera, taking a picture and sending it to Google Cloud Vision API. The API returns a label for the object, used then as a key, for a query of the grasping type database. This will generate grasping type suggestions sorted by most likely choices. Using the contraction detector system, the user will, one by one, accept the suggestion or ask for the next one. When accepted, the controller mediates the contact to the hand prosthetic, which at development stage is simulated in V-REP<sup>2</sup>. **Relevance:** The hand prostheses present on the market have high costs and a hectic human machine interface, making difficult their acquisition and use. This project aims to reduce the costs and facilitate the use of the human-hand prosthesis, by decreasing the number of electrodes on a 3D printed hand like.

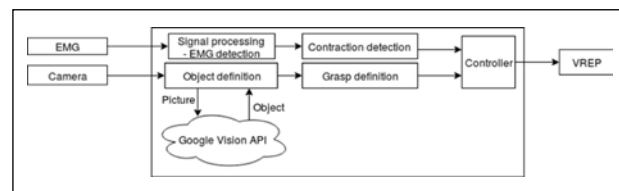


Figure 1. Overview of the proposed platform.

**References:** [1] Cummings D. Prosthetics in the developing world: a review of the literature. Prosthet Orthot Int. 1996;20(1):51-60; [2] Rohmer E, Singh SPN, Freese M. V-REP: A versatile and scalable robot simulation framework. In 2013 IEEE/RSJ Int Conf on Intel Robots; Sys. 2013;1321-26; [3] Fajardo J, Ferman V, Lemus A, Rohmer E. An Affordable Open-Source Multifunctional Upper-Limb Prosthesis with Intrinsic Actuation. In 2017 IEEE Workshop on Adv. Robotics and its Social Impact, 2017.

# O 1º PASSO para uma vida com NOVAS POSSIBILIDADES



- ▶ **Keppra® é o único FAE considerado nível A de evidência para o tratamento de crises focais, em terapia adjuvante, pelos guidelines da ILAE\*, em pediatria¹**
- ▶ **Keppra® tem bom perfil de tolerabilidade, baixa incidência de eventos adversos significativos, sem interação medicamentosa clinicamente significativa²**
- ▶ **Keppra® é um fármaco antiepiléptico de amplo espectro de ação²**

\*International League Against Epilepsy

**CONTRAINDICAÇÃO:** Hipersensibilidade ao princípio ativo ou a outros derivados da pirrolidona ou a qualquer um dos excipientes. **INTERAÇÃO MEDICAMENTOSA:** Foram observados relatos isolados de diminuição de eficácia quando o laxante osmótico macrogol foi administrado concomitantemente a levetiracetam oral. Assim, a administração oral de macrogol não deve ser realizada dentro de 1 hora (antes ou após) da administração de levetiracetam.

**Referência Bibliográfica:** 1. Wilmschurst JM. Summary of recommendations for the management of infantile seizures: Task Force Report for the ILAE Commission of Pediatrics. - Epilepsia, 56(8):1185-97. Aug. 2015. 2. Panayiotopoulos CP. A Clinical Guide to Epileptic Syndromes and their Treatment - Revised Second Edition - Chapter 18, Symptomatic and Cryptogenic (Probably Symptomatic) Focal Epilepsies, -ed. London UK - Springer-Verlag; page 485, 2007.

**Keppra® (levetiracetam). Apresentação:** comprimidos revestidos de 250 mg em embalagens com 30 ou 60 comprimidos ou comprimidos de 750 mg também em embalagens com 30 ou 60 comprimidos. **Indicações:** é indicado como monoterapia para o tratamento de crises parciais, com ou sem generalização secundária em pacientes a partir dos 16 anos com diagnóstico recente de epilepsia. Keppra® também é indicado como terapia adjuvante no tratamento de: - crises convulsivas parciais com ou sem generalização secundária em adultos, adolescentes e crianças com idade superior a 6 anos, com epilepsia; - crises convulsivas mioclônicas em adultos, adolescentes e crianças com idade superior a 12 anos, com epilepsia mioclônica juvenil; - crises convulsivas tônico-clônicas primárias generalizadas em adultos, adolescentes e crianças com mais de 6 anos de idade, com epilepsia idiopática generalizada. **Contraindicações:** Hipersensibilidade ao princípio ativo ou a outros derivados da pirrolidona ou a qualquer um dos excipientes. **Cuidados e Advertências:** para informações completas de advertências, vide bula do produto. A administração de Keppra® em pacientes com comprometimento renal poderá necessitar de um ajuste da dose. Foram notificados suicídio, tentativa de suicídio e ideias e comportamento suicida em pacientes tratados com levetiracetam. **Gravidez** categoria C de risco de gravidez. Este medicamento não deve ser utilizado por mulheres grávidas sem orientação médica ou do cirurgião-dentista. Levetiracetam é excretado no leite humano materno. **Keppra®** é um medicamento. Durante seu uso, não dirija veículos ou opere máquinas, pois sua agilidade e atenção podem estar prejudicadas. **Interações medicamentosas (vide bula completa do produto):** Dados indicam que levetiracetam não influencia as concentrações séricas de medicamentos antiepilépticos existentes (fenitoína, carbamazepina, ácido valproico, fenobarbital, lamotrigina, gabapentina e primidona) e que estes medicamentos antiepilépticos não influenciam a farmacocinética de levetiracetam. A probenecida (500 mg quatro vezes ao dia), um agente bloqueador da secreção tubular renal, mostrou inibir a depuração renal do metabólito primário, mas não a do levetiracetam. Contudo, a concentração deste metabólito permanece baixa. Levetiracetam 1000 mg por dia não influenciou a farmacocinética dos contraceptivos orais (etinilestradiol e levonorgestrel). Foram observados relatos isolados de diminuição de eficácia quando o laxante osmótico macrogol foi administrado concomitantemente a levetiracetam oral. Assim, a administração oral de macrogol não deve ser realizada dentro de 1 hora (antes ou após) da administração de levetiracetam. A extensão de absorção do levetiracetam não sofreu qualquer alteração com a ingestão de alimentos, mas a taxa de absorção diminuiu ligeiramente. Não estão disponíveis dados sobre a interação do levetiracetam com o álcool. **Reações Adversas:** para informações completas de reações adversas, vide bula do produto. Os eventos adversos mais comumente reportados nos estudos clínicos foram astenia, fadiga, dor de cabeça e sonolência. Adicionalmente às reações adversas relatadas durante os estudos clínicos, as seguintes reações adversas foram reportadas na experiência pós-comercialização, além de outras mencionadas na bula completa do produto: comportamento anormal, raiva, ataque de pânico, ansiedade, estado de confusão, alucinação, distúrbios psicóticos, suicídio, tentativa de suicídio e ideação suicida, parestesia, coreoatetose, discinesia, letargia. **Posologia:** A dose inicial recomendada para monoterapia no tratamento de crises parciais, com ou sem generalização secundária em pacientes a partir dos 16 anos com diagnóstico recente de epilepsia, é de 250 mg duas vezes ao dia, a qual poderá ser aumentada para uma dose terapêutica inicial de 500 mg duas vezes ao dia, após duas semanas. A dose máxima é de 1500 mg duas vezes ao dia. Nos casos de terapia adjuvante, para adultos e crianças acima de 12 anos e com mais de 50 kg, a dose terapêutica inicial é de 500 mg/duas vezes ao dia. Esta dose poderá ser iniciada no primeiro dia de tratamento, a dose diária poderá ser aumentada até o máximo de 1500 mg/duas vezes ao dia. Ainda nos casos de terapia adjuvante, para crianças (dos 6 aos 11 anos) e adolescentes com peso inferior a 50 kg a dose terapêutica inicial é de 10 mg/kg duas vezes ao dia, a dose pode ser aumentada até 30 mg/kg duas vezes ao dia. A alteração das doses não deve exceder aumentos ou reduções de 10 mg/kg duas vezes ao dia, a cada duas semanas. Deve ser utilizada a dose eficaz mais baixa. A posologia em crianças com peso igual ou superior a 50 kg é igual à dos adultos. A forma farmacêutica comprimido revestido não é adaptada para bebês e crianças com menos de 6 anos. Keppra® solução oral é a forma farmacêutica ideal para uso nesta população. **USO ADULTO E PEDIÁTRICO ACIMA DE 06 ANOS DE IDADE. USO ORAL. VENDA SOB PRESCRIÇÃO MÉDICA - SO PODE SER VENDIDO COM RETENÇÃO DA RECEITA. SE PERSISTIREM OS SINTOMAS, O MÉDICO DEVERÁ SER CONSULTADO.** Para maiores informações, consulte a bula completa do produto. (0302040013 R9 Rev. Agosto 2015).

[www.ucb-biopharma.com.br](http://www.ucb-biopharma.com.br) Reg. MS - 1.2361.0083





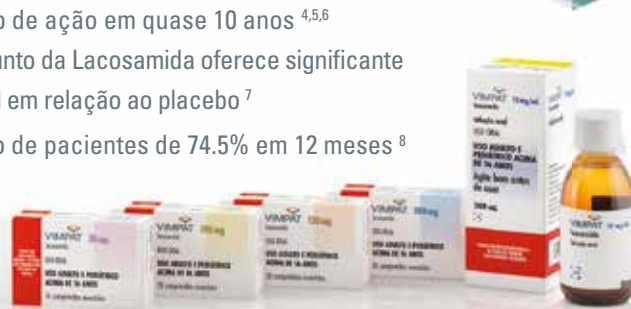
QUANDO A MONOTERAPIA NÃO É SUFICIENTE

# AVANÇAMOS

## VIMPAT: CONTROLE COMPROVADO EM PACIENTES COM CRISES DE INÍCIO FOCAL.<sup>2,3</sup>

- ▶ Melhor controle das crises independente da terapia de antiepilépticos atual ou prévia<sup>2,3</sup>
- ▶ Novo mecanismo de ação em quase 10 anos<sup>4,5,6</sup>
- ▶ O tratamento adjunto da Lacosamida oferece significativa eficácia adicional em relação ao placebo<sup>7</sup>
- ▶ Taxa de retenção de pacientes de 74.5% em 12 meses<sup>8</sup>

Disponível em mais de  
**40 países**<sup>1</sup>



**VIMPAT**™  
lacosamida

**CONTRAINDICAÇÃO:** em casos de hipersensibilidade ao princípio ativo (lacosamida) ou a qualquer um dos excipientes.  
**INTERAÇÃO MEDICAMENTOSA:** medicamentos conhecidos por prolongar o intervalo PR e antiarrítmicos classe I.

**Referências Bibliográficas:** 1. Alemanha, Argentina, Austrália, Áustria, Bélgica, Bulgária, Canadá, Chile, Chipre, Colômbia, Coreia do Sul, Dinamarca, Equador, Eslováquia, Eslovênia, Espanha, Estados Unidos, Filipinas, Finlândia, França, Grécia, Holanda, Hong Kong, Hungria, Índia, Irlanda, Israel, Itália, Luxemburgo, Malásia, México, Moldávia, Noruega, Nova Zelândia, Polónia, Portugal, Reino Unido, República Tcheca, Rússia, Suécia, Suíça, Tailândia, Turquia e Ucrânia. 2. Rosenfeld W, et al. Evaluation of long-term treatment with lacosamide for partial-onset seizures: a pooled analysis of open-label extension trials. Presented at the 65th Annual Meeting of the American Epilepsy Society (AES); 2011. Dec 2-6; Baltimore, USA. [www.aesnet.org](http://www.aesnet.org). 3. Chung S, et al. Examining the clinical utility of lacosamide: pooled analyses of three phase I/II clinical trials. CNS Drugs. 2010;24(12):1041-54. 4. Cross SA, et al. Lacosamide: in partial-onset seizures. Drugs 2009; 69 (4):449-459. 5. Fountain NB et al. Safety and tolerability of adjunctive Lacosamide intravenous loading dose in lacosamide-naïve patients with partial-onset seizures. Epilepsia 2013; 54(1):58-65. 6. Kellinghaus C, et al. Intravenous lacosamide treatment for treatment of status epilepticus. Acta Neurol Scand. 2011; 123(2): 137-41. 7. Sake J-K, et al. A pooled analysis of lacosamide clinical trial data grouped by mechanism of action of concomitant antiepileptic drugs. CNS Drugs. 2010;24(12):1055-68. 8. Rosenow F<sup>1</sup>, Kelemen A<sup>2</sup>, Ben-Menachem E<sup>3</sup>, McShea C<sup>4</sup>, Isojarvi J<sup>4</sup>, Doty P<sup>4</sup>: SP774 study investigators. Long-term adjunctive lacosamide treatment in patients with partial-onset seizures. Acta Neurol Scand. 2015 Jul 2. doi: 10.1111/ane.12451. [Epub ahead of print]. 9. Vimpat comprimidos revestidos 50, 100, 150 e 200 mg. Informação para prescrição. Reg. MS - 1.2361.0081. 10. Vimpat solução oral 10 mg/mL. Informação para prescrição. Reg. MS - 1.2361.0081.

### INFORMAÇÕES PARA PRESCRIÇÃO

**VIMPAT™ lacosamida** (lista C1 Port 344/98)

**Vimpat™** (lacosamida) comprimidos revestidos de 50 mg em embalagem com 14 comprimidos ou de 100, 150 e 200 mg em embalagens com 28 comprimidos. **Indicações:** terapia adjuvante no tratamento de crises parciais com ou sem generalização secundária em pacientes a partir de 16 anos de idade com epilepsia. **Contraindicações:** em casos de hipersensibilidade ao princípio ativo (lacosamida) ou a qualquer um dos excipientes. **Cuidados e Advertências:** (vide bula completa do produto): Vimpat pode causar tonturas, que podem aumentar o risco de acidente ou queda. Um pequeno número de pessoas que iniciaram tratamento com antiepilépticos, como a lacosamida, apresentaram pensamentos de autoagressão ou suicídio. Não é recomendável tomar Vimpat com álcool, pois Vimpat pode provocar tonturas ou sensação de cansaço. Vimpat é um medicamento. Durante seu uso, não dirija veículos ou opere máquinas, pois sua agilidade e atenção podem estar prejudicadas. Nos estudos clínicos foram observados prolongamentos no intervalo PR com o uso de lacosamida. Bloqueio AV de segundo grau ou maior foi reportado na experiência pós-comercialização. **Gravidez:** categoria C de risco de gravidez. **Interações medicamentosas** (vide bula completa do produto): A lacosamida deve ser usada com cautela em pacientes tratados com medicamentos conhecidos por prolongar o intervalo PR e em pacientes tratados com medicamentos antiarrítmicos classe I. Dados in vitro sugerem que a lacosamida possui potencial para inibir CYP2C19 em concentrações terapêuticas. A análise farmacocinética populacional estimou que o tratamento concomitante com outros medicamentos antiepilépticos indutores enzimáticos (carbamazepina, fenitoína, fenobarbital, em várias doses) reduz a exposição sistêmica geral da lacosamida em 25%. **Reações adversas** (vide bula completa do produto): Muito comuns: tontura, dor de cabeça, náusea e diplopia. Comuns: distúrbio cognitivo, nistagmo, distúrbio de equilíbrio, coordenação anormal, falha de memória, tremor, sonolência, disartria, distúrbio de atenção, hipostesia, parestesia, visão embaçada, vertigem, zumbido, vômitos, constipação, flatulência, dispepsia, boca seca, diarreia, prurido, espasmos musculares, distúrbio ao andar, astenia, fadiga, irritabilidade, sensação de embriaguez, quedas, laceração da pele, contusão. **Posologia:** A dose inicial recomendada é de 50 mg duas vezes por dia, a qual deverá ser aumentada para uma dose terapêutica inicial de 100 mg duas vezes por dia após uma semana. O tratamento com lacosamida também pode ser iniciado com uma dose de ataque única de 200 mg, seguida por uma dose de regime de manutenção, após aproximadamente 12 horas, de 100 mg duas vezes ao dia (200 mg/dia). A dose de ataque deve ser administrada sob supervisão médica considerando sua farmacocinética e o potencial para o aumento de incidência de reações adversas relacionadas ao SNC. A administração da dose de ataque não foi estudada em condições agudas em estados epilépticos. Dependendo da resposta clínica e tolerabilidade, a dose de manutenção pode ser aumentada 50 mg, duas vezes por dia, a cada semana, até uma dose diária máxima de 400 mg (200 mg duas vezes por dia). **USO ADULTO E PEDIÁTRICO ACIMA DE 16 ANOS DE IDADE. USO ORAL. VENDA SOB PRESCRIÇÃO MÉDICA – SO PODE SER VENDIDO COM RETENÇÃO DA RECEITA. SE PERSISTIREM OS SINTOMAS, O MÉDICO DEVERÁ SER CONSULTADO.** Para maiores informações, consulte a bula completa do produto. (0302040001R5 Rev. Dezembro 2014). [www.ucb-biopharma.com.br](http://www.ucb-biopharma.com.br) Reg. MS – 1.2361.0081

**Vimpat™** (lacosamida) solução oral 10mg/mL em embalagem contendo 1 frasco de 200mL e um copo-medida. **Indicações:** terapia adjuvante no tratamento de crises parciais com ou sem generalização secundária em pacientes a partir de 16 anos de idade com epilepsia. **Contraindicações:** em casos de hipersensibilidade ao princípio ativo (lacosamida) ou a qualquer um dos excipientes. **Cuidados e Advertências:** (vide bula completa do produto): Vimpat pode causar tonturas, que podem aumentar o risco de acidente ou queda. Um pequeno número de pessoas que iniciaram tratamento com antiepilépticos, como a lacosamida, apresentaram pensamentos de autoagressão ou suicídio. Não é recomendável tomar Vimpat com álcool, pois Vimpat pode provocar tonturas ou sensação de cansaço. Vimpat é um medicamento. Durante seu uso, não dirija veículos ou opere máquinas, pois sua agilidade e atenção podem estar prejudicadas. Nos estudos clínicos foram observados prolongamentos no intervalo PR com o uso de lacosamida. Bloqueio AV de segundo grau ou maior foi reportado na experiência pós-comercialização. **Gravidez:** categoria C de risco de gravidez. **Interações medicamentosas** (vide bula completa do produto): A lacosamida deve ser usada com cautela em pacientes tratados com medicamentos conhecidos por prolongar o intervalo PR e em pacientes tratados com medicamentos antiarrítmicos classe I. Dados in vitro sugerem que a lacosamida possui potencial para inibir CYP2C19 em concentrações terapêuticas. A análise farmacocinética populacional estimou que o tratamento concomitante com outros medicamentos antiepilépticos indutores enzimáticos (carbamazepina, fenitoína, fenobarbital, em várias doses) reduz a exposição sistêmica geral da lacosamida em 25%. **Reações adversas** (vide bula completa do produto): Muito comuns: tontura, dor de cabeça, náusea e diplopia. Comuns: distúrbio cognitivo, nistagmo, distúrbio de equilíbrio, coordenação anormal, falha de memória, tremor, sonolência, disartria, distúrbio de atenção, hipostesia, parestesia, visão embaçada, vertigem, zumbido, vômitos, constipação, flatulência, dispepsia, boca seca, diarreia, prurido, espasmos musculares, distúrbio ao andar, astenia, fadiga, irritabilidade, sensação de embriaguez, quedas, laceração da pele, contusão. **Posologia:** A dose inicial recomendada é de 50 mg duas vezes por dia, a qual deverá ser aumentada para uma dose terapêutica inicial de 100 mg duas vezes por dia após uma semana. O tratamento com lacosamida também pode ser iniciado com uma dose de ataque única de 200 mg, seguida por uma dose de regime de manutenção, após aproximadamente 12 horas, de 100 mg duas vezes ao dia (200 mg/dia). A dose de ataque deve ser administrada sob supervisão médica considerando sua farmacocinética e o potencial para o aumento de incidência de reações adversas relacionadas ao SNC. A administração da dose de ataque não foi estudada em condições agudas em estados epilépticos. Dependendo da resposta clínica e tolerabilidade, a dose de manutenção pode ser aumentada 50 mg, duas vezes por dia, a cada semana, até uma dose diária máxima de 400 mg (200 mg duas vezes por dia). **USO ADULTO E PEDIÁTRICO ACIMA DE 16 ANOS DE IDADE. USO ORAL. VENDA SOB PRESCRIÇÃO MÉDICA – SO PODE SER VENDIDO COM RETENÇÃO DA RECEITA. SE PERSISTIREM OS SINTOMAS, O MÉDICO DEVERÁ SER CONSULTADO.** Para maiores informações, consulte a bula completa do produto. (0302040001R5 Rev. Dezembro 2014). [www.ucb-biopharma.com.br](http://www.ucb-biopharma.com.br) Reg. MS – 1.2361.0081